1965

The thermodynamics of the ZnO-Fe_2O_3-Fe_3O_4 system

Robert Lee Benner

THE THERMODYNAMICS OF THE $ZnO-Fe_2O_3-Fe_3O_4$ SYSTEM

A Dissertation

Presented to

the Faculty of the Graduate School

University of Missouri

In Partial Fulfillment

of the Requirements for the Degree

Doctor of Philosophy

By

Robert Lee Benner, 1933

February 1965

ACKNOWLEDGMENTS

The author wishes to take this opportunity to express his deep appreciation to Mr. James A. Rowland, Research Director, Rolla Metallurgy Research Center, and to the Federal Bureau of Mines for making this research possible through a cooperative fellowship agreement with the University of Missouri at Rolla. Special gratitude is extended to Mr. H. Kenworthy for the time and assistance he so willingly devoted to this work.

The author is also indebted to the faculty of the University of Missouri at Rolla who were consulted at various times for technical advice and gratitude is extended to Dr. D. S. Eppelsheimer, the author's advisor, for his advice throughout this course of study and to Dr. W. J. James and Dr. G. Lewis for their many stimulating discussions on the theoretical thermodynamics.

TABLE OF CONTENTS

LIST OF TABLES

LIST OF FIGURES

FIGURE PAGE

CHAPTER I

INTRODUCTION

Statement of the problem. The purpose of this investigation was to (1) experimentally locate certain phase boundaries in three isothermal sections of the zinc oxide - ferric oxide - magnetite phase diagram, (2) to experimentally determine some of the thermodynamic properties of the zinc oxide - ferric oxide - magnetite system, (3) to use the thermodynamic properties of the zinc oxide - ferric oxide - magnetite system to evaluate the pseudo-binary system between zinc ferrite and magnetite, (4) to construct a compound stability diagram for the zinc-iron-oxygen-sulfur system.

Importance of the study. For many years the electrolytic refining of zinc has maintained an increasingly important position in the zinc industry and recently accounted for approximately thirty-eight percent of the primary zinc refined in the United States.[1] Because the process yields high-purity zinc and can treat certain types of complex ores, it would be desirable to increase the amount of zinc produced by this method. However, one of the serious obstacles encountered in the electrolytic process is the formation of a compound that is insoluble during normal leaching of roasted zinc ores containing iron. This insoluble compound is a zinc-iron oxide called zinc ferrite, and its formation during roasting creates subsequent zinc losses that are directly proportional to the iron content of the ore. Needless to say, zinc ferrite is an undesirable by-product, and methods are constantly

---

[1]Minerals yearbook (1961), Vol. 1, Metals and Minerals U.S. Dept. of Interior, Bureau of Mines.

being sought to reduce its formation. On the other hand, the electronics industry requires and produces considerable amounts of zinc ferrite as well as products in which zinc ferrite is combined with other ferrites. These ferrites have found extensive use in magnetic applications; however, their composition must be closely controlled in order to retain the desired magnetic properties. The amount of ferrous ion, a decomposition product of the ferrites, is an important constituent that must be controlled and, in certain cases, reduced to a minimum. Thus the electronics industry is constantly looking for methods of improving ferrite production and controlling its composition.

This investigation was initiated in order to provide these industries with basic data on the thermodynamic properties of zinc ferrite, zinc oxide, ferric oxide, and magnetite. With this information, industry can devise more effective methods to reduce or control the formation of zinc ferrite.

Because of the trend toward high-temperature roasting (above 950° C) and because the electronics industry utilizes temperatures from 1100° C to 1300° C in the production of ferrites, this investigation was confined to studies of systems at 1100° C, 1300° C and 1400° C.

CHAPTER II

REVIEW OF THE LITERATURE

Zinc as a metal has been known to man from prehistoric times and was probably first smelted commercially in India as early as the fourteenth century.[1] During the seventeenth and eighteenth centuries large quantities of slab zinc were imported from the East and about the year 1730 the knowledge of zinc smelting itself was brought from China to England. The process of smelting at that time consisted of distilling the zinc from a mixture of zinc ore and carbon in a sealed clay pot. A tube projected downward from the pot and the zinc condensed in it and then dripped into a receiver. Until 1758 only zinc oxide ores were used, but during that year, a patent was granted for making zinc from a sulfide ore by a process of roasting, mixing the roasted ore with charcoal, and smelting the mixture.

With the advent of zinc hydrometallurgy, roasted zinc sulfide ores became more widely used because, in the process of roasting, a portion of the sulfide is converted to sulfate, and thus the zinc was more easily leached. However, this procedure was not without drawbacks as O. C. Ralston stated: "It was soon discovered that hydrometallurgy has its limitations. It has also been found that certain ores can not be leached successfully by the present standard methods."[2] One of the serious obstacles encountered in the electrolytic process was the

---

[1]American Zinc Institute. "Zinc--The Science and Technology of the Metal, Its Alloys and Compounds" Am. Chem. Soc. Monograph No. 142, Reinhold Pub. Corp., New York, New York (1959), pp. 1-7.

[2]O. C. Ralston "Electrolytic Deposition and Hydrometallurgy of Zinc" McGraw-Hill and Company, New York, New York (1921), p. 7.

formation of dilute sulfuric acid-insoluble zinc compounds when iron-bearing zinc ores were roasted. The insoluble zinc was retained in the form of a zinc-iron-oxygen complex called zinc ferrite with the chemical formula $ZnFe_2O_4$.

In the early history of zinc hydrometallurgy much of the investigation of zinc ferrite was directed toward reclaiming the zinc from the ferrite by a separate process. Most of these processes involved the reduction of the ferrite by carbon or a reducing gas. Much of this early work gave contradictory results regarding the reducibility of the ferrite. Hommel[3] stated that it could not be reduced in normal zinc retort practice. Tafel and Grosse[4] found indications of a reversal in the relative stabilities of zinc oxide and ferrite in that zinc ferrite was less reducible than the oxide in the temperature range of 950°-1000° C, but was equally reducible at 1050° C. On the other hand, Prost and Van DePutte[5] reported that at 1150°-1240° C zinc ferrite was more easily reduced than was the oxide.

Hopkins and Adlington[6] reported that the reduction of the ferrite occurred in steps. The low temperature step involved the reduction of a portion of the ferric ion to ferrous ion, thereby replacing some of the zinc oxide in the ferrite structure with ferrous oxide and yielding free zinc oxide and magnetite as a final product.

---

[3]Hommel, Metallurgie, Vol. 9 (1912), p. 281.

[4]Tafel and Grosse, Metall u. Erz, Vol. 26 (1929), p. 354.

[5]Prost and Van DePutte, Rev. Univ. Des Mines, June 1, 1926.

[6]D. W. Hopkins and A. G. Adlington, Inst. of Mining and Metallurgy Trans., Vol. 60 (1950-1951), pp. 117-128.

The high-temperature step yielded free zinc oxide together with ferrous oxide or free iron as final products. However, they did not consider how zinc recovery would be effected by solid solution formation between zinc ferrite and magnetite.

In an investigation of the magnetic properties of zinc ferrite, Takei and Kato[7] were the first to mention the possibility of extensive solid solution of zinc ferrite and magnetite. The extent of the solubility was not fully investigated until much later[8] when the electronics industry became interested in the properties of zinc ferrite and the effect of zinc ferrite on other magnetic ferrites. In line with these investigations Yamaguchi and Takei[9] investigated the zinc oxide-ferric oxide-magnetite system in air between 1000° C and 1400° C. During their investigation they found a solid solution region, between zinc ferrite and magnetite, that was capable of dissolving excess ferric oxide as well as some excess zinc oxide. In addition, they found that the decomposition of zinc ferrite increased as the temperature increased.

---

[7] T. Takei and Y. Kato, Trans. Electrochem. Soc., Vol. 57 (1930), pp. 297-312.

[8] N. A. Toropov and A. I. Borisenko. Doklady Akad. Nauk, SSSR, Vol. 82 (1952), p. 607.

I. Kushima and T. Amanuma, Mem. Fac. Eng. Kyoto Univ., Vol. 16

[9] T. Yamaguchi and T. Takei. Sci. Papers Inst. Phys. Chem. Research, Tokyo, Vol. 53 (1959), p. 207.

The findings of Yamaguchi and Takei[10] were contrary to the thinking of many zinc metallurgists[11] up to that time. For many years they had noted that zinc ferrite formation became more prevalent as the zinc roasting temperatures were increased above 650°-700° C. On the other hand, if temperatures were not sufficiently high for complete oxidation, zinc losses would be encountered by retention of sulfuric acid insoluble zinc sulfide in the calcine.

More recently, a different approach has been made to the problem of roasting on the basis that zinc ferrite can be decomposed by high temperature. A paper presented by Roggero[12] at the February 1962 meeting of the AIME describes the new process. In this process, the roasting temperature of the fluid-bed roaster was increased from 951° C to 1147° C and the over-all zinc extraction was increased by 2 to 3 percent. However, to obtain the higher temperatures, the feed of excess air into the roaster had to be reduced from 73 to 21 percent thus changing the atmospheric conditions. Because of this unfortunate set of circumstances it was impossible to determine whether the higher temperatures produced decomposition of portions of the zinc ferrite or whether the changes in atmospheric conditions caused the decomposition.

The present investigation was undertaken to determine the source of foregoing contradictions by studying the ZnO-Fe_2O_3-Fe_3O_4 system and its thermodynamic properties at elevated temperatures.

---

[10] Ibid.

[11] O. C. Ralston, "Electrolytic Deposition and Hydrometallurgy of Zinc" McGraw-Hill Book Co., New York, New York (1921), p. 5.
D. W. Hopkins, J. Electrochem. Soc., Vol. 96, p. 195 (1949).

[12] C. E. Roggero, Trans. Met. Soc. AIME, Vol. 227, p. 105 (1963).

CHAPTER III

EXPERIMENTAL TECHNIQUE

DESCRIPTION OF APPARATUS AND MATERIALS

Apparatus. The equilibrium apparatus used in this investigation is shown schematically in Figure 1 and photographically in Figure 2.

Furnace and reaction chamber. The furnace was of the three-bar silicon-carbide resistance type and was controlled by a Leeds and Northrup mechanical type controller. The controller was sensitive to temperature changes of $\pm 1^{\circ}$ C, and regulated temperature to within $\pm 2^{\circ}$ C. A 6-inch heat zone in which the thermal gradient was only 3° C was established within the mullite reaction chamber. The maximum error at the temperatures of the experiments was $\pm 5^{\circ}$ C.

The Pt-Pt 13 percent Rh thermocouple used for the temperature measurements was standardized against a National Bureau of Standards thermocouple that had been calibrated at the zinc, aluminum, and copper points. The temperature measurements were taken on a Leeds and Northrup potentiometer capable of detecting temperature changes of $\pm 0.5^{\circ}$ C.

The sample crucibles were fabricated from 0.001-inch Pt and were capable of holding from 3 to 5 grams of sample. By placing the crucibles into two connected Pt boats capable of holding 6 crucibles, a complete series of specimens could be heated at one time under the same conditions of temperature and oxygen pressure. A Pt wire was attached to the boats to allow samples to be quickly moved from the hot zone into a copper heat-sink.

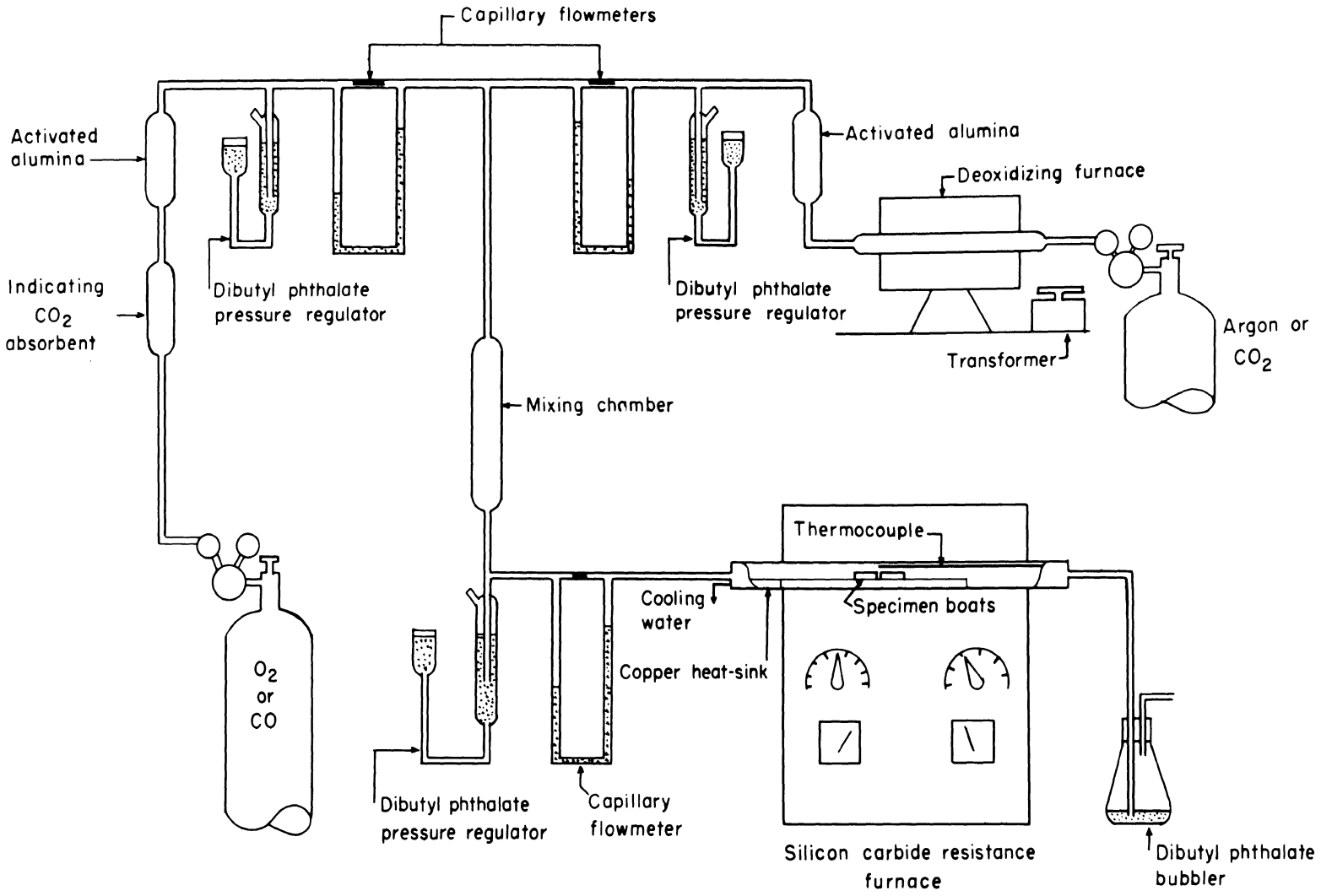

FIGURE 1. - Schematic Diagram of Equilibrium Apparatus.

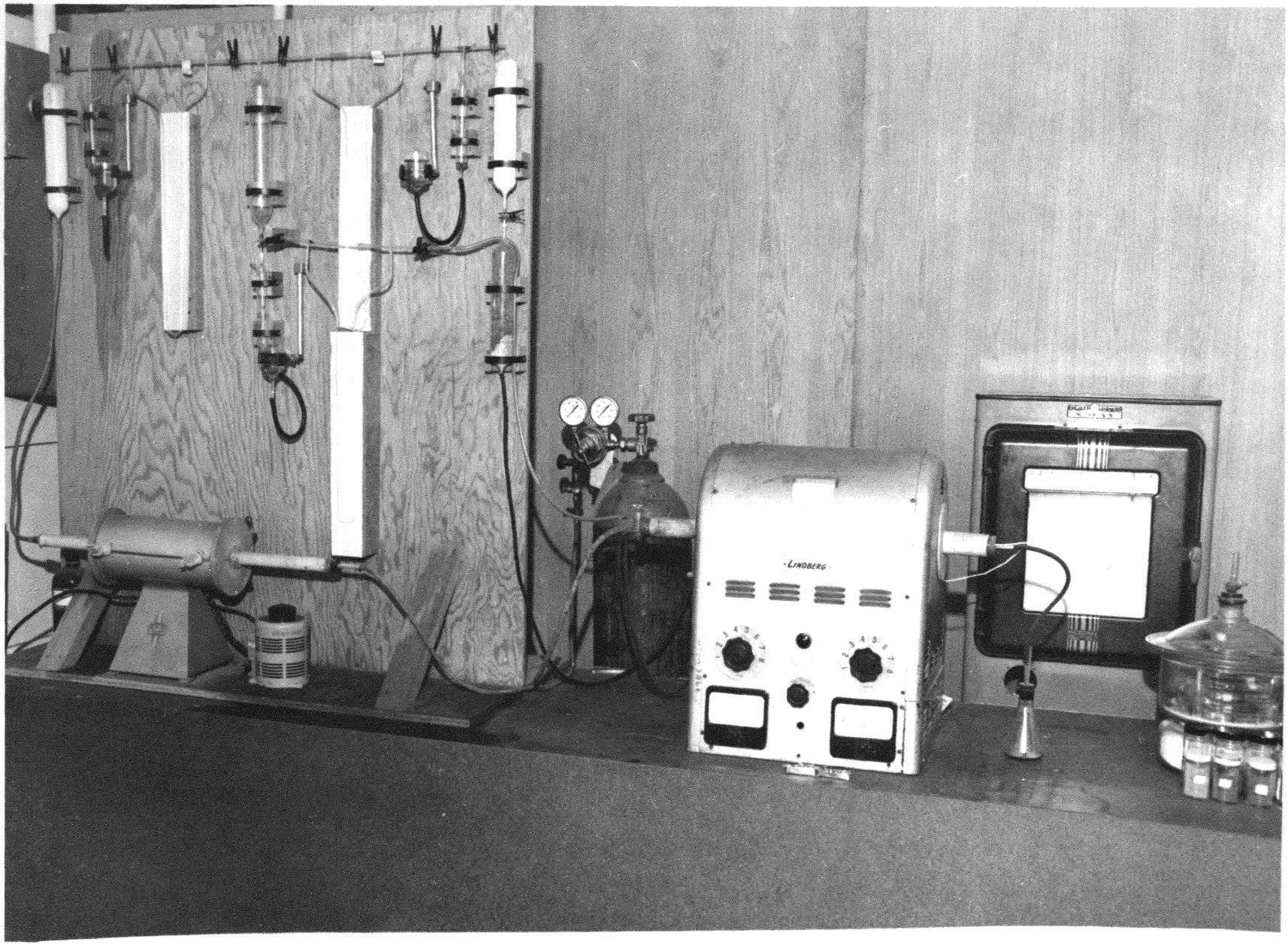

FIGURE 2. - Photograph of Equilibrium Apparatus.

The copper heat-sink was used in place of a water quench to eliminate the possibility of sample-water reactions that might alter the structure and composition of samples at elevated temperatures.

Control of atmosphere. The desired oxygen pressure for the reaction chamber was attained by using mixtures of O_2-A or CO_2-CO. The purity of the gases, as stated by the manufacturer, was:

Gas	Purity, mole percent
Argon	99.99
Oxygen	99.9
Carbon dioxide	99.9
Carbon monoxide	99.8

With the exception of the 10 percent O_2-90 percent A composition, all O_2-A mixtures were from cylinders containing commercially mixed and analyzed gases. The 10 percent O_2-90 percent A mixture and the 91 percent CO_2-9 percent CO mixture were prepared in a gas-mixing train similar to that described by Darken and Gurry[1] (see Figs. 1 and 2). Before the gases entered the mixing unit, they were treated by one of the following processes: The argon and the carbon dioxide were passed through a deoxidizing furnace filled with copper gauze at 650° C and then through an activated alumina-type drying agent; the oxygen and the carbon monoxide were passed through a CO_2 absorber and then through the drying agent.

After these purification steps, the gases were forced through their respective orifices and into the mixing chamber. The gas

---

[1] L. S. Darken and R. W. Gurry, J. Amer. Chem. Soc., Vol. 67, p. 1398 (1945)

mixture forced through another orifice and into the reaction chamber. Once through the reaction chamber the gas was vented to the atmosphere through a low-vapor-pressure oil bubbler that prevented atmospheric oxygen from back diffusing into the reaction chamber. The exhaust gases were collected and were analyzed on an Orsat gas analyzer.

Equilibration and quenching procedure. A series of five or six charges, each weighing 3 to 5 grams, were packed firmly into Pt crucibles, the crucibles were placed in Pt boats, and the boats were positioned in the preheated reaction zone of the tube furnace. The furnace was then sealed, and the reaction chamber was flushed with a rapid flow of premixed gas. The gas flow was then reduced to between 0.5 and 1.0 cm^3/sec., and the samples were allowed to come to equilibrium with the atmosphere.

The equilibration times used in the investigation were 72, 24, and 12 hours at 1100, 1300, and 1400° C, respectively. These times are slightly longer than those used by Yamaguchi and Takei[4] in their investigation.

Once equilibrium time had been reached, the charges were quickly pulled into the heat-sink to cool.

Several charges of $ZnFe_2O_4$ plus Fe_2O_3 were sintered in 1.0 atmosphere of oxygen at 1400° C to determine whether quenching was sufficient to minimize reoxidation of the thermally decomposed Fe_2O_3. After the charges had reached equilibrium with the atmosphere, they

---

[4]T. Yamaguchi and T. Takei. Sci. Papers Inst. Phy. Chem. Research, Tokyo, Vol. 53, p. 207 (1959).

were pulled into the heat-sink and allowed to cool in the oxygen atmosphere. The charges were then polished and examined for evidence of reoxidation. A comparison of the surface versus the interior condition of the pellet is shown in Figure 3. Although the surface layer did show some signs of reoxidation, the amount was small in comparison to the total amount of sample. The oxidation apparently took place along certain directions in each grain as shown in Figure 4. The white constituent is the Fe_2O_3, the gray is the ferrite, and voids are black. This same directional reoxidation was noted by Greig, Posnjak, Merwin, and Sosman[5], in their work on the Fe_2O_3-Fe_3O_4 system. As a further indication of sufficient cooling rates, substantial amounts of FeO were retained to room temperature in the samples of the CO_2-CO experiments. FeO generally decomposes below 560°C unless it is cooled quite rapidly thus any retentions of FeO to room temperature would indicate rapid cooling.

In an effort to further reduce reoxidation, pure argon was flushed through the reaction chamber during the sample cooling period.

Materials. In order to form the starting $ZnFe_2O_4$ equal molar portions of analytical-grade ZnO and Fe_2O_3 were mixed in a wet-blender for 8 hours, filtered, and dried in a drying oven at 110°C. The mixture was then sintered in 1 atmosphere of oxygen for 96 hours at 1150° C and allowed to furnace cool under the same atmospheric conditions. The mixing and sintering times used for the experimental materials were

---

[5]Greig, Posnjak, Merwin, and Sosman. Amer. J. Sci., Vol. 30, p. 293, (1935).

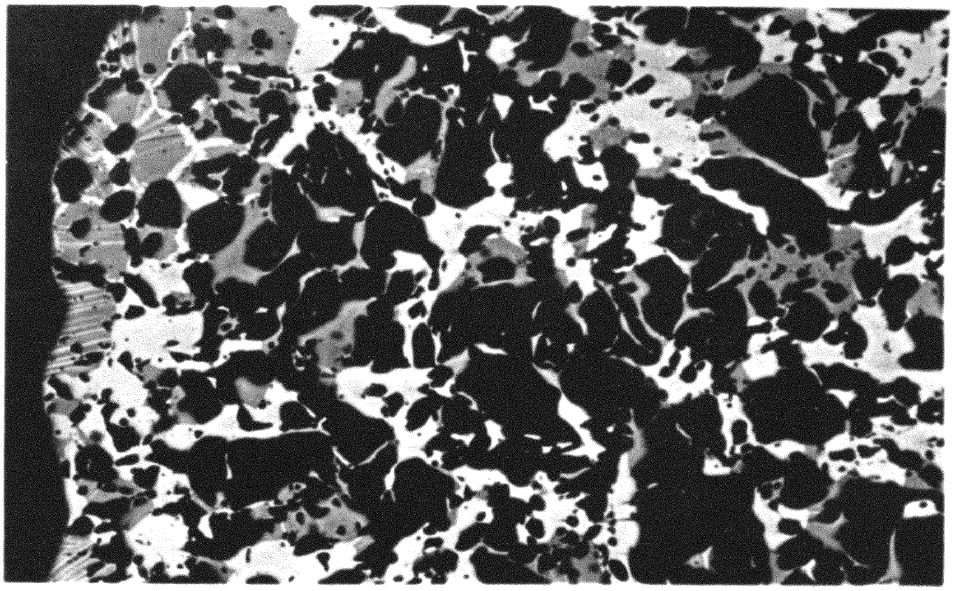

FIGURE 3. - Surface and Interior of Reoxidized Sample, Mechanically Polished, Unetched, X100.

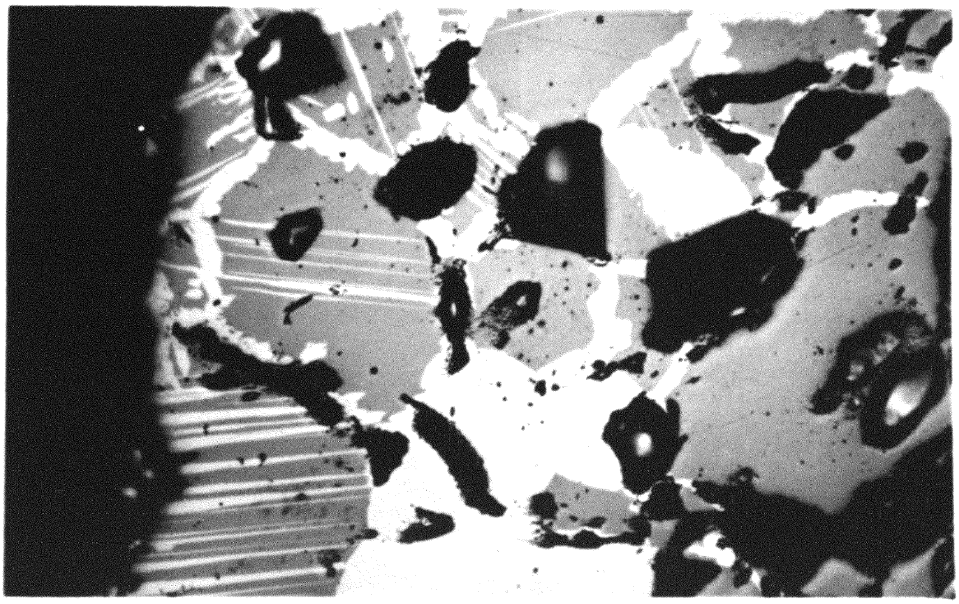

FIGURE 4. - Surface of Reoxidized Sample, Mechanically Polished, Unetched, X500.

much longer than those used in the manufacture of commercial ferrites[6] to insure a homogeneous starting material. The product analyzed in weight percent: $ZnFe_2O_4$, 99.6; free ZnO, 0.2; and Fe_3O_4, 0.2.

The starting material was then ground to minus 200 mesh (less than 74 microns) and was mixed in a wet-blender with excess ZnO or Fe_2O_3 to the proportions shown in Table 1.

The Fe_3O_4 used in the reversal reactions was made by decomposing a portion of the analytical grade Fe_2O_3 according to the reaction

$$6Fe_2O_3 \rightleftharpoons 4Fe_3O_4 + O_2 \qquad (3\text{-}1)$$

This reaction was accomplished at 1400°C in a continuous flow of He. Analysis of the end product showed the material to be, in weight percent: Fe_3O_4, 91.2; Fe_2O_3, 8.8. This material was then dry-mixed with ZnO to the proportions shown in Table 1.

CHEMICAL ANALYSIS AND PHASE IDENTIFICATION

Chemical Analysis

Magnetite. Determination of the ferrous ion was by an analytical method developed for ferrites and chromites by J. R. Wells, Supervisory Chemist, Bureau of Mines, Metallurgy Research Center, Rolla, Missouri. A description of this method is currently being prepared for publication so only a brief summary of the procedure will be given here.

A small portion of the sample (0.5 to 1.0 gram) is dissolved in a boiling solution of four parts concentrated H_3PO_4 to one part H_2SO_4. The ferrous ion reacts with the H_2SO_4 to form SO_2. An atmosphere of

---

[6] J. E. Pippin and C. L. Hogan. The Preparation of Polycrystalline Ferrites for Microwave Applications. ASTIA Document No. AD 117295.

TABLE I

COMPOSITION OF STARTING MATERIAL

Material Sample Designation	Sample Composition					
	Weight Percent			Mole Percent		
	ZnO	Fe_2O_3	Fe_3O_4	ZnO	Fe_2O_3	Fe_2O_3 Eq.-Fe_3O_4
30	54.32	45.68	--	70.00	30.00	--
30R	55.09	--	44.91	70.00	--	30.00
50	33.76	66.24	--	50.00	50.00	--
55	29.42	70.58	--	45.00	55.00	--
60	25.36	74.64	--	40.00	60.00	--
70	17.92	82.08	--	30.00	70.00	--
70R	18.38	--	81.62	30.00		70.00
80	11.30	88.70	--	20.00	80.00	--
90	5.36	94.64	--	10.00	90.00	--

CO_2 covers the sample and carries the SO_2 over into a solution of $K_2Cr_2O_7$. The SO_2 reduces an equivalent amount of $K_2Cr_2O_7$. This solution is then mixed with a KI solution, and the unreduced $K_2Cr_2O_7$ reacts to release free I. The free I is then titrated with a $Na_2S_2O_3$ solution.

The method has been calibrated with U. S. Bureau of Standards samples containing ferrous ion as well as with samples in which ferrous ion has been determined by other methods. In all cases the method agreed to within $\pm$0.3 percent of the ferrous ion calculated as Fe_3O_4 for a 0.5 to 1.0 gram sample.

Free zinc oxide. Free zinc oxide was determined by leaching a 0.5 gram sample with 50 ml of solution containing 100 grams of NH_4Cl and 100 ml of concentrated NH_4OH per 1000 ml of H_2O.

The sample was filtered and after driving off the excess NH_3 and diluting to 200 ml, the filtrate was titrated with a $K_4Fe(CN)_6$ solution. $K_3Fe(CN)_6$ and diphenylbenzidine solution was used as the indicator.

The error of the analysis was found to be $\pm$0.2 percent of the amount present.

Total zinc. Total zinc was determined by fluorescent analysis.[7] A 0.25 gram sample was dissolved in 2500 grams of fused borax by heating to 1000° C in a platinum crucible. The fused borax sample was then poured into buttons on an aluminum plate heated to 450° C. The buttons were made to fluoresce; the intensity was measured at a

---

[7]F. Claisse. Norelco Reporter, Vol. 4, No. 1, p. 3 (1957).

predetermined peak, and this intensity was compared to a standard curve.

The percent of total zinc reported was accurate to within ±0.5 percent.

Total iron. The total iron was determined in the same manner as the total zinc, using the same borax buttons.

The percent of total iron reported was accurate to within ±0.5 percent.

Phase identifications. The phases present in the samples were identified by X-ray diffraction and reflected-light microscopy. The X-ray diffraction was carried out with Cobalt Kα radiation.

CHAPTER IV

EXPERIMENTAL RESULTS

The experimental results of this investigation are presented in two parts to facilitate tabulation. The first of these deals with the chemical composition of charges brought to equilibrium in the various oxygen atmospheres. The second contains the lattice parameter measurements of a selected group of these materials.

Chemical composition of samples. The chemical composition of the samples is given in Table II and is plotted on ternary diagrams in Figures 5, 6, and 7. Frequently, several samples would have approximately the same composition therefore not all of these compositions were plotted on the figures. The composition, given in mole percent ZnO, Fe_2O_3 and Fe_3O_4, was calculated from the percentage of total Fe, total Zn, Fe_3O_4 and free ZnO. Because chemical analysis was more accurate in the region of low Fe_3O_4 content, the results given in Table II are reported to the tenth of a percent. However very little significance can be affixed to this tenth-percent figure at higher Fe_3O_4 contents. When the mole-percents of the ZnO, Fe_2O_3, and Fe_3O_4 were summed, they were found to be 100 ± 3 percent. The variance in this case was probably caused by the errors in the analyses.

The lines of constant oxygen pressure or potential,[1] shown in Figures 5, 6, and 7, represent the compositions that would exist in equilibrium with the oxygen potential of the atmosphere. These lines

---

[1]Throughout this investigation the activity of the oxygen was assumed equal to the square-root of its pressure and that oxygen behaves as an ideal gas.

TABLE II

RESULTS OF EQUILIBRATION EXPERIMENTS AT VARIOUS OXYGEN PRESSURES AND TEMPERATURES

Sample Designation	Composition of Starting Materials, Mole Percent			Temperature °C	Oxygen Pressure Atmospheres	Final Composition, Mole Percent		
	ZnO	Fe_2O_3	Fe_2O_3 Equivalent For Fe_3O_4			ZnO	Fe_2O_3	Fe_3O_4
1-1-30	70.0	30.0		1,100	0.1	49.7	50.2	0.1
1-1-50	50.0	50.0		1,100	0.1	50.0	49.8	0.2
1-1-55	45.0	55.0		1,100	0.1	46.2	48.0	5.8
1-1-60	40.0	60.0		1,100	0.1	41.4	51.1	7.5
1-1-70	30.0	70.0		1,100	0.1	30.8	63.1	6.1
1-1-30R	70.0		30.0	1,100	0.1	49.7	49.6	0.7
1-1-70R	30.0		70.0	1,100	0.1	30.6	64.0	5.4
1-2-30	70.0	30.0		1,100	0.01	50.5	48.9	0.6
1-2-50	50.0	50.0		1,100	0.01	51.1	48.6	0.3
1-2-55	45.0	55.0		1,100	0.01	48.3	45.5	6.2
1-2-60	40.0	60.0		1,100	0.01	42.2	45.5	12.3
1-2-70	30.0	70.0		1,100	0.01	31.7	56.0	12.3
1-2-30R	70.0		30.0	1,100	0.01	50.4	48.8	0.8
1-2-70R	30.0		70.0	1,100	0.01	31.7	55.0	13.3
1-3-30	70.0	30.0		1,100	0.001	50.4	48.5	1.1
1-3-50	50.0	50.0		1,100	0.001	49.5	49.6	0.9
1-3-60	40.0	60.0		1,100	0.001	42.5	43.5	14.0
1-3-70	30.0	70.0		1,100	0.001	33.3	44.1	22.6
1-3-80	20.0	80.0		1,100	0.001	22.4	51.4	26.2
1-3-90	10.0	90.0		1,100	0.001	10.6	76.1	13.3
1-4-30	70.0	30.0		1,100	0.0001	49.5	49.2	1.3
1-4-50	50.0	50.0		1,100	0.0001	49.0	49.8	1.2
1-4-55	45.0	55.0		1,100	0.0001	46.4	46.7	6.9
1-4-60	40.0	60.0		1,100	0.0001	42.5	43.4	14.1
1-4-70	30.0	70.0		1,100	0.0001	34.0	36.5	29.5

TABLE II
(continued)

Sample Designation	Composition of Starting Materials, Mole Percent ZnO	Fe_2O_3	Fe_2O_3 Equivalent For Fe_3O_4	Temperature °C	Oxygen Pressure Atmospheres	Final Composition, Mole Percent ZnO	Fe_2O_3	Fe_3O_4
1-4-90	10.0	90.0		1,100	0.0001	12.3	36.8	50.9
1-5-30	70.0	30.0		1,100	0.00001	50.0	48.0	2.0
1-5-70	30.0	70.0		1,100	0.00001	33.8	37.8	28.4
1-5-30R	70.0		30.0	1,100	0.00001	50.1	48.6	1.3
1-5-70R	30.0		70.0	1,100	0.00001	34.0	36.8	29.8
2-0-30	70.0	30.0		1,300	1.0	49.7	49.5	0.8
2-0-50	50.0	50.0		1,300	1.0	49.1	50.3	0.6
2-0-60	40.0	60.0		1,300	1.0	41.9	45.3	12.8
2-0-70	30.0	70.0		1,300	1.0	32.9	45.8	21.3
2-0-80	20.0	80.0		1,300	1.0	22.4	62.8	14.8
2-0-90	10.0	90.0		1,300	1.0	10.8	82.1	7.1
2-0-30R	70.0		30.0	1,300	1.0	49.6	49.3	1.1
2-0-70R	30.0		70.0	1,300	1.0	31.7	52.9	15.4
2-1-30	70.0	30.0		1,300	0.1	50.1	48.6	1.3
2-1-50	50.0	50.0		1,300	0.1	50.4	47.8	1.8
2-1-60	40.0	60.0		1,300	0.1	42.4	45.0	12.6
2-1-70	30.0	70.0		1,300	0.1	33.5	40.3	26.2
2-1-80	20.0	80.0		1,300	0.1	22.5	49.5	28.0
2-1-90	10.0	90.0		1,300	0.1	11.0	65.8	23.2
2-2-30	70.0	30.0		1,300	0.01	49.6	48.6	1.8
2-2-50	50.0	50.0		1,300	0.01	50.4	48.1	1.5
2-2-60	40.0	60.0		1,300	0.01	43.0	44.1	12.9
2-2-70	30.0	70.0		1,300	0.01	35.3	35.4	29.3
2-2-90	10.0	90.0		1,300	0.01	14.3	19.8	65.9
2-2-30	70.0		30.0	1,300	0.01	49.2	48.0	2.8
2-2-70	30.0		70.0	1,300	0.01	33.7	36.9	29.5
2-3-30	70.0	30.0		1,300	0.001	49.2	46.4	4.4

TABLE II
(continued)

Sample Designation	Composition of Starting Materials, Mole Percent ZnO	Fe_2O_3	Fe_2O_3 Equivalent For Fe_3O_4	Temperature °C	Oxygen Pressure Atmospheres	Final Composition, Mole Percent ZnO	Fe_2O_3	Fe_3O_4
2-3-50	50.0	50.0		1,300	0.001	50.9	45.3	3.8
2-3-60	40.0	60.0		1,300	0.001	42.1	46.1	11.8
2-3-70	30.0	70.0		1,300	0.001	33.9	37.4	28.7
2-3-90	10.0	90.0		1,300	0.001	13.1	17.4	69.5
2-4-30	70.0	30.0		1,300	0.0001	49.4	45.0	5.6
2-4-50	50.0	50.0		1,300	0.0001	48.9	45.9	5.2
2-4-55	45.0	55.0		1,300	0.0001	45.2	46.3	8.5
2-4-60	40.0	60.0		1,300	0.0001	42.1	43.3	14.6
2-4-90	10.0	90.0		1,300	0.0001	15.9	16.1	68.0
2-5-30	70.0	30.0		1,300	0.00001	49.5	42.5	8.0
2-5-70	30.0	70.0		1,300	0.00001	33.9	37.2	28.9
2-5-30R	70.0		30.0	1,300	0.00001	49.5	42.3	8.2
2-5-70R	30.0		70.0	1,300	0.00001	34.7	29.8	35.5
3-0-30	70.0	30.0		1,400	1.0	46.9	50.7	2.4
3-0-50	50.0	50.0		1,400	1.0	50.0	48.7	1.3
3-0-60	40.0	60.0		1,400	1.0	42.6	43.3	14.1
3-0-70	30.0	70.0		1,400	1.0	33.8	38.2	28.0
3-0-90	10.0	90.0		1,400	1.0	11.2	62.5	26.3
3-0-30R	70.0		30.0	1,400	1.0	47.7	50.7	1.6
3-0-70R	30.0		70.0	1,400	1.0	32.2	49.9	17.9
3-1-30	70.0	30.0		1,400	0.1	48.0	49.6	2.4
3-1-50	50.0	50.0		1,400	0.1	50.5	47.3	2.2
3-1-60	40.0	60.0		1,400	0.1	41.7	44.1	14.2
3-1-70	30.0	70.0		1,400	0.1	34.0	36.2	29.8
3-1-90	10.0	90.0		1,400	0.1	14.2	24.4	61.4
3-2-30	70.0	30.0		1,400	0.1	48.0	47.9	4.1

TABLE II
(continued)

Sample Designation	Composition of Starting Materials, Mole Percent ZnO	Fe_2O_3	Fe_2O_3 Equivalent For Fe_3O_4	Temperature °C	Oxygen Pressure Atmospheres	Final Composition, Mole Percent ZnO	Fe_2O_3	Fe_3O_4
3-2-50	50.0	50.0		1,400	0.01	51.1	45.1	3.8
3-2-60	40.0	60.0		1,400	0.01	42.1	41.9	16.0
3-2-70	30.0	70.0		1,400	0.01	34.1	33.6	32.3
3-2-90	10.0	90.0		1,400	0.01	13.3	19.4	67.3
3-2-30R	70.0		30.0	1,400	0.01	47.8	47.4	4.8
3-2-70R	30.0		70.0	1,400	0.01	35.0	28.2	36.8
3-3-30	70.0	30.0		1,400	0.001	47.7	44.3	8.0
3-3-50	50.0	50.0		1,400	0.001	51.5	42.0	6.5
3-3-60	40.0	60.0		1,400	0.001	41.9	43.3	14.8
3-3-70	30.0	70.0		1,400	0.001	33.6	33.9	32.5
3-3-90	10.0	90.0		1,400	0.001	13.8	14.2	72.0
3-4-30	70.0	30.0		1,400	0.0001	45.5	39.8	14.7
3-4-50	50.0	50.0		1,400	0.0001	52.2	37.9	9.9
3-4-55	45.0	55.0		1,400	0.0001	47.3	41.0	11.7
3-4-60	40.0	60.0		1,400	0.0001	42.6	42.5	15.1
3-4-70	30.0	70.0		1,400	0.0001	35.8	32.3	31.9
3-4-90	10.0	90.0		1,400	0.0001	20.1	18.2	61.7
3-5-30	70.0	30.0		1,400	0.00001	47.9	41.2	10.9
3-5-70	30.0	70.0		1,400	0.00001	34.1	35.8	30.1
3-5-30R	70.0		30.0	1,400	0.00001	47.7	44.2	8.1
3-5-70R	30.0		70.0	1,400	0.00001	34.0	35.7	30.3

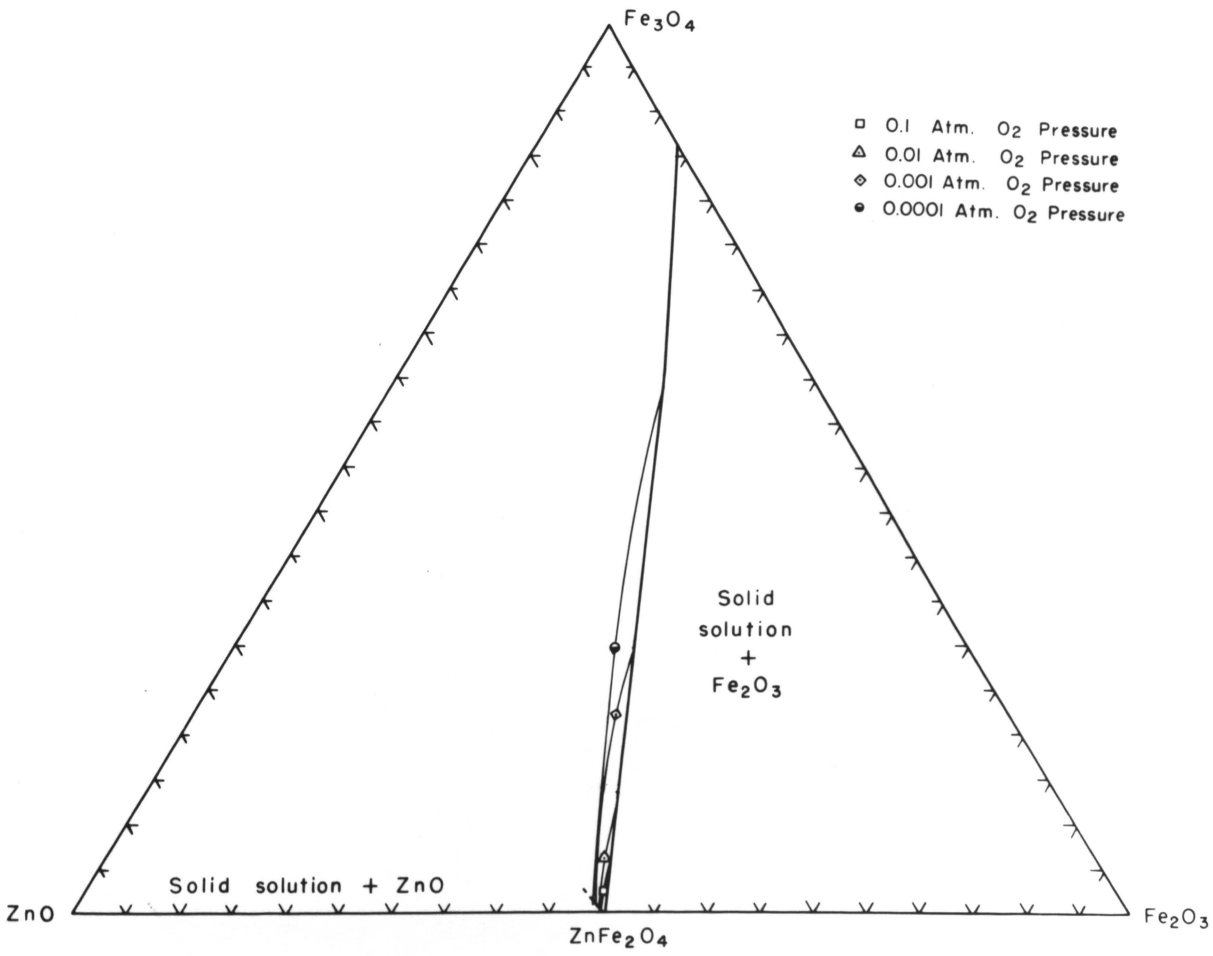

FIGURE 5. - Iso-thermal Section of the ZnO-Fe_2O_3-Fe_3O_4 System at 1,100° C Showing the Iso-activity of Oxygen Lines.

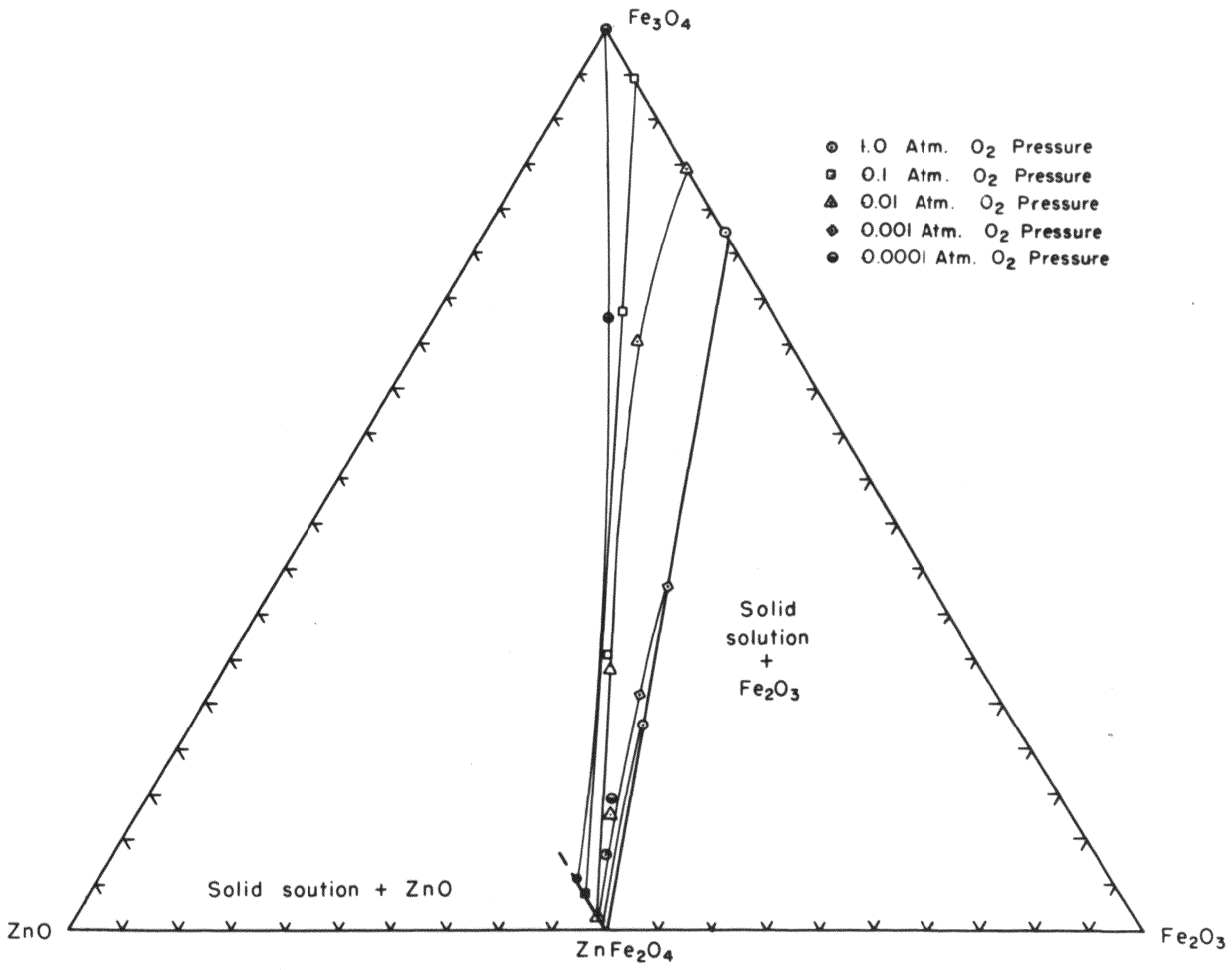

FIGURE 6. - Iso-thermal Section of the ZnO-Fe_2O_3-Fe_3O_4 System at 1,300° C Showing the Iso-activity of Oxygen Lines.

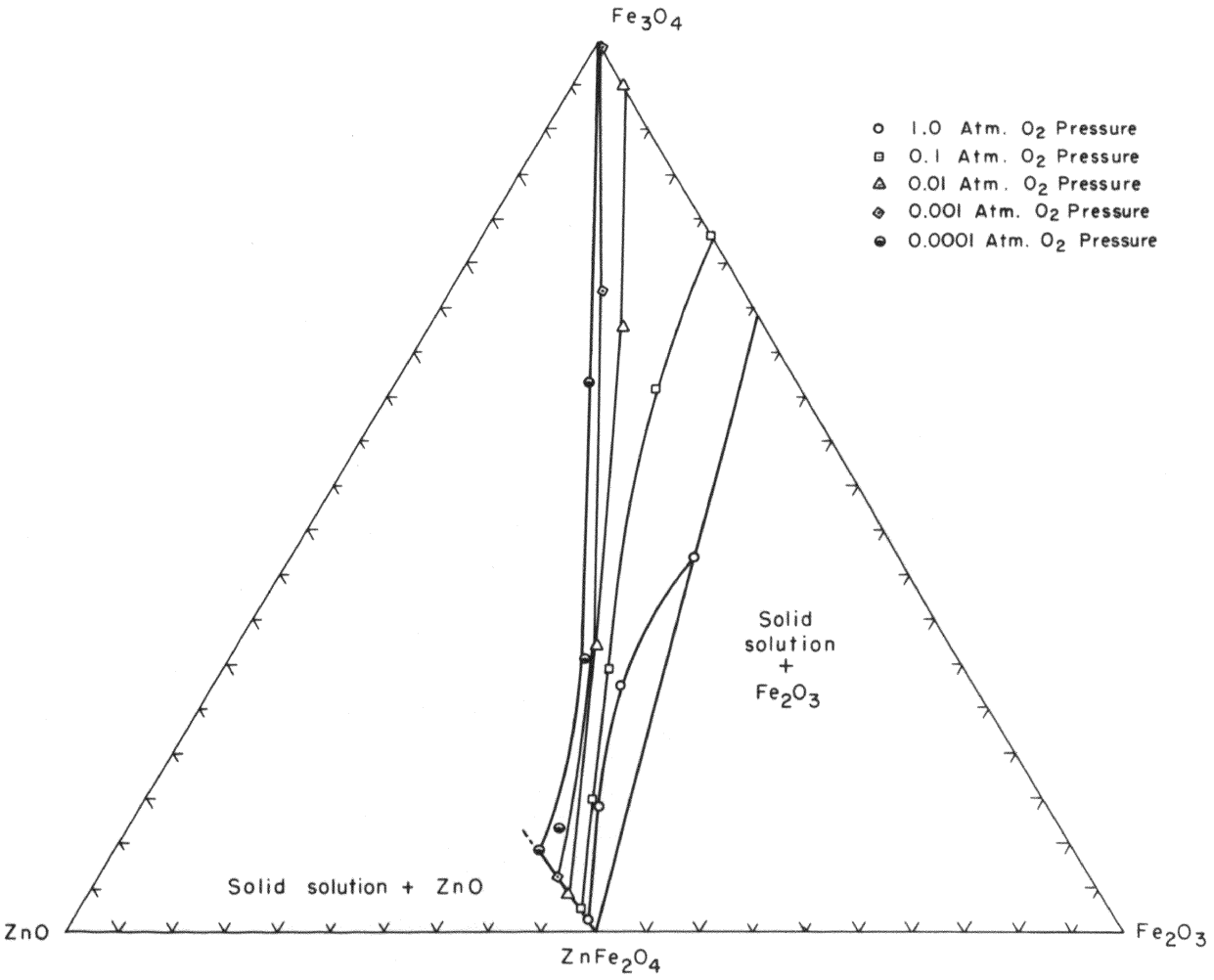

FIGURE 7. - Iso-thermal Section of the ZnO-Fe_2O_3-Fe_3O_4 System at 1,400° C Showing the Iso-activity of Oxygen Lines.

were derived from the groups of charges which were sintered under the same conditions of temperature and oxygen pressure. The compositions and respective oxygen pressures for the Fe_2O_3-Fe_3O_4 binary system were taken from the work of Darken and Gurry.[2]

The boundary lines between the solid solution region and the solid solution plus ZnO region were determined by subtracting the free ZnO from the total ZnO. Unfortunately, the boundary between the solid solution region and the solid solution plus Fe_2O_3 could not be determined in a similar manner because there is no known analytical method of distinguishing between the free Fe_2O_3 and the Fe_2O_3 in the solid solution. In this case X-ray analysis and graphical methods were employed to establish the boundary. The graphical method was the same as that of Yamaguchi and Takei[3] and was achieved by plotting the ratio of the weight-percent Fe_3O_4 to the original weight-percent of Fe_2O_3 versus the mole-percent Fe_2O_3 in the original charge. The ratio of Fe_3O_4 to original Fe_2O_3 is sometimes referred to as the degree of dissociation and is shown schematically in Figure 8 for a number of oxygen pressures at 1300°C. The straight line portions of the curves represent the two phase regions. Those on the right, which pass through the abcissa at pure Fe_2O_3, represent the Fe_2O_3 plus solid solution region. In this region, as the amount of Fe_2O_3 in the original material is increased beyond the limits of solubility for

---

[2] L. S. Darken and R. W. Gurry. J. Amer. Chem. Soc., Vol. 68, p. 798 (1959).

[3] T. Yamaguchi and T. Takei. Sci. Papers Inst. Phys. Chem. Research, Tokyo, Vol. 53, p. 207 (1959).

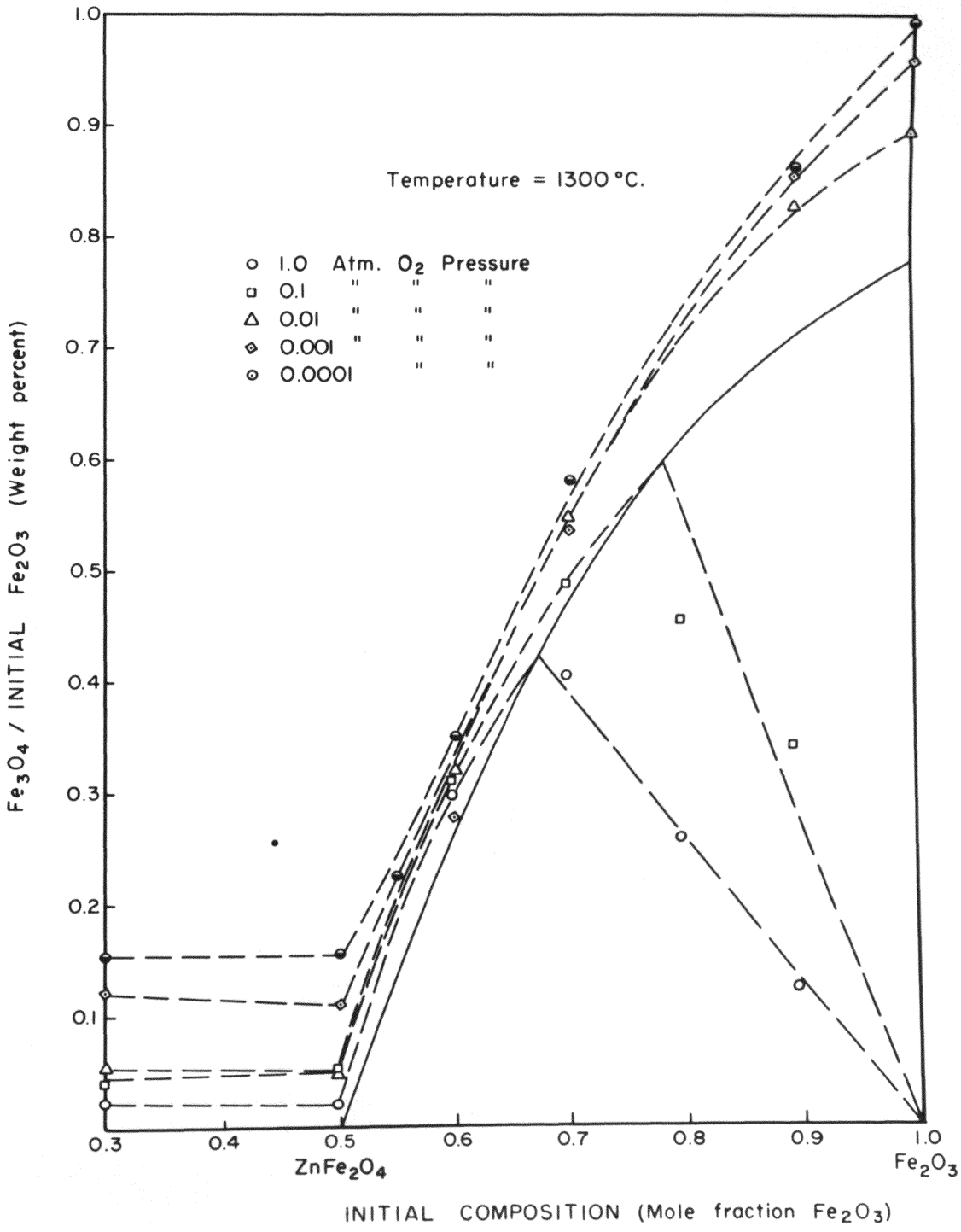

FIGURE 8. - Degree of Dissociation as a Function of Initial Composition.

Fe_2O_3, the degree of dissociation decreases proportionately. The straight line portions on the left hand side of the diagram represent the two-phase region of solid solution plus ZnO. It can be noted from the figure that, in most cases, the degree of dissociation was greater for charges having excess ZnO, indicating that excess ZnO promoted the decomposition of Fe_2O_3. This was even more evident at 1400°C where the degree of dissociation of the 0.3, Fe_2O_3 (degree of dissociation = .208) was as much as 11 percent greater than that of the 0.5 Fe_2O_3 (degree of dissociation = .187). Upon X-ray examination, it was found that the hexagonal ZnO structure increased as much as 3 percent in the C-direction, suggesting that ZnO is able to take some ferrous ion into its structure. This indicates that some solid solubility would be encountered in the binary diagram of ZnO-FeO. No change was noted in the A-direction of the ZnO structure.

Between these two straight line portions exists a single-phase solid solution region in which the degree of dissociation increases as the amount of original Fe_2O_3 is increased. The boundary of the single-phase region was determined by the intersection of the single-phase curve and the solid solution plus Fe_2O_3 curve.

The number of phases present in the samples were also determined by X-ray analysis and, in certain cases, reflected-light microscopy.

The results of the CO_2-CO mixtures were not included in Figures 5, 6, 7, or 8 or in the tables. Apparently the atmosphere in these experiments reduced a portion of the ZnO to Zn vapor that was then transported into a cooler portion of the reaction chamber and reoxidized to ZnO.

Experiments with 0.00001 atmosphere of oxygen were included only to determine reversibility at the low oxygen pressure.

X-ray analysis. In Figure 7 the lines of constant oxygen pressure tend to cluster in the area of 34 percent Fe_3O_4, 33 percent ZnO and 33 percent Fe_2O_3. This suggested the possibility of compound formation in this area and a study of the change in the cubic lattice parameter with composition was undertaken to determine whether the structure changed significantly in the area of clustering. The specimens chosen for this study were taken from the pseudo-binary system between $ZnFe_2O_4$ and Fe_3O_4. Two other groups of specimens were also studied to determined the effect that excesses of Fe_2O_3 or ZnO had on the spinel structure. The specimens chosen for the excess Fe_2O_3 study were taken from a system between $ZnFe_2O_4$ and the 18 percent Fe_2O_3 - 82 percent Fe_3O_4 point in the Fe_2O_3 - Fe_3O_4 binary system. The excess ZnO study was taken from a system between $ZnFe_2O_4$ and the 61 percent ZnO - 39 percent Fe_3O_4 point in the ZnO - Fe_3O_4 binary system. Table III gives the results of the study, and Figure 9 graphically portrays the data.

The best estimate of the lattice parameter was obtained by utilizing the 6 highest-angle diffraction lines. The angles of these diffraction lines were measured with the Straumanis technique and the lattice parameter was calculated for each diffraction line. A curve of lattice parameter versus the Nelson-Riley function was plotted for each specimen and the curve extrapolated to 90° to obtain the best estimate of the lattice parameter. Because the experiment was primarily concerned with the change in lattice parameter, the

TABLE III

LATTICE PARAMETERS OF SELECTED SAMPLES

Sample Number	Composition Mole Percent ZnO	Fe_2O_3	Fe_3O_4	Fraction Solute	Fraction $ZnFe_2O_4$	Lattice Parameter
3-4-50	52.2	37.9	9.9	.238	.762	8.439A°
50[a]	50.0	50.0			1.000	8.442
3-4-60	42.7	42.0	15.3	.153	.847	8.435
3-3-70	34.4	32.0	32.6	.326	.674	8.426
3-3-90	13.3	14.6	72.1	.721	.279	8.405
100R[b]			100.0	1.000		8.396
3-0-70	33.8	38.2	28.0	.323	.677	8.426
3-1-90	12.7	27.4	59.9	.748	.252	8.402
78R[c]		22.0	78.0	1.000		8.386

[a]Lattice parameter obtained from zinc ferrite starting material.

[b]Basta, Min. Mag., Vol. 31, p. 431 (1957).

[c]J. W. Greig, E. Posnjak, H. E. Merwin, R. B. Sosman. Amer. J. Sci., Vol. 30, p. 239 (1935)

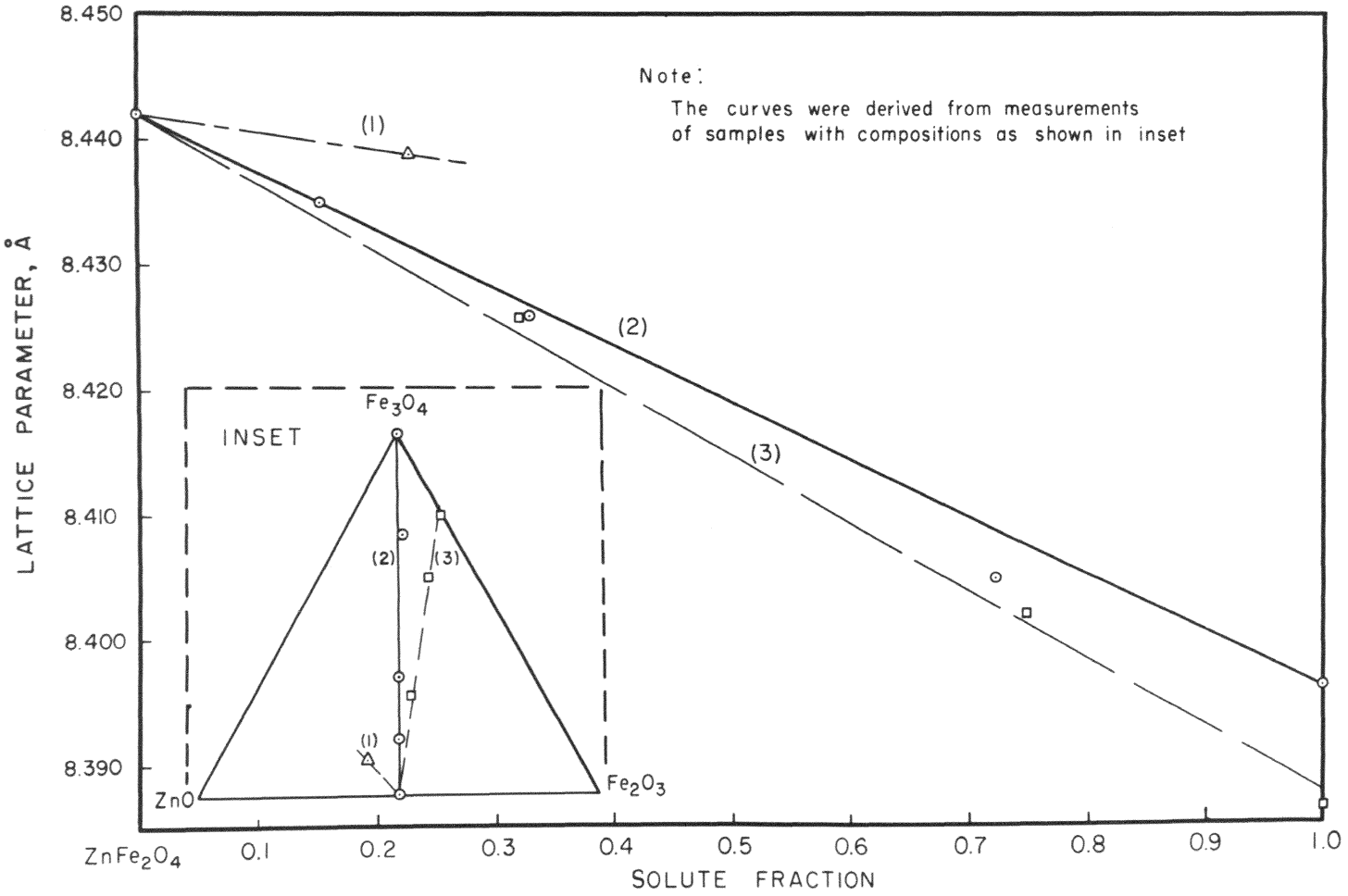

FIGURE 9. - Lattice Parameters of Three Systems in the Spinel Solid Solution Region as a Function of Composition.

accuracy of the extrapolation method was sufficient for this investigation. The lattice parameters for the pure solute in lines 2 and 3 were taken from the literature.

The lattice parameter obtained from extrapolation was then plotted in Figure 9 versus the solute fraction. The solute in this case is defined as that point on the binary system that is intersected by a straight line extending from the $ZnFe_2O_4$ composition through the composition of the specimen. The solute of line 1 probably consists of 2 phases therefore the lattice parameter, as it would exist in this diagram, is imaginary. However it does show how excess ZnO effects the lattice parameter as will be explained later. The solute fraction was calculated using the lever rule.

It can be seen from the figure that the lattice parameter of the $ZnFe_2O_4$ system (line 2) apparently follows Vegards law and agrees with the work of Miyata.[4] On the other hand, the investigation of Popov, Simonova, Vgolnikova and Chufavov[5] indicates a curve composed of two straight lines which deviate positively from Vegards law and intersect at 30 percent Fe_3O_4. This discontinuity in the curve would suggest compound formation in the same manner as the clustering of oxygen lines. However some question can be raised with regard to the compositions of the samples because of the method of preparation. According to their investigation, the samples were made by mechanically mixing ZnO, FeO, and Fe_2O_3 in proportions such that the composition fell on the $ZnFe_2O_4$-

---

[4] N. Miyata. J. Phys. Soc., Vol. 16, p. 1291 (1959).

[5] G. P. Popov, M. I. Simonova, T. A. Vgolnikova, G. I. Chufavov. Dokl. Akad. Nauk SSSR Vol. 148, No. 2 (1963).

Fe_3O_4 pseudo-binary system. These mechanically mixed samples were then sintered, however no mention was made of the sintering conditions. The measured lattice parameters of these samples were plotted versus the composition before sintering. If the composition changed by oxidation or reduction during sintering, then the composition would no longer lie on the pseudo-binary system but would contain an excess (line 3 of inset, Figure 9) or a deficiency (line 1 of inset, Figure 9) of Fe_2O_3. Likewise the lattice would contract (line 3) or expand (line 1) and lead to incorrect results.

Even though this investigation showed no deviations in the area of 30 percent Fe_3O_4 it does not necessarily mean there is no compound in this region. Ordering of the zinc, ferrous and ferric ions could occur within the spinel structure without significant changes in the lattice parameter. This type of ordering would require application of diffraction techniques of greater sensitivity to detect the ordering. Because of the time limitations no further studies were made along these lines.

In addition to the apparent ideality of the lattice parameters of the $ZnFe_2O_4$ system (line 2) it would appear that the system between $ZnFe_2O_4$ and 79 percent Fe_3O_4 - 21 percent Fe_2O_3 follows the same relationship where the point of 78 percent Fe_3O_4 - 22 percent Fe_2O_3 was given in the work of Greig, Posnjak, Merwin and Sosman.[6] This would suggest the possible existence of a linear relationship

---

[6] J. W. Greig, E. Posnjak, H. E. Merwin, and R. B. Sosman. Amer. J. Sci., Vol. 30, series 5, p. 239 (1935).

between the lattice parameter and the solute fraction throughout the entire solid solution region.

CHAPTER V

THERMODYNAMIC CALCULATIONS

Thermodynamic calculations based upon the experimental results reported in the previous chapter are presented in three parts. The first of these deals with the method of calculating thermodynamic activities of two components of a ternary system from the activities of the third. The second part deals with the application of this method to the ZnO-Fe_2O_3-Fe_3O_4 system. The third part utilizes the activities of Fe_3O_4 to calculate the activities of the $ZnFe_2O_4$-Fe_3O_4 system and to apply these activities in the calculation of free energy, enthalpy, and entropies of mixing in the $ZnFe_2O_4$-Fe_3O_4 system.

METHOD OF CALCULATING PARTIAL MOLAR QUANTITIES IN A TERNARY SYSTEM

In the study of multicomponent systems the Gibbs-Duhem equation has become an invaluable tool in calculating partial molar quantities of certain components of a system from the partial molar quantities of the other components. Most of the application of the Gibbs-Duhem equation has been in binary systems; however, since 1950, a number of methods[1-5] have been proposed for calculating the partial molar properties of the two components in a ternary system when those of the

---

[1] L. S. Darken, J. Am. Chem. Soc., Vol. 72, 2909 (1950)

[2] C. Wagner, "Thermodynamics of Alloys", Addison-Wesley Press, p. 19, (1952).

[3] H.A.C. McKay, Nature, Vol. 169, 464 (1952).

[4] R. Schuhmann, Jr., Acta Met., Vol. 3, 219 (1955).

[5] N. A. Gokcen, J. Phys. Chem., Vol. 64, 401 (1960).

third are known. Of these, the method of Schuhmann[6] was the most applicable to this investigation. A brief description of the derivation of this method is given below:

The Gibbs-Duhem equation for a system of three components at constant pressure and temperature may be written

$$n_1 \, d\mu_1 + n_2 \, d\mu_2 + n_3 \, d\mu_3 = 0 \qquad (5\text{-}1)$$

when n_1, n_2, and n_3 represent the moles, and μ_1, μ_2 and μ_3 represent the chemical potentials, or partial molar free energies of the respective components 1, 2, and 3. The chemical potentials or partial molar free energies are defined as

$$\mu_1 = \left[\frac{\partial F}{\partial n_1}\right]_{n_2,n_3} \qquad (5\text{-}2a)$$

$$\mu_2 = \left[\frac{\partial F}{\partial n_2}\right]_{n_1,n_3} \qquad (5\text{-}2b)$$

$$\mu_3 = \left[\frac{\partial F}{\partial n_3}\right]_{n_1,n_2} \qquad (5\text{-}2c)$$

where F is the free energy of the system and is generally a function of temperature, pressure, and composition. In a three component system, however, if the temperature, pressure, and n_3 are held constant, the free energy of the system, as well as the chemical potentials μ_1 and μ_2 become functions of n_1 and n_2. Under these restrictions the partial derivative of μ_1 with respect to n_2 is written

$$\left[\frac{\partial \mu_1}{\partial n_2}\right]_{n_1,n_3} = -\left[\frac{\partial \mu_1}{\partial n_1}\right]_{n_2,n_3} \left[\frac{\partial n_1}{\partial n_2}\right]_{\mu_1,n_3} \qquad (5\text{-}3)$$

In addition, the partial derivation of μ_2 with respect to μ_1 can be expressed as

---

[6] R. Schuhmann, Jr., op. cit., p. 219

$$\left(\frac{\partial \mu_2}{\partial n_1}\right)_{n_2,n_3} = \left(\frac{\partial \mu_2}{\partial \mu_1}\right)_{n_2,n_3} \left(\frac{\partial \mu_1}{\partial n_1}\right)_{n_2,n_3} \qquad (5\text{-}4)$$

Additional equations for $(\partial\mu_1/\partial n_2)_{n_1,n_3}$ and $(\partial\mu_2/\partial n_1)_{n_2,n_3}$ can be derived by differentiating Equation 5-2a with respect to n_2, and, utilizing the principle that the order of differentiation is immaterial, the following expression results:

$$\left(\frac{\partial \mu_1}{\partial n_2}\right)_{n_1,n_3} = \left(\frac{\partial^2 F}{\partial n_1 \partial n_2}\right)_{n_3} = \left(\frac{\partial \mu_2}{\partial n_1}\right)_{n_2,n_3} \qquad (5\text{-}5)$$

Substituting Equations 5-3 and 5-4 in Equation 5-5 gives the following important equation:

$$\left(\frac{\partial \mu_2}{\partial \mu_1}\right)_{n_2,n_3} = \left(\frac{\partial n_1}{\partial n_2}\right)_{\mu_1,n_3} \qquad (5\text{-}6)$$

Equation 5-6 can be integrated through a one-phase field, along a path of constant n_2 and n_3, to obtain the chemical potential of component 2 from that of component 1. A path of constant n_2 and n_3 means a compositional path of constant ratio of n_2/n_3. Such a path follows a straight line that passes through the corner corresponding to component 1 on a composition triangle. The integration of Equation 5-6 can be expressed as

$$\mu_2^{II} = \left[\mu_2^{I} - \int_{\mu_1^{I}}^{\mu_1} \left(\frac{\partial u_1}{\partial n_2}\right)_{\mu_1,n_2} d\mu_1\right]_{n_2/n_3} \qquad (5\text{-}7)$$

in which the path of integration extends from point I to point II in the ternary isotherm as shown in Figure 10. This integration can be carried out to evaluate μ_2^{II} when at the starting point, μ_2^{I} is known and when the experimental data of μ_1 are sufficiently complete that the partial derivative $(\partial n_1/\partial n_2)_{\mu_1,n_3}$ can be evaluated as a function of μ_1 along the entire path of integration.

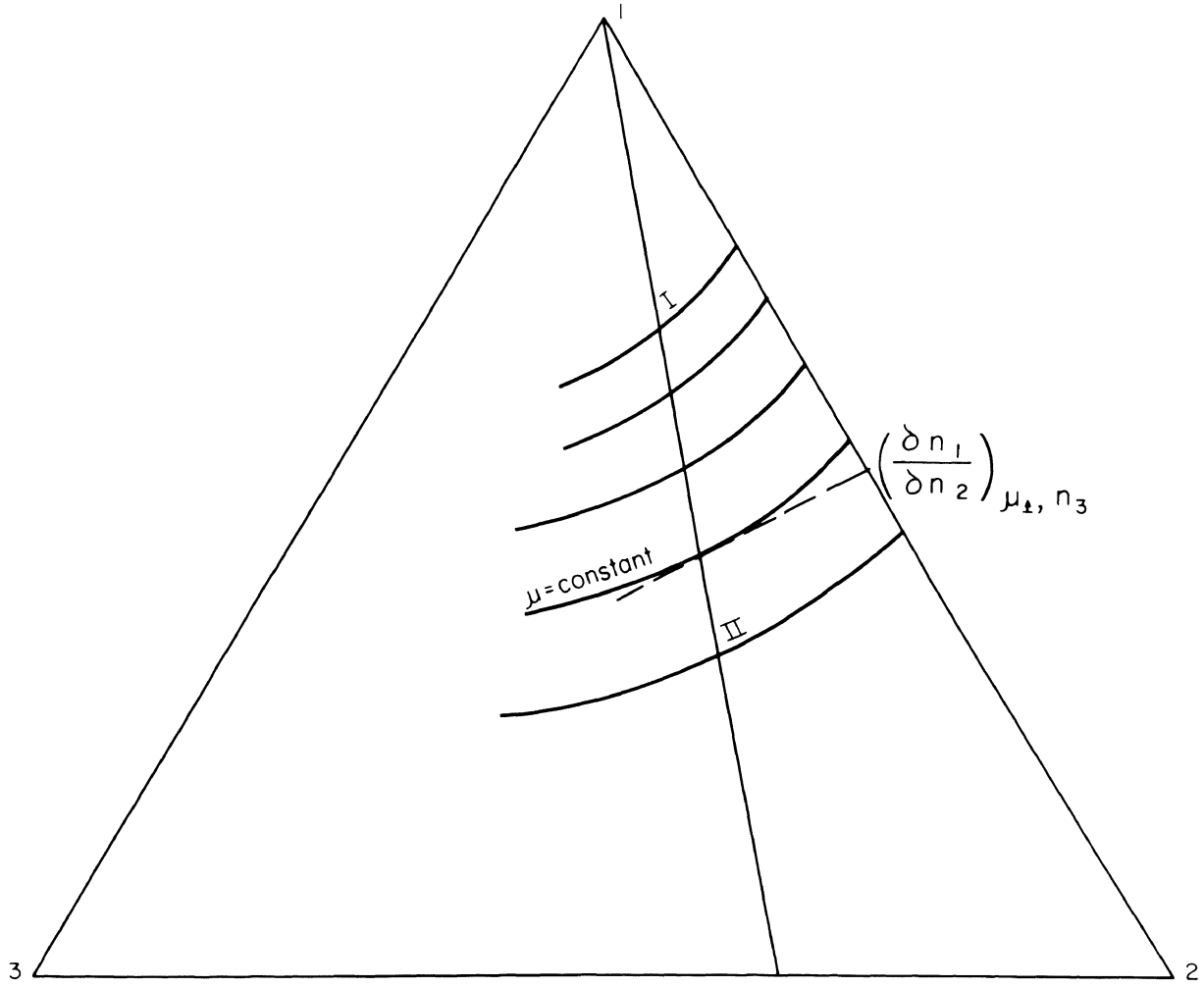

FIGURE 10. - Idealized Ternary Showing Graphic Evaluation of the Parameters Needed to Calculate μ_1, From μ_2.

The quantity $(\partial n_1/\partial n_2)_{\mu_1,n_3}$ describes the direction of the tangent to the μ_1 isoactivity curve at a certain point. This quantity is determined by the intersection of the tangent with the binary system between components 1 and 2 as shown in Figure 10.

A more useful equation is obtained by substituting the definition of chemical potential, $\mu = RT \ln\alpha = 2.303RT \log_{10}\alpha$, into Equation 5-7 and dividing through by 2.303 RT, thus obtaining:

$$\text{Log}_{10}\alpha_2^{II} = \left[\text{Log}_{10}\alpha_2^{I} - \int_{\text{Log}_{10}\alpha_1^{I}}^{\text{Log}_{10}\alpha_1^{II}} \left(\frac{\partial n_1}{\partial n_2}\right)_{\text{Log}_{10}\alpha_1, n_3} d\,\text{Log}_{10}\alpha_1\right]_{n_3/n_3} \qquad (5\text{-}8)$$

THERMODYNAMIC ACTIVITIES OF THE ZnO-Fe_2O_3-Fe_3O_4 SYSTEM

Activities of Fe_2O_3. Application of Equation 5-8 of the preceding section will now be made in order to calculate the activities of Fe_2O_3 in the spinel solid solution region from the experimentally determined activities of oxygen.

A number of different sets of components, corresponding to n_1, n_2 and n_3 can be used to describe the ZnO-Fe_2O_3-Fe_3O_4 system. Perhaps the easiest to work with, however, is the ZnO-Fe_2O_3-O set where

$$\left(\frac{\partial n_1}{\partial n_2}\right)_{\text{Log}_{10}\alpha_1, n_3} = \left(\frac{\partial O}{\partial Fe_2O_3}\right)_{\text{Log}_{10}O, ZnO} \qquad (5\text{-}9)$$

---

[7] See Appendix A for a description of the calculation with ZnO, Fe, and O as components. The activities of Fe_2O_3 and the partial value of the derivative, $(n_1/n_2)_{u_1,n_3}$ are the same in both cases which is to be expected.

Unfortunately the system is not defined in terms of ZnO, Fe_2O_3 and O; therefore, $(\partial O/\partial Fe_2O_3)_{\log_{10}O,ZnO}$ must be transformed into terms of Fe_2O_3 and Fe_3O_4. This transformation is easily accomplished with the aid of the equation

$$2Fe_3O_4 + O = 3Fe_2O_3 \qquad (5\text{-}10)$$

If the initial oxygen is defined as Y and the initial Fe_2O_3 as Z then, according to Equation 5-10, the final amounts of Fe_2O_3 and Fe_3O_4 after transformation, are

$$Fe_2O_3 = Z + 3Y$$

$$Fe_3O_4 = -2Y$$

The intersection of the tangent to the oxygen isoactivity curve with the Fe_2O_3 - Fe_3O_4 binary represents the partial derivative of Fe_2O_3 with respect to Fe_3O_4 and can be written in transformed coordinates as

$$\left(\frac{\partial Fe_2O_3}{\partial Fe_3O_4}\right)_{\log_{10}O,ZnO} = \frac{N_{Fe_2O_3}}{N_{Fe_3O_4}} = \frac{Z + 3Y}{-2Y}$$

and

$$\frac{Z}{Y} = -3 + 2\,\frac{N_{Fe_2O_3}}{N_{Fe_3O_4}} \quad .$$

However,

$$\frac{Y}{Z} = \frac{N_O}{N_{Fe_2O_3}} = \left(\frac{\partial O}{\partial Fe_2O_3}\right)_{\log_{10}O,ZnO}.$$

Therefore,

$$\left(\frac{\partial O}{\partial Fe_2O_3}\right)_{\log_{10}O,ZnO} = \frac{-1}{3+2\,\dfrac{N_{Fe_2O_3}}{N_{Fe_3O_4}}}$$

The quantities $N_{Fe_2O_3}$ and $N_{Fe_3O_4}$ are the respective mole fractions of Fe_2O_3 and Fe_3O_4 in the Fe_2O_3-Fe_3O_4 binary system. By substituting Equations 5-9 and 5-11 into Equation 5-8, it can be expressed as

$$\log_{10} \alpha_{Fe_2O_3} = \left[\log_{10} \alpha^{I}_{Fe_2O_3} + \int_{\log_{10} O_I}^{\log_{10} O} \frac{1}{3+2\frac{N_{Fe_2O_3}}{N_{Fe_3O_4}}} \, d \log_{10} O \right]_{Fe_2O_3/ZnO} \quad (5\text{-}12)$$

The standard state for Fe_2O_3, chosen as free Fe_2O_3, is represented by the phase boundary between the solid solution region and the Fe_2O_3 plus solid solution region. This requires the path of integration to pass through the intersection of the phase boundary with the oxygen isoactivity curve. Under these conditions Equation 5-12 reduces to

$$\log_{10} Fe_2O_3 = \left[\int_{\log_{10} O \text{ for } Fe_2O_3 = \text{free}}^{\log_{10} O} \frac{1}{3+2\frac{N_{Fe_2O_3}}{N_{Fe_3O_4}}} \, d \log_{10} O \right]_{Fe_2O_3/ZnO} \quad (5\text{-}13)$$

Because of the lack of an analytical expression for the partial derivative $(\partial O/\partial Fe_2O_3)_{\log_{10} O, ZnO}$ in terms of $\log_{10} O$, all of the Fe_2O_3 activities were calculated by graphical integration.[8] The integration was accomplished with the aid of a polar planimeter and the Fe_2O_3 activities obtained were plotted against the atomic percent of oxygen along the path of integration. The activities of Fe_2O_3, expressed in terms of tenths, were then interpolated from these curves, and the values were plotted in Figures 11, 12, and 13. Table IV gives the Fe_2O_3 activities and the quantities needed to calculate the activities.

Activities of Fe_3O_4. The activities of Fe_3O_4 were calculated from the thermochemical data[9] of the reaction

---

[8]Since the differential $\log_{10} O_2$ was substituted for $\log 10^0$ in the integration of Equation 5-13, the area under the curve had to be divided by 2. This stems from the relationship

$$\log_{10} O = \log_{10} P_O = \log_{10} P_{O\frac{1}{2}} = \tfrac{1}{2} \log_{10} P_{O_2}$$

[9]J. P. Couglin, U. S. Bureau of Mines, Bull. 542 (1954).

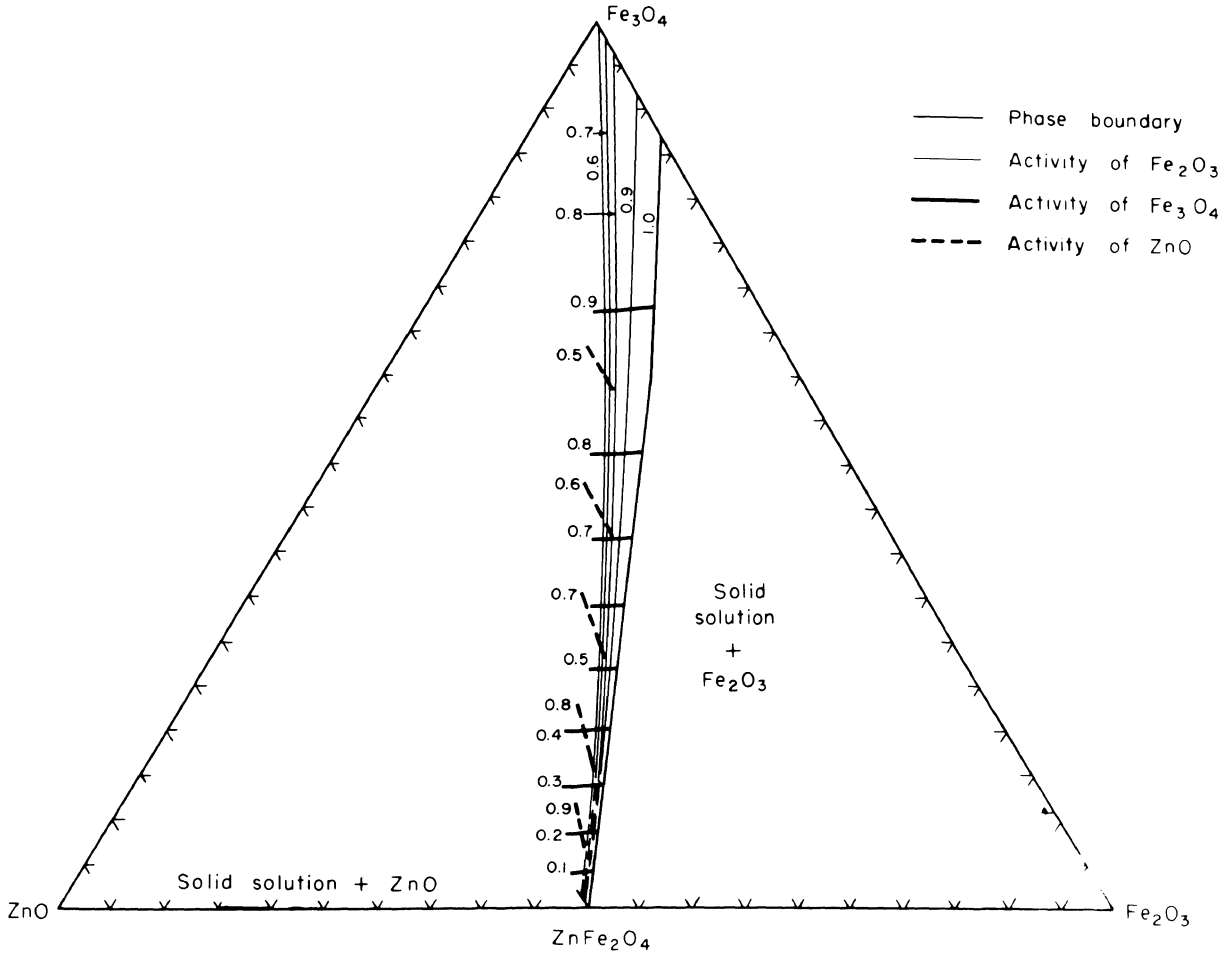

FIGURE 11. - Iso-Activity Curves in the ZnO-Fe_2O_3-Fe_3O_4 System at 1,100° C.

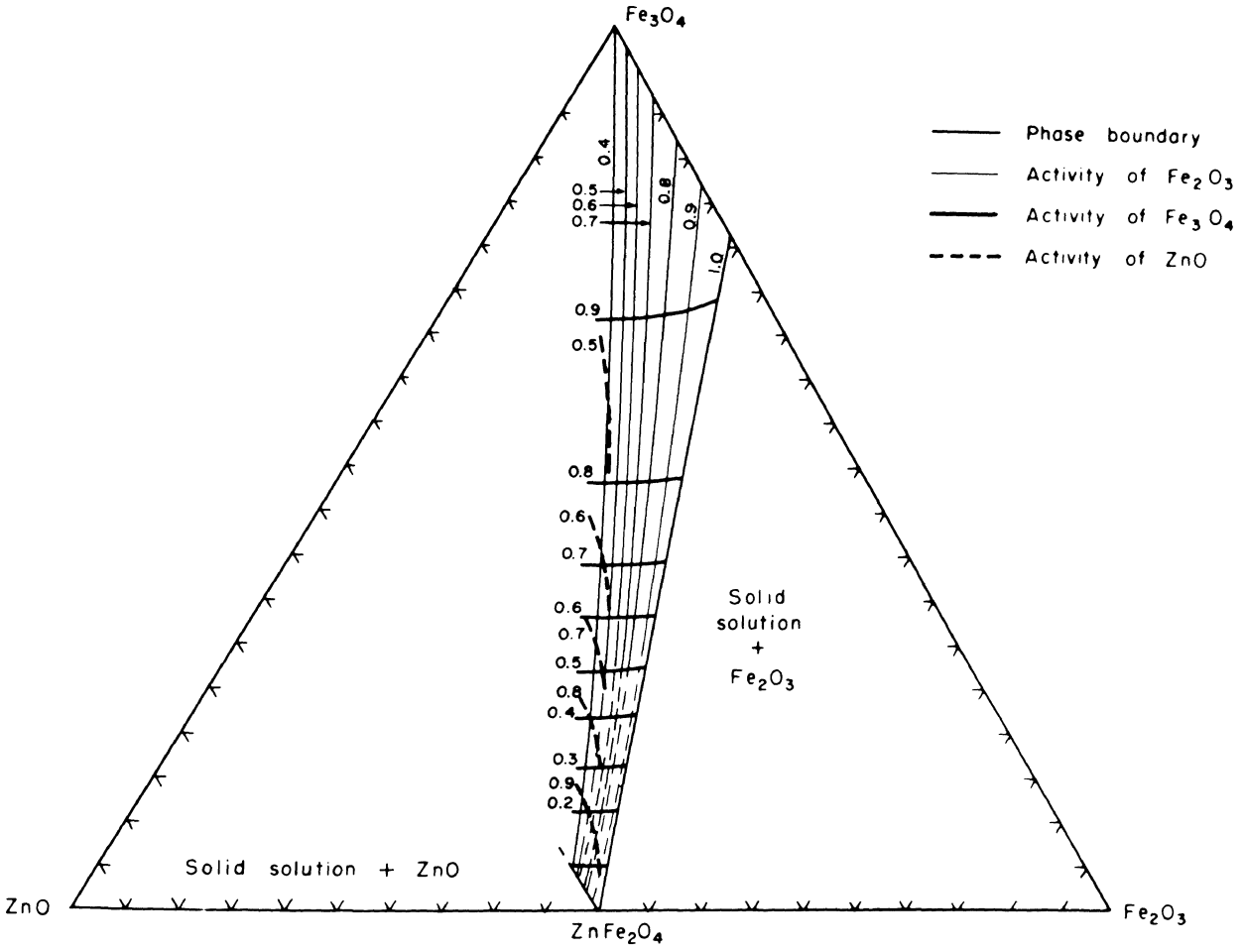

FIGURE 12. - Iso-Activity Curves in the ZnO-Fe_2O_3-Fe_3O_4 System at 1,300° C.

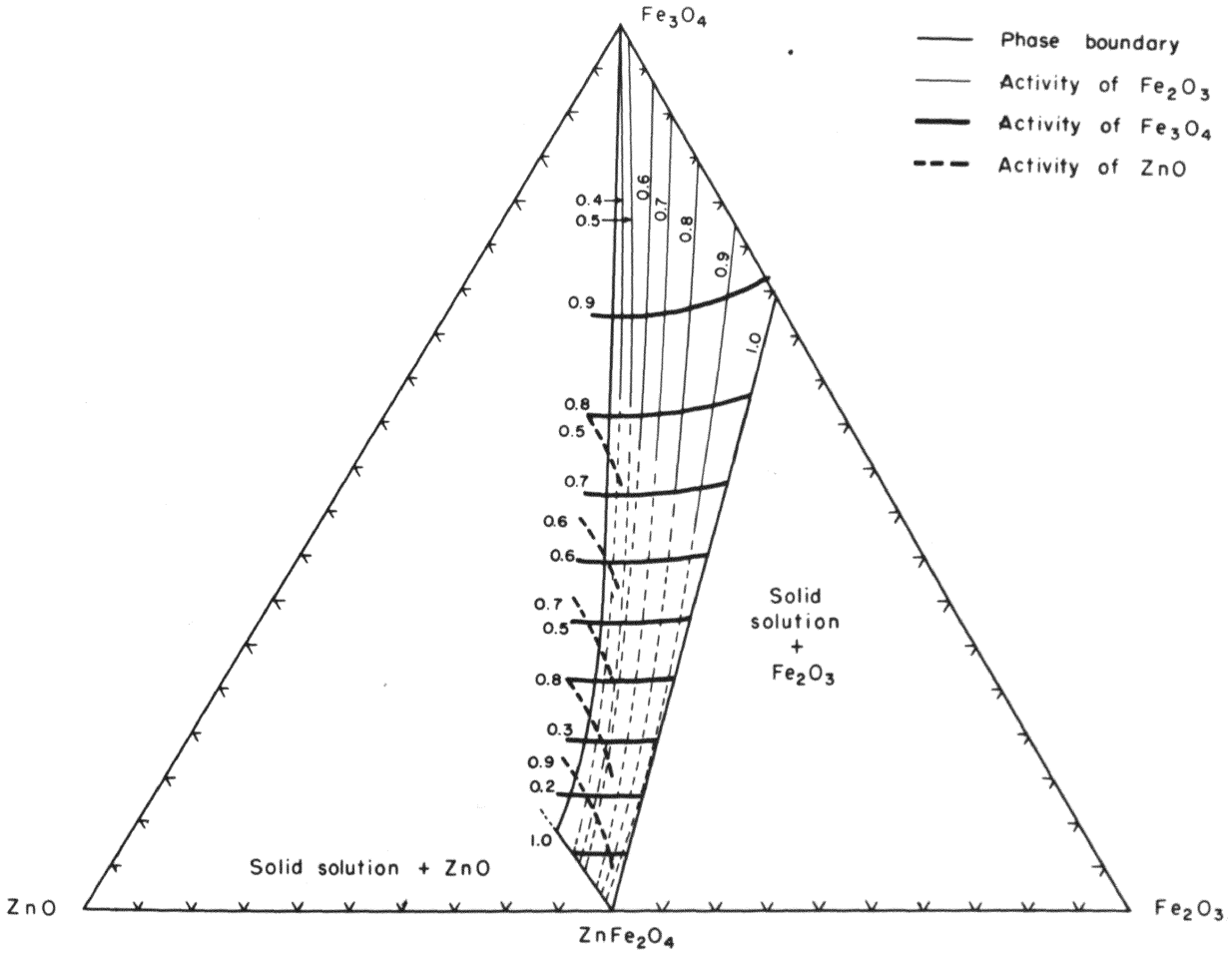

FIGURE 13. - Iso-Activity Curves in the ZnO-Fe_2O_3-Fe_3O_4 System at 1,400° C.

TABLE IV

Fe_2O_3 ACTIVITIES CALCULATED FROM OXYGEN ISOACTIVITY CURVES

Temperature	Oxygen Pressure at Boundary Intersection	Isoactivity of Oxygen Curve	$\frac{\partial O}{\partial Fe_2O_3}$	$\alpha_{Fe_2O_3}$	Atomic Percent Oxygen
1100°C	$1X10^{-1}$ ATM	$1X10^{-1}$ ATM	0.2660	1.000	57.20
		$1X10^{-2}$	0.2880	0.726	57.17
		$1X10^{-3}$	0.3026	0.516	57.14
		$1X10^{-4}$	0.3068	0.363	57.12
	$1X10^{-2}$	$1X10^{-2}$	0.2690	1.000	57.21
		$1X10^{-3}$	0.2982	0.720	57.19
		$1X10^{-4}$	0.3084	0.639	57.15
	$1X10^{-3}$	$1X10^{-3}$	0.2860	1.000	57.30
		$1X10^{-4}$	0.2998	0.714	57.23
	Fe_2O_3-Fe_3O_4 Boundary	$7.54X10^{-5}$	0.3045	1.000	57.39
		$2.4X10^{-5}$	0.3185	0.830	57.34
		$1X10^{-5}$	0.3260	0.726	57.20
		$3.98X10^{-7}$	0.3330	0.424	57.14
1300°C	1.0	1.0	0.2606	1.000	57.36
		$1X10^{-1}$	0.2728	0.737	57.31
		$1X10^{-2}$	0.3200	0.522	57.19
		$1X10^{-3}$	0.3200	0.361	57.17
		$1X10^{-4}$	0.3278	0.249	57.13
	$1X10^{-1}$	$1X10^{-1}$	0.2632	1.000	57.47
		$1X10^{-2}$	0.3095	0.716	57.22
		$1X10^{-3}$	0.3200	0.498	57.20
		$1X10^{-4}$	0.3318	0.343	57.14
	Fe_2O_3-Fe_3O_4 Boundary	$3.5X10^{-2}$	0.2800	1.000	57.60
		$1X10^{-2}$	0.2970	0.832	57.45
		$1X10^{-3}$	0.3248	0.582	57.20
		$1X10^{-4}$	0.3333	0.398	57.14
1400°C	1.0 ATM	1.0 ATM	0.2246	1.000	57.57
		$1X10^{-1}$	0.2834	0.745	57.46
		$1X10^{-2}$	0.3188	0.525	57.27
		$1X10^{-3}$	0.3316	0.360	57.21
		$1X10^{-4}$	0.3316	0.246	57.16
	Fe_2O_3-Fe_3O_4 Boundary	$2.37X10^{-1}$	0.2563	1.000	57.94
		$1X10^{-1}$	0.2838	0.890	57.60
		$1X10^{-2}$	0.3174	0.627	57.30
		$1X10^{-3}$	0.3333	0.432	57.14
		$1X10^{-4}$	0.3333	0.294	57.14

$$\frac{3}{2}\,Fe_2O_3(solid) \rightleftharpoons Fe_3O_4(solid) + \frac{1}{4}\,O_2(gas) \qquad (5\text{-}14)$$

for which

$$K = \frac{(\alpha_{Fe_3O_4})(P_{O_2})^{1/4}}{(\alpha_{Fe_2O_3})^{3/2}} \qquad (5\text{-}15)$$

where K is the equilibrium constant for Equation 5-14 at a certain temperature.[10] Thus, the activity of Fe_3O_4 can be calculated from Equation 5-15 if K, Fe_2O_3 and P_{O_2} are all known at a point. Since P_{O_2} was experimentally determined and Fe_2O_3 was calculated in the previous section, the only quantity needed to calculate the Fe_3O_4 activity was K.

The value of K was calculated from the free energy change of Equation 5-14, however, to be consistent with the experimental results of Darken and Gurry,[11] it was necessary to use a free energy value slightly different from that tabulated by Coughlin. The value used is well within the limit of error of the tabulated value. A tabulation of the free energy values at the various temperatures, together with the equilibrium constant, are shown in Table V.

TABLE V

THERMOCHEMICAL DATA FOR THE REACTION $\frac{3}{2}\,Fe_2O_3 \rightleftharpoons Fe_3O_4 + \frac{1}{4}\,O_2$

Temperature	Free Energy		Equilibrium Constant
	Tabulated Value Cal.	Utilized Value Cal.	
1,100	11,924	13,150	0.00800
1,300	5,645	5,750	0.159
1,400	3,307	3,170	0.386

[10] See Appendix B for a thermodynamic validation of this method of calculation.

[11] L. S. Darken and R. W. Gurry. J. American Chem. Soc., Vol. 68, p. 798 (1946).

The calculated Fe_3O_4 activities, along with the oxygen pressure and the activities of Fe_2O_3, are given in Table VI.

Because of the limited number of Fe_3O_4 activities determined and because their distribution was not uniform throughout the spinel solid solution region, certain assumptions had to be made regarding the contour of the Fe_3O_4 isoactivity lines. A contour that is symmetrical about the Fe_3O_4 corner of the ZnO-Fe_2O_3-Fe_3O_4 composition triangle was finally selected. These contour lines appear as segments of concentric circles about the Fe_3O_4 corner as shown in Figures 11, 12, and 13.

Activity values of straight contour lines, parallel to the ZnO-Fe_2O_3 side, differ by less than 3 percent from the circular lines assumed in this investigation. Inasmuch as these two activity contours are the most prevalent types found in other ternary systems, it is felt that the Fe_3O_4 isoactivity curves shown in Figures 11, 12, and 13 are fair estimates of the actual Fe_3O_4 isoactivity curves.

Activities of ZnO. The activities of ZnO were calculated from Equation 5-8 and the Fe_3O_4 isoactivity curves developed in the preceding section. The components used in the calculation were ZnO, Fe_2O_3, and Fe_3O_4 where

$$\left(\frac{\partial n_1}{\partial n_2}\right)_{\log_{10}\alpha_1, n_3} = \left(\frac{\partial Fe_3O_4}{\partial ZnO}\right)_{\log_{10}\alpha_{Fe_3O_4}, Fe_2O_3} \qquad (5\text{-}16)$$

and

$$\left(\frac{\partial Fe_3O_4}{\partial ZnO}\right)_{\log_{10}\alpha_{Fe_3O_4}, Fe_2O_3} = \frac{N_{Fe_3O_4}}{N_{ZnO}} \cdot \qquad (5\text{-}17)$$

TABLE VI

Fe_3O_4 ACTIVITIES CALCULATED FROM Fe_2O_3 AND OXYGEN ACTIVITIES

Temperature	Oxygen Pressure At Boundary Intersection	Oxygen Pressure	Activity Fe_2O_3	Activity Fe_3O_4
1100°C	$1X10^{-1}$ATM	$1X10^{-1}$ATM	1.000	0.159
		$1X10^{-2}$	0.726	0.175
		$1X10^{-3}$	0.516	0.186
		$1X10^{-4}$	0.363	0.196
	$1X10^{-2}$	$1X10^{-2}$	1.000	1.283
		$1X10^{-3}$	0.720	0.307
		$1X10^{-4}$	0.639	0.457
	$1X10^{-3}$	$1X10^{-3}$	1.000	0.503
		$1X10^{-4}$	0.714	0.540
	Fe_2O_3-Fe_3O_4 Boundary	$7.54X10^{-5}$	1.000	0.960
		$2.4X10^{-5}$	0.830	0.966
		$1X10^{-5}$	0.726	0.984
		$3.98X10^{-7}$	0.424	1.000
1300°C	1.0	1.0	1.000	0.399
		$1X10^{-1}$	0.737	0.449
		$1X10^{-2}$	0.522	0.476
		$1X10^{-3}$	0.361	0.486
		$1X10^{-4}$	0.249	0.495
	$1X10^{-1}$	$1X10^{-1}$	1.000	0.709
		$1X10^{-2}$	0.716	0.764
		$1X10^{-3}$	0.498	0.788
		$1X10^{-4}$	0.343	0.801
	Fe_2O_3-Fe_3O_4 Boundary	$3.5X10^{-2}$	1.000	0.922
		$1X10^{-2}$	0.832	0.957
		$1X10^{-3}$	0.582	0.996
		$1X10^{-4}$	0.398	1.000
1400°C	1.0 ATM	1.0 ATM	1.000	0.621
		$1X10^{-1}$	0.745	0.710
		$1X10^{-2}$	0.525	0.747
		$1X10^{-3}$	0.360	0.755
		$1X10^{-4}$	0.246	0.758
	Fe_2O_3-Fe_3O_4 Boundary	$2.37X10^{-1}$	1.000	0.890
		$1X10^{-1}$	0.890	0.928
		$1X10^{-2}$	0.627	0.975
		$1X10^{-3}$	0.432	1.000
		$1X10^{-4}$	0.294	1.000

Here, $N_{Fe_3O_4}$ and N_{ZnO} are the respective mole fractions of Fe_3O_4 and ZnO in the ZnO-Fe_3O_4 binary system. By substituting Equations 5-16 and 5-17 in Equation 5-8 the integral can be expressed as

$$\log_{10}\alpha_{ZnO} = \left[\log_{10}\alpha_{ZnO_I} - \int_{\log_{10}\alpha_{Fe_3O_4\,I}}^{\log_{10}\alpha_{Fe_3O_4}} \frac{N_{Fe_3O_4}}{N_{ZnO}}\, d\log_{10}\alpha_{Fe_3O_4}\right]_{ZnO/Fe_2O_3} \qquad (5\text{-}18)$$

By choosing free ZnO as the standard state and integrating along a straight line between the Fe_3O_4 corner of the composition triangle and the phase boundary between the solid solution and solid solution plus ZnO regions, Equation 5-18 reduces to

$$\log_{10}\alpha_{ZnO} = \left[-\int_{\log_{10}\alpha_{Fe_3O_4,\,ZnO=Free}}^{\log_{10}\alpha_{Fe_3O_4}} \frac{N_{Fe_3O_4}}{N_{ZnO}}\, d\log_{10}\alpha_{Fe_3O_4}\right]_{ZnO/Fe_2O_3} \qquad (5\text{-}19)$$

The ZnO activities obtained from graphical integration of this equation were then plotted against the mole fraction Fe_3O_4 along the path of integration. The activities plotted in Figures 11, 12, and 13 were then interpolated from the activity versus Fe_3O_4 mole-fraction graphs.

Table VII shows the ZnO activities obtained from integration, together with the mole percents of Fe_3O_4 and the Fe_3O_4 activities.

THERMODYNAMIC PROPERTIES OF THE $ZnFe_2O_4$-Fe_3O_4 SYSTEM

Zinc ferrite and magnetite are both classified as a spinel-type crystal structure; however, because they exhibit different cation distributions within the parent oxygen lattice, they are respectively

TABLE VII

ZnO ACTIVITIES CALCULATED FROM Fe_3O_4 ACTIVITIES

Temperature	Fe_3O_4 At Boundary Intersection	Isoactivity of Fe_3O_4 Curve	$\frac{\partial Fe_3O_4}{\partial ZnO}$	α_{ZnO}	Mole Percent Fe_3O_4
1100°C	0.048	0.048	0.024	1.000	2.0
		0.100	0.043	0.975	4.3
		0.200	0.090	0.931	8.5
		0.300	0.160	0.880	14.0
		0.400	0.257	0.822	20.4
		0.500	0.373	0.774	27.0
		0.600	0.530	0.710	34.1
		0.700	0.710	0.652	41.6
		0.800	1.056	0.575	51.1
		0.900	2.030	0.486	66.9
	0.000	0.000	0.010	1.000	0.0
		0.100	0.040	0.907	4.2
		0.200	0.090	0.864	8.4
		0.300	0.160	0.825	13.9
		0.400	0.253	0.769	20.3
		0.500	0.370	0.726	26.9
		0.600	0.515	0.674	34.0
		0.700	0.704	0.609	41.5
		0.800	1.042	0.544	51.0
		0.900	2.010	0.459	66.8
1300°C	0.100	0.100	0.056	1.000	5.5
		0.200	0.128	0.936	11.0
		0.300	0.196	0.880	16.5
		0.400	0.283	0.814	22.1
		0.500	0.383	0.760	27.7
		0.600	0.503	0.698	33.5
		0.700	0.653	0.639	39.7
		0.800	0.938	0.574	48.4
		0.900	2.037	0.495	67.2
	0.050	0.050	0.028	1.000	2.8
		0.100	0.050	0.972	5.4
		0.200	0.127	0.916	10.9
		0.300	0.195	0.857	16.4
		0.400	0.282	0.796	22.0
		0.500	0.382	0.742	27.6
		0.600	0.501	0.684	33.4
		0.700	0.650	0.621	39.6
		0.800	0.934	0.562	48.2
		0.900	2.030	0.484	67.1
	0.000	0.000	0.000	1.000	0.0
		0.100	0.053	0.891	5.3

TABLE VII
(continued)

Temperature	Fe_3O_4 At Boundary Intersection	Isoactivity of Fe_3O_4 Curve	$\frac{\partial Fe_3O_4}{\partial ZnO}$	α_{ZnO}	Mole Percent Fe_3O_4
		0.200	0.127	0.839	10.8
		0.300	0.195	0.790	16.3
		0.400	0.282	0.734	21.9
		0.500	0.380	0.680	27.5
		0.600	0.500	0.629	33.3
		0.700	0.660	0.569	39.5
		0.800	0.933	0.512	48.1
		0.900	2.020	0.444	67.0
1400°C	0.140	0.140	0.112	1.000	9.3
		0.200	0.178	0.951	13.2
		0.300	0.255	0.881	19.6
		0.400	0.370	0.802	26.1
		0.500	0.505	0.730	32.7
		0.600	0.678	0.655	39.5
		0.700	0.925	0.579	47.1
		0.800	1.315	0.501	56.1
		0.900	2.125	0.419	67.1
	0.100	0.100	0.072	1.000	6.7
		0.200	0.150	0.923	13.1
		0.300	0.247	0.855	19.4
		0.400	0.359	0.778	26.0
		0.500	0.490	0.708	32.6
		0.600	0.652	0.636	39.4
		0.700	0.900	0.562	47.0
		0.800	1.280	0.486	56.0
		0.900	2.057	0.416	67.0
	0.000	0.000	0.000	1.000	0.0
		0.100	0.066	0.889	6.5
		0.200	0.145	0.822	12.9
		0.300	0.236	0.762	19.2
		0.400	0.347	0.705	25.7
		0.500	0.481	0.642	32.5
		0.600	0.650	0.575	39.5
		0.700	0.886	0.514	46.9
		0.800	1.243	0.441	55.5
		0.900	2.020	0.371	66.9

subclassified as normal and inverse spinel structures. The normal spinel structure of $ZnFe_2O_4$ is made up of a cubic, close-packed lattice of oxygen ions with the cubic unit cell containing thirty-two oxygen ions. The divalent zinc ions are distributed among the tetrahedral voids of the oxygen lattice, and the trivalent ferric ions are distributed among the octrahedral voids of the lattice. The magnetic inverse spinel structure of the Fe_3O_4 is likewise made up of the cubic, close-packed lattice of oxygen with thirty-two oxygen ions per unit cell. However, in this case, half of the trivalent ferric ions are now distributed in the tetrahedral voids with the remaining ferric ions and the divalent ferrous ions distributed among the octrahedral voids. This difference in cation distribution gives rise to markedly different magnetic properties, and because the spinels form complete solid solutions, the magnetic properties of the inverse spinel structure can be effectively controlled by additions of the normal spinel structure.

Because the magnetic properties are so closely related to the structure of the solid solution, a study was made of the thermodynamic properties of the $ZnFe_2O_4$-Fe_3O_4 system in an attempt to gain some insight into the structure.

Activities of the System. Figures 14, 15, and 16 show the activity curves for Fe_3O_4 and $ZnFe_2O_4$ at 1100°C, 1300°C, and 1400° C respectively. The experimental points shown in the figures were taken from the Fe_3O_4 activities of the ternary system. Because Figures 15 and 16 exhibit a relatively uniform distribution of Fe_3O_4 activity

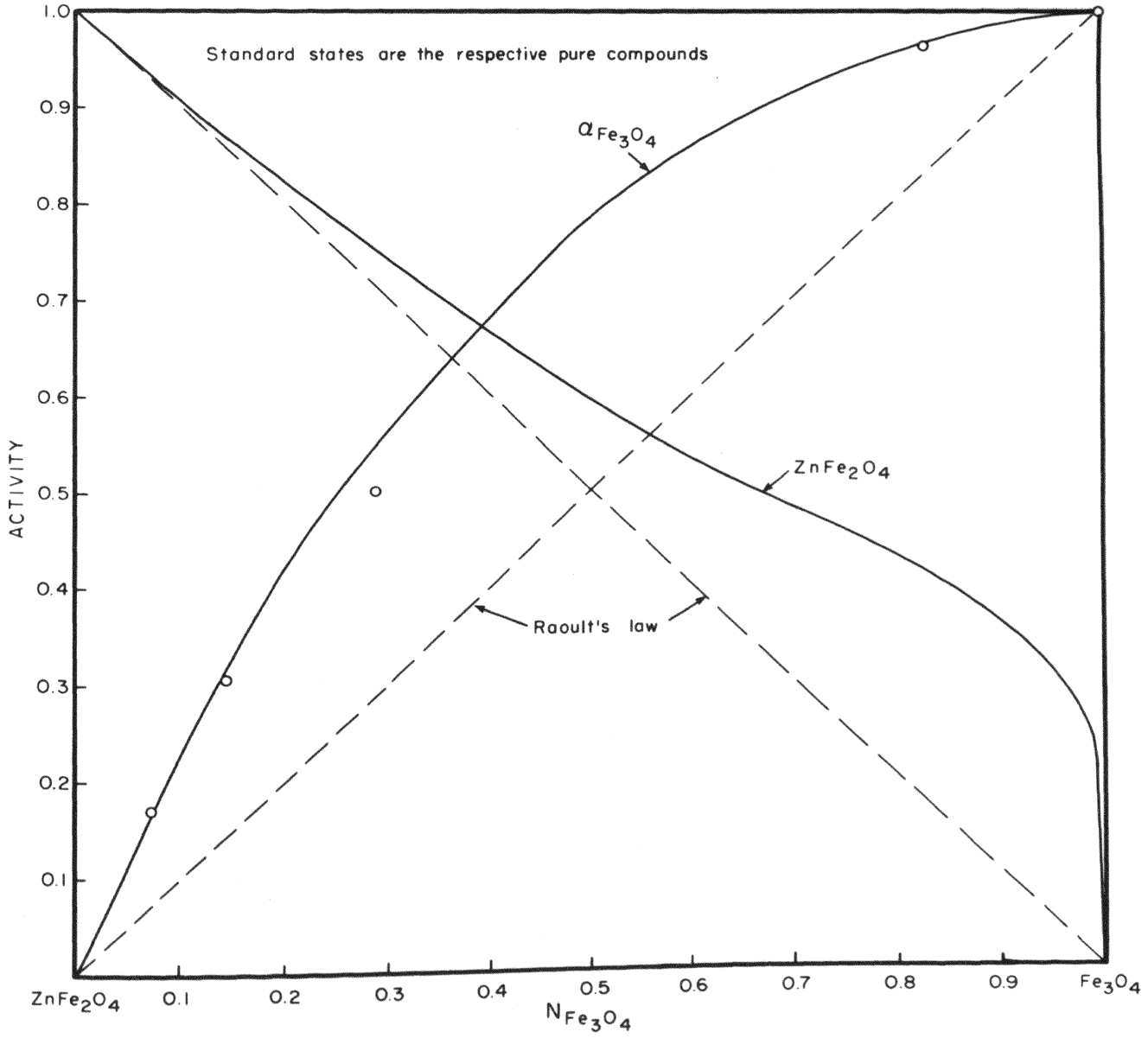

FIGURE 14. - Activities in the Pseudo-Binary System $ZnFe_2O_4$-Fe_3O_4 at 1,100° C.

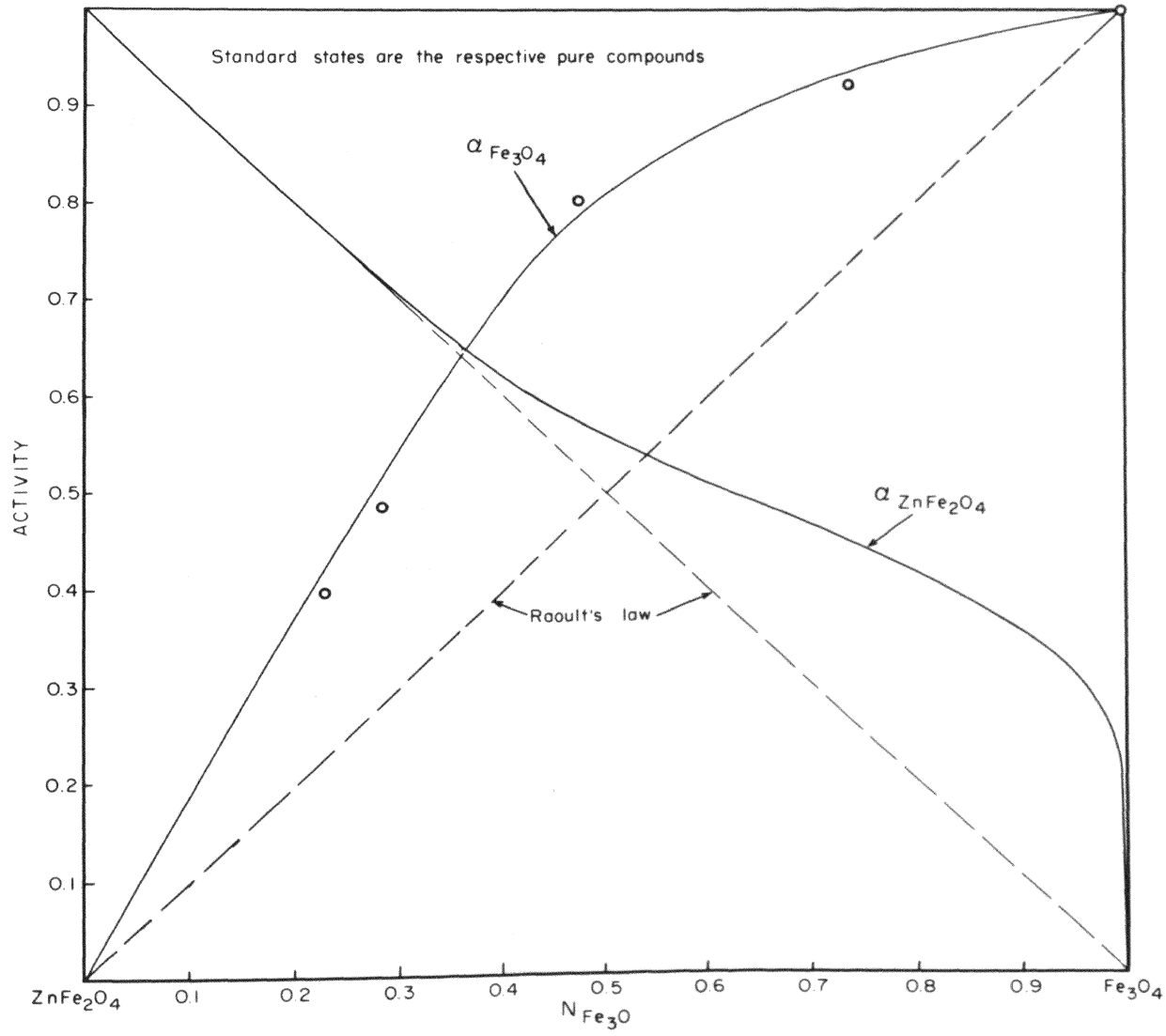

FIGURE 15. - Activities in the Pseudo-Binary System $ZnFe_2O_4$-Fe_3O_4 at 1,300° C.

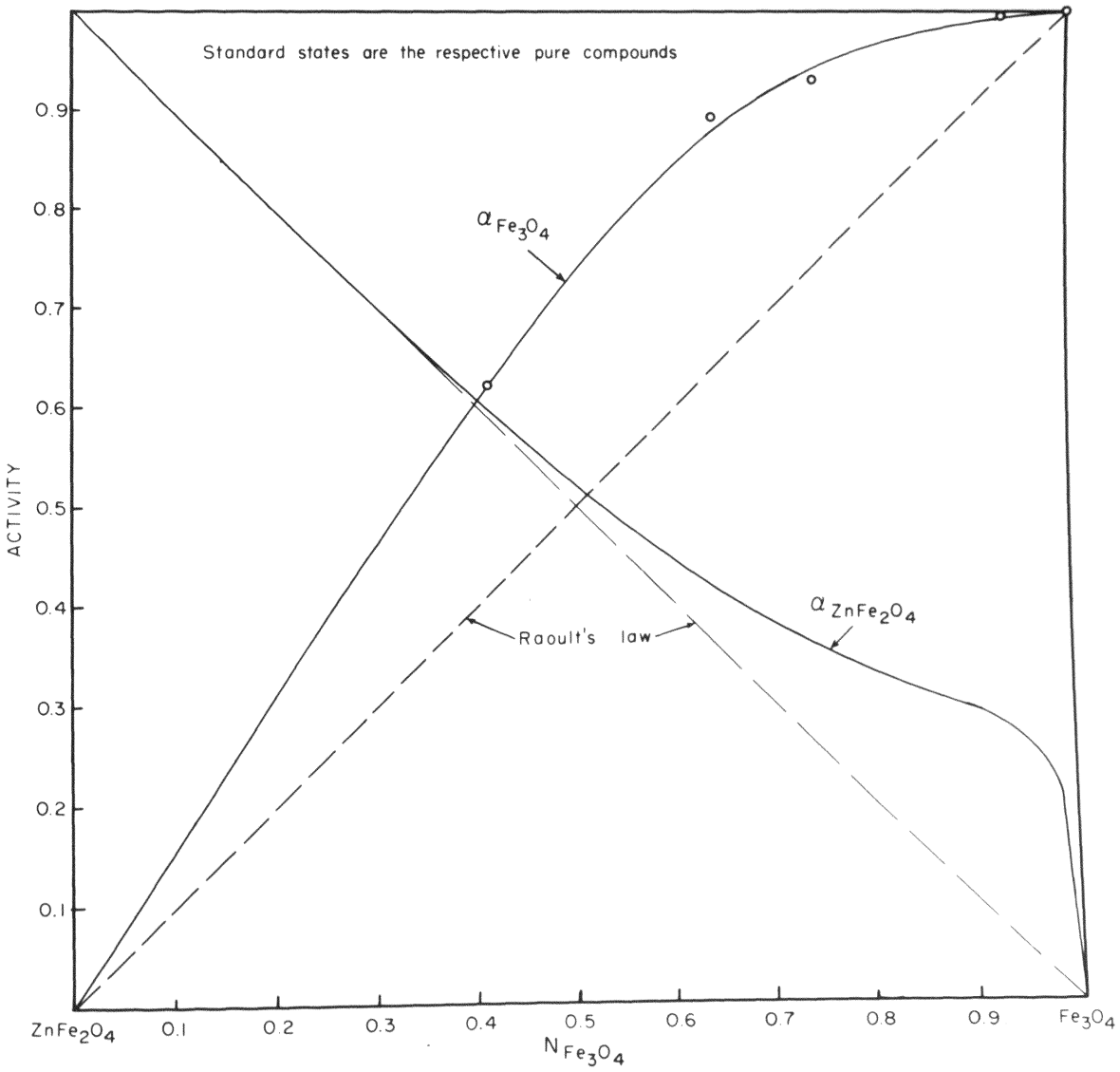

FIGURE 16. - Activities in the Pseudo-Binary System $ZnFe_2O_4$-Fe_3O_4 at 1,400° C.

points, the general configuration of these curves was used as a prototype in the construction of the Fe_3O_4 activity curve of Figure 14. This same prototype has been noted for Fe_3O_4 activities in the Fe_2O_3-Fe_3O_4 system.

The $ZnFe_2O_4$ activity curves were then calculated by utilizing the curves of Fe_3O_4 activity and the Gibbs-Duhem equation for binary systems:

$$N_1 d\ln\alpha_1 + N_2 \ d\ln\alpha_2 = 0 \qquad (5\text{-}20)$$

Because of the limits of integration, however, several substitutions were made to simplify the calculations.

By first differentiating the mole fraction equation, $N_1+N_2=1$, the relationship

$$dN_1 + dN_2 = 0$$

is obtained. Multiplying the first term by N_1/N_1 and the second by N_2/N_2 gives the expression

$$N_1 \ \frac{dN_1}{N_1} \ + \ N_2 \ \frac{dN_2}{N_2} \ = \ 0$$

or

$$N_1 \ d\ln N_1 + \ N_2 \ d\ln N_2 = 0$$

Subtracting this from Equation 5-20 yields

$$N_1 \ d\ln \frac{\alpha_1}{N_1} \ + \ N_2 \ d\ln \frac{\alpha_2}{N_2} \ = 0$$

By definition, the activity coefficient γ_i is equal to α_i/N_i; therefore,

$$N_1 \ d\ln \gamma_1 \ + \ N_2 \ d\ln \gamma_2 \ = \ 0$$

Transforming to logarithm to the base 10 and dividing by 2.303 yields

$$N_1 \, d \log_{10} \gamma_1 + N_2 \, d \log_{10} \gamma_2 = 0$$

Transposing the second term, dividing by N_1, and substituting the components of the system into the equation, the results can be expressed

$$\log_{10} \gamma_{ZnFe_2O_4} = - \int_{\log_{10} \gamma_{Fe_3O_4, ZnFe_2O_4}}^{\log_{10} \gamma_{Fe_3O_4}} \frac{N_{Fe_3O_4}}{N_{ZnFe_2O_4}} \, d \log_{10} \gamma_{Fe_3O_4} \qquad (5\text{-}21)$$

Equation 5-21 was then graphically integrated to obtain $\gamma ZnFe_2O_4$ which, in turn, was used to calculate the activities of $ZnFe_2O_4$ that are plotted in Figures 14, 15, and 16.

Table VIII shows the activity coefficients and activities of $ZnFe_2O_4$ together with the quantities needed to calculate them.

Thermodynamic Properties of Mixing of the System. Statistical methods have found extensive use in the field of thermochemistry because they provide a link between the atomistic viewpoint and classical thermodynamics. Through this link, certain thermodynamic properties can be used to gain some insight into the structure of a system. This is generally accomplished by assuming some structural model and calculating certain of its thermodynamic properties. Then the thermodynamic properties of the real system are compared with those of the model. Probably the easiest property to work with is the entropy of mixing, because fewer assumptions are needed to derive it statistically and because it can be compared directly with experimental values without the knowledge of additional quantities such as bonding energies.[12]

---

[12] C. Wagner. Op.Cit. p. 32

TABLE VIII

$ZnFe_2O_4$ ACTIVITIES CALCULATED FROM THE ACTIVITIES OF Fe_3O_4

Temperature	$N_{ZnFe_2O_4}$	$\alpha_{Fe_3O_4}$	$\gamma_{Fe_3O_4}$	$\frac{N_{Fe_3O_4}}{N_{ZnFe_2O_4}}$	$\gamma_{ZnFe_2O_4}$	$\alpha_{ZnFe_2O_4}$
1100°C	0.005	0.9999	1.005	199.000	42.660	0.213
	0.010	0.999	1.009	99.000	23.660	0.237
	0.020	0.998	1.018	49.000	14.890	0.298
	0.030	0.997	1.028	32.333	10.002	0.300
	0.040	0.996	1.038	24.000	7.638	0.306
	0.050	0.995	1.047	19.000	6.339	0.317
	0.060	0.994	1.057	15.667	5.200	0.312
	0.070	0.993	1.068	13.290	4.732	0.331
	0.080	0.991	1.077	11.500	4.266	0.341
	0.090	0.988	1.086	10.111	3.820	0.344
	0.100	0.986	1.096	9.000	3.451	0.345
	0.150	0.970	1.141	5.667	2.606	0.391
	0.200	0.955	1.194	4.000	2.051	0.410
	0.250	0.937	1.249	3.000	1.764	0.441
	0.300	0.913	1.304	2.333	1.629	0.489
	0.350	0.890	1.369	1.860	1.459	0.511
	0.400	0.863	1.438	1.500	1.358	0.543
	0.450	0.831	1.511	1.222	1.234	0.555
	0.500	0.791	1.582	1.000	1.169	0.585
	0.550	0.741	1.647	0.818	1.133	0.623
	0.600	0.678	1.695	0.667	1.105	0.663
	0.650	0.610	1.743	0.538	1.089	0.708
	0.700	0.540	1.800	0.429	1.074	0.752
	0.750	0.470	1.880	0.333	1.050	0.788
	0.800	0.395	1.975	0.250	1.041	0.832
	0.850	0.315	2.100	0.177	1.017	0.865
	0.900	0.230	2.300	0.111	1.003	0.903
	0.950	0.120	2.400	0.053	1.000	0.950
	0.990	0.024	2.400	0.010	1.000	0.990
1300°C	0.005	0.9999	1.005	199.000	42.460	0.212
	0.010	0.999	1.009	99.000	23.550	0.236
	0.020	0.998	1.018	49.000	14.830	0.297
	0.030	0.997	1.028	32.333	10.000	0.300
	0.040	0.996	1.038	24.000	7.603	0.304
	0.050	0.995	1.047	19.000	6.310	0.316
	0.060	0.993	1.056	15.667	5.176	0.311
	0.070	0.992	1.067	13.290	4.457	0.312
	0.080	0.990	1.076	11.500	4.055	0.324
	0.090	0.987	1.085	10.111	3.656	0.329
	0.100	0.985	1.094	9.000	3.389	0.339
	0.150	0.971	1.142	5.667	2.489	0.373

TABLE VIII
(continued)

Temperature	$N_{ZnFe_2O_4}$	$\alpha_{Fe_3O_4}$	$\gamma_{Fe_3O_4}$	$\frac{N_{Fe_3O_4}}{N_{ZnFe_2O_4}}$	$\gamma_{ZnFe_2O_4}$	$\alpha_{ZnFe_2O_4}$
	0.200	0.954	1.193	4.000	2.039	0.408
	0.150	0.971	1.142	5.667	2.489	0.373
	0.200	0.954	1.193	4.000	2.039	0.408
	0.250	0.935	1.247	3.000	1.726	0.432
	0.300	0.913	1.304	2.333	1.535	0.461
	0.350	0.891	1.371	1.860	1.374	0.481
	0.400	0.867	1.445	1.500	1.271	0.508
	0.450	0.843	1.533	1.222	1.165	0.524
	0.500	0.813	1.626	1.000	1.090	0.545
	0.550	0.771	1.713	0.818	1.041	0.573
	0.600	0.707	1.768	0.667	1.016	0.610
	0.650	0.628	1.794	0.538	1.008	0.655
	0.700	0.544	1.813	0.429	1.002	0.701
	0.750	0.455	1.820	0.333	1.000	0.750
	0.800	0.364	1.820	0.250	1.000	0.800
	0.850	0.275	1.820	0.177	1.000	0.850
	0.900	0.185	1.820	0.111	1.000	0.900
	0.950	0.093	1.820	0.053	1.000	0.950
	0.990	0.018	1.820	0.010	1.000	0.990
1400°C	0.005	0.9999	1.005	199.000	36.140	0.181
	0.010	0.999	1.009	99.000	20.040	0.200
	0.020	0.998	1.018	49.000	12.620	0.252
	0.030	0.997	1.028	32.333	8.492	0.255
	0.040	0.996	1.038	24.000	6.471	0.259
	0.050	0.995	1.047	19.000	5.370	0.268
	0.060	0.994	1.057	15.667	4.539	0.272
	0.070	0.993	1.068	13.290	3.963	0.277
	0.080	0.992	1.078	11.500	3.524	0.282
	0.090	0.991	1.089	10.111	3.177	0.286
	0.100	0.990	1.100	9.000	2.877	0.288
	0.150	0.978	1.151	5.667	2.061	0.309
	0.200	0.963	1.204	4.000	1.642	0.328
	0.250	0.945	1.260	3.000	1.408	0.350
	0.300	0.920	1.314	2.333	1.259	0.378
	0.350	0.887	1.365	1.860	1.161	0.406
	0.400	0.846	1.410	1.500	1.099	0.439
	0.500	0.738	1.476	1.000	1.036	0.518
	0.550	0.675	1.500	0.818	1.019	0.560
	0.600	0.606	1.515	0.667	1.011	0.607
	0.650	0.536	1.531	0.538	1.007	0.655
	0.700	0.462	1.540	0.429	1.004	0.703
	0.750	0.239	1.556	0.333	1.000	0.750
	0.800	0.311	1.556	0.250	1.000	0.800

TABLE VIII
(continued)

Temperature	$N_{ZnFe_2O_4}$	$\alpha_{Fe_3O_4}$	$\gamma_{Fe_3O_4}$	$\frac{N_{Fe_3O_4}}{N_{ZnFe_2O_4}}$	$\gamma_{ZnFe_2O_4}$	$\alpha_{ZnFe_2O_4}$
	0.850	0.232	1.556	0.177	1.000	0.850
	0.900	0.155	1.556	0.111	1.000	0.900
	0.950	0.077	1.556	0.053	1.000	0.950
	0.990	0.016	1.556	0.010	1.000	0.990

In an attempt to gain some insight into the structure of the $ZnFe_2O_4$-Fe_3O_4 system, the entropies of mixing were calculated for the system and compared with those derived from idealized structures.

In order to obtain the entropies, however, it was found necessary to calculate first the free energies and enthalpies of mixing and then, utilizing the relationship

$$\Delta F^M = \Delta H^M - T\Delta S^M,$$

to calculate the entropies.

Free energies of mixing. The free energy of mixing is a molar quantity defined as

$$\Delta F^M = RT\ (N_1 \ln \alpha_1 + N_2 \ln \alpha_2), \qquad (5\text{-}22)$$

and it represents the difference between the free energy of formation of the solution (F) and the sum of the free energies of formation of the components in their standard states (F^o) multiplied by their respective mole fractions (N); that is

$$\Delta F^M = F - N_1F_1^o - N_2F_2^o \cdot$$

In this case, the free energy of mixing represents the relative stability of the system as compared to equivalent amounts of its pure components.

The activities of $ZnFe_2O_4$ and Fe_3O_4, developed in the preceding section, were used in Equation 5-22 to calculate the free energies of mixing for the system. The results are given in Table IX and are represented graphically in Figure 17. It can be seen from the figure that the free energy curves are skewed toward the $ZnFe_2O_4$ side (Figure 17) and have a minimum in the region of $N_{Fe_3O_4} = 0.35$. This is the same region where clustering of the oxygen-isoactivity lines was noted in the experimental results.

Enthalpies of mixing. The enthalpies of mixing were calculated from the free energies of mixing by using the Gibbs-Helmholtz equation:

$$\frac{\partial\left(\frac{\Delta F^M}{T}\right)}{\partial\left(\frac{1}{T}\right)} = \Delta H^M \qquad (5\text{-}23)$$

where ΔF^M is the free energy of mixing,

T is the absolute temperature, and

ΔH^M is the enthalpy of mixing.

It can be seen from the equation that ΔH^M is the slope of the curve $\Delta F^M/T$ versus $1/T$.

In order to simplify calculations, the enthalpies of mixing were assumed to be temperature independent, and the functions of $\Delta F^M/T$ versus $1/T$ were assumed to be linear. The method of least squares was used to calculate the equation of this function at a constant composition, and the slope of this equation is equal to enthalpy of mixing at this composition. These values of ΔH^M are given in Table X and are represented graphically in Figure 18.

TABLE IX

MOLAR FREE ENERGY OF MIXING

Mole Fraction Fe_3O_4	Molar Free Energy of Mixing cal/mole 1100°C	1300°C	1400°C
0.00	000	000	000
0.05	-422	-527	-586
0.10	-643	-829	-934
0.15	-820	-1041	-1187
0.20	-937	-1190	-1370
0.25	-1021	-1290	-1502
0.30	-1074	-1348	-1590
0.35	-1094	-1369	-1640
0.40	-1092	-1361	-1662
0.45	-1066	-1323	-1648
0.50	-1040	-1272	-1598
0.55	-994	-1203	-1528
0.60	-932	-1114	-1428
0.65	-859	-1035	-1308
0.70	-775	-925	-1164
0.75	-670	-813	-1009
0.80	-565	-678	-841
0.85	-450	-541	-648
0.90	-314	-381	-444
0.95	-171	-203	-235
1.00	000	000	000

The assumption of temperature-independence was not strictly accurate because a plot of the function $\Delta F^M/T$ versus 1/T showed some curvature, indicating that ΔH^M is a function of temperature. Because of the limited number of values available for calculating the equation, any other assumption regarding the shape of the curve would probably introduce the same amount of error. In spite of any error that might have been introduced by the assumption of linearity, the graph of enthalpy of mixing versus mole fraction Fe_3O_4 (See Fig. 18) appears to be a substantially uniform locus of points.

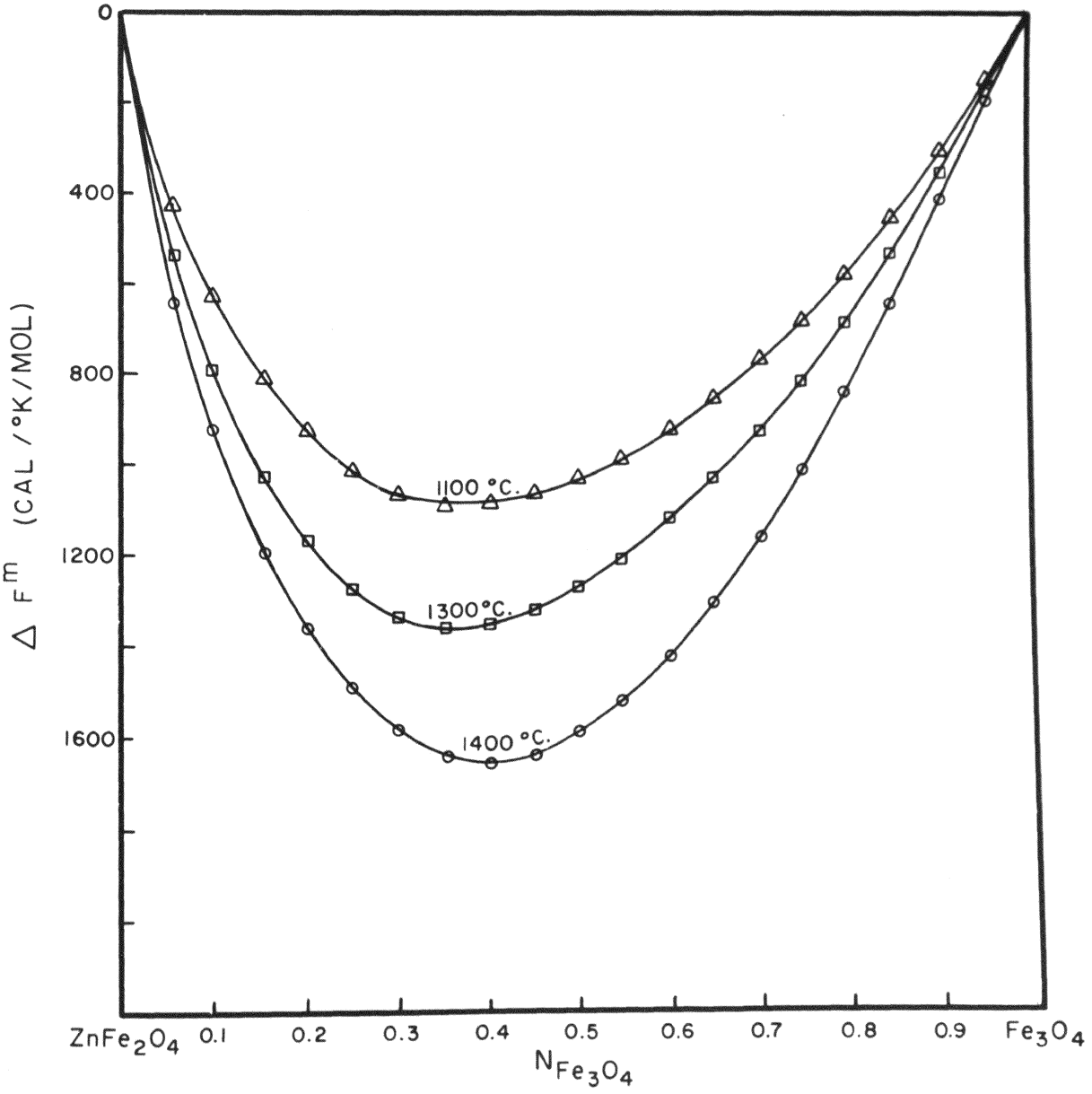

FIGURE 17. - Molar Free Energy of Mixing for the $ZnFe_2O_4$-Fe_3O_4 System.

TABLE X

MOLAR ENTHALPY OF MIXING

Mole Fraction Fe_3O_4	Enthalpy of Mixing cal/mole
0.00	000
0.05	324
0.10	675
0.15	830
0.20	995
0.25	1115
0.30	1197
0.35	1287
0.40	1374
0.45	1430
0.50	1338
0.55	1260
0.60	1149
0.65	1038
0.70	869
0.75	773
0.80	610
0.85	407
0.90	254
0.95	105
1.00	000

Entropy of Mixing. The foregoing free energies and enthalpies of mixing were used to calculate the entropies of mixing from the equation

$$\Delta S^M = \frac{\Delta H^M - \Delta F^M}{T} \qquad (5\text{-}24)$$

The experimental results are given in Table XI together with the values for two structural models, which were calculated from statistical considerations. The experimental results and the values for the models are also shown in Figure 19.

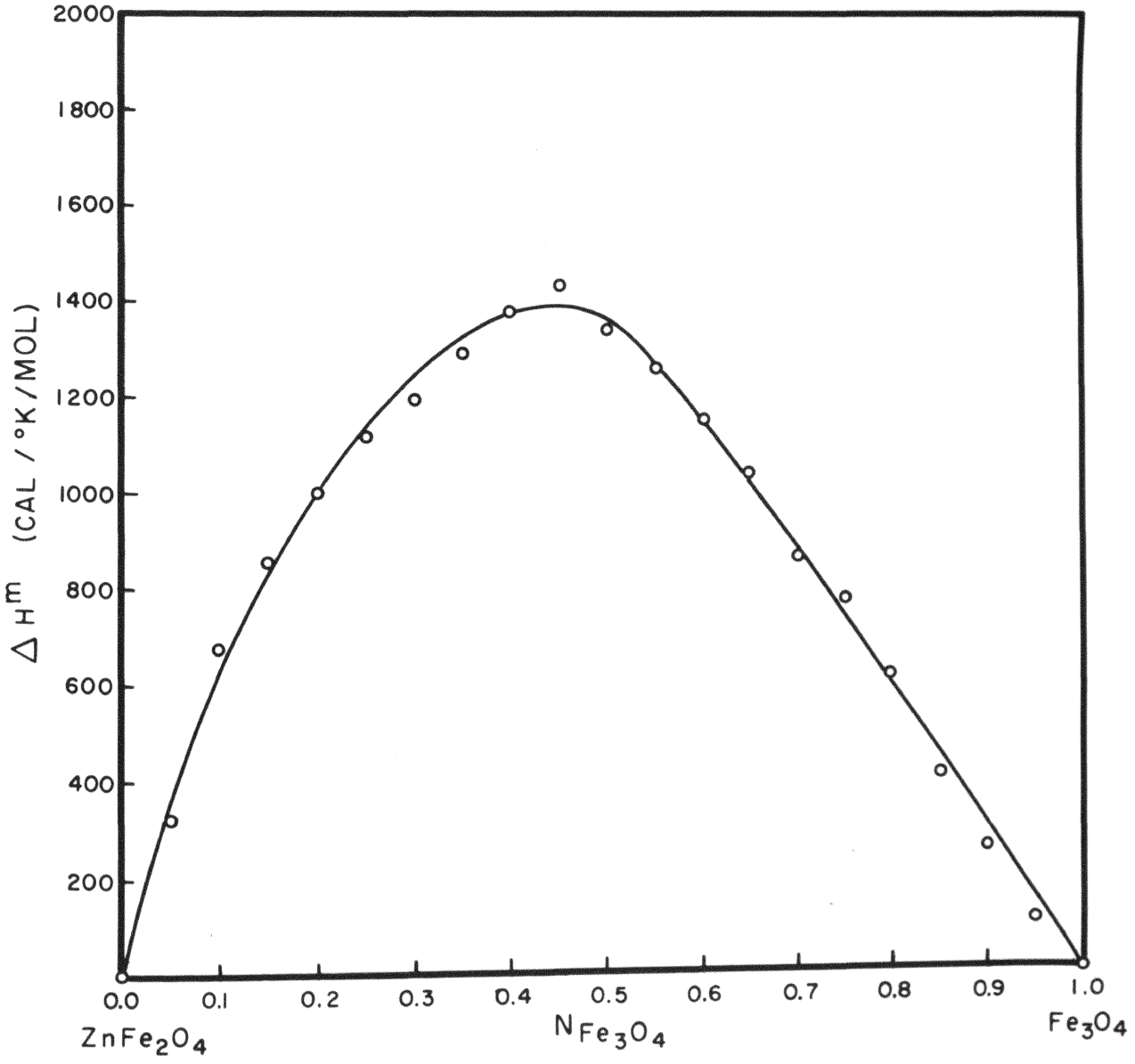

FIGURE 18. - Molar Enthalpy of Mixing for the $ZnFe_2O_4$-Fe_3O_4 System.

TABLE XI

MOLAR ENTROPIES OF MIXING

Mole Fraction Fe_3O_4	Experimental Values 1100°C	1300°C	1400°C	Statistical Models Ideal Solutions	Normal Plus Inverse Spinels
0.00	0.000	0.000	0.000	0.000	0.000
0.05	0.543	0.540	0.544		0.721
0.10	0.960	0.956	0.962	0.647	1.160
0.15	1.201	1.189	1.205		1.486
0.20	1.408	1.389	1.414	0.995	1.735
0.25	1.556	1.529	1.564		1.926
0.30	1.655	1.618	1.666	1.215	2.067
0.35	1.735	1.689	1.750		2.165
0.40	1.796	1.738	1.814	1.338	2.224
0.45	1.818	1.750	1.840		2.247
0.50	1.732	1.660	1.755	1.377	2.235
0.55	1.641	1.565	1.666		2.190
0.60	1.516	1.439	1.541	1.338	2.112
0.65	1.381	1.318	1.402		2.002
0.70	1.197	1.141	1.216	1.215	1.859
0.75	1.052	1.009	1.065		1.681
0.80	0.856	0.819	0.868	0.995	1.465
0.85	0.624	0.602	0.631		1.208
0.90	0.414	0.404	0.417	0.647	0.902
0.95	0.201	0.196	0.203		0.527
1.00	0.000	0.000	0.000	0.000	0.000

It can be noted from the figure that all the experimental curves exhibit the same general configuration. The 1100 and 1400°C curves coincide, and the values of the 1300°C curve are slightly lower. However, the most important feature to be noted is that all the curves are skewed toward the $ZnFe_2O_4$ side, with a maximum at $N_{Fe_3O_4} = 0.45$.

The structural models in this investigation represent two different methods of distributing the cations throughout a rigid oxygen ion lattice. The first of these represents an ideal-solution type of distribution. In this structure any cation, regardless of charge, has an equal probability of being found in a tetrahedral or

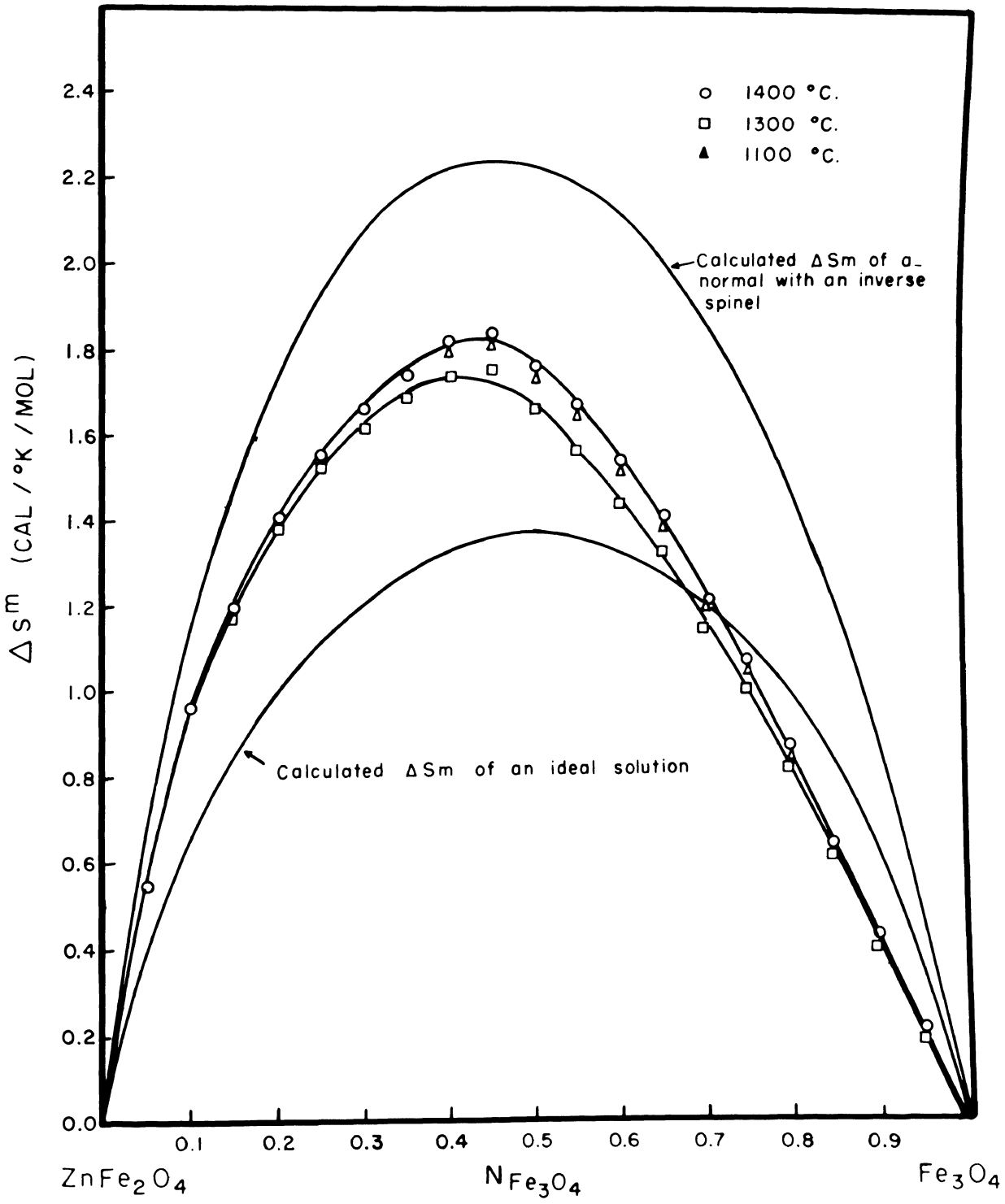

FIGURE 19. - Molar Entropies of Mixing for the $ZnFe_2O_4$-Fe_3O_4 System.

an octahedral void. The anions, however, are assumed fixed in a cubic close-packed lattice and are not affected by compositional change. The assumption of a rigid anion lattice is supported by experimental evidence: the number and relative position of the lines in the diffraction pattern remain constant for all the samples between $ZnFe_2O_4$ and Fe_3O_4.

By utilizing these assumptions and a knowledge of the structure, the entropy of mixing for the ideal-solution type structure can be derived as follows:

If the structure contained N oxygen ions, it would follow, from structural considerations, that the lattice would also contain 2N tetrahedral voids and N octahedral voids. Since the tetrahedral and octahedral voids are equivalent, there is a total of 3N voids throughout the lattice. If there are $\left(\frac{N}{4} - X\right)$ zinc ions, X ferrous ions, and $\frac{N}{2}$ ferric ions, all of which must be distributed over the 3N voids, then there are

$$W_p = \frac{(3N)!}{\left(\frac{N}{4} - x\right)!\,(x)!\left(\frac{N}{2}\right)!\left(3N - \frac{3N}{4}\right)!} \qquad (5\text{-}25)$$

ways of arranging all of the ions and the unoccupied voids.

If X = zero (pure $ZnFe_2O_4$) or if $X = \frac{N}{4}$ (pure Fe_3O_4), Equation 5-25 reduces to

$$W_p = W_{ZnFe_2O_4} = W_{Fe_3O_4} = \frac{(3N)!}{\left(\frac{N}{4}\right)!\,\left(\frac{N}{2}\right)!\,\left(3N - \frac{3N}{4}\right)!} \qquad (5\text{-}26)$$

Assuming no change in vibrational entropy, the entropy of mixing for the structure can be defined as

$$\Delta S^M = k(\ln W_p - X \ln W_{p_{Fe_3O_4}} - (1-X) \ln W_{p_{ZnFe_2O_4}}) \qquad (5\text{-}27)$$

where k is defined as the Boltzmann's constant. Substituting Equations 5-25 and 5-26 into Equation 5-27, and simplifying, gives

$$\Delta S^M + K \ln \frac{(\frac{N}{4})!}{(\frac{N}{4} - x)!\,(x)!} \qquad (5\text{-}28)$$

Equation 5-28 can be reduced further by using Stirling's approximation

$$\ln A! = A \ln A - A$$

where A is a very large number. The resultant equation is

$$\Delta S^M = k \left[\frac{N}{4} \ln \frac{N}{4} - X \ln X - \frac{N}{4} - X) \ln (\frac{N}{4} - X) \right] \qquad (5\text{-}29)$$

If N is defined as 4 No, where No is Avagadro's number, and each term of Equation 5-29 is divided by No, the result is

$$\Delta S^M = -R \left[Y \ln Y + (1-Y) \ln (1-Y) \right] \qquad (5\text{-}30)$$

where Y is the mole fraction Fe_3O_4. This equation is the ΔS^M of an ideal solution (See Fig. 19), with a maximum of 1.38 cal/degree/mol at Y = 0.50.

It is apparent from Figure 19 that the experimentally determined entropies of mixing do not approach that of the ideal solution. The experimental values show a maximum at Y = 0.45, and the general configuration of the curves does not exhibit much resemblance to that of the ideal solution. This comparison would imply that, although some randomness might exist within the structure, the majority of the cations exhibit some other type of distribution.

The second structural model represents the mixing of a normal with an inverse spinel structure. In this model the cations do not

have an equal probability of occupying the octrahedral and the tetrahedral voids, but they must occupy the same type void which they would occupy in the pure component. Thus, the zinc ions of the normal spinel and one-half of the ferric ions of the inverse spinel are randomly distributed throughout the tetrahedral voids while the ferric ions of the normal spinel together with the ferrous ions and remaining one-half of the ferric ions of the inverse spinel are randomly distributed throughout the octahedral voids. The oxygen lattice is, once again, assumed to be constant and unaffected by compositional change.

The derivation of the entropy of mixing for the second structural model is very similar to that of the ideal solution and proceeds as follows: For a structure containing N oxygen ions, there are 2N tetrahedral voids and N octahedral voids which are now distinguishable. If there are $\left(\frac{N}{4} - X\right)$ zinc ions and X ferric ions distributed over 2N tetrahedral voids, then there are

$$W_T = \frac{(2N)!}{\left(\frac{N}{4} - x\right)!(x)!\left(2N - \frac{N}{4}\right)!} \qquad (5\text{-}31)$$

ways of arranging the ions and the unoccupied tetrahedral voids.

Likewise, if X ferrous ions and $\left(\frac{N}{2} - X\right)$ ferric ions are distributed over N octahedral voids, then there are

$$W_o = \frac{(N)!}{\left(\frac{N}{2} - x\right)!(x)!\left(N - \frac{N}{2}\right)!} \qquad (5\text{-}32)$$

ways of arranging the ions and the unoccupied octahedral voids. If the distributions of Equations 5-31 and 5-32 are independent and show no interaction, there are

$$W_P = W_T W_O = \frac{(2N)!\ (N)!}{\left(\frac{N}{4}-x\right)!\left(\frac{N}{2}-x\right)!(x!)^2\left(\frac{7N}{4}\right)!\ \left(\frac{N}{2}\right)!} \qquad (5\text{-}33)$$

total ways of distributing the cations throughout the lattice. If X = zero (pure $ZnFe_2O_4$), Equation 5-33 reduces to

$$W_{P_{ZnFe_2O_4}} = \frac{(2N)!\ (N)!}{\left(\frac{N}{4}\right)!\ \left[\left(\frac{N}{2}\right)!\right]^2\ \left(\frac{7N}{4}\right)!} \qquad (5\text{-}34)$$

Similarly, if $X = \frac{N}{4}$ (pure Fe_3O_4), Equation 5-33 reduces to

$$W_{P_{Fe_3O_4}} = \frac{(2N)!\ (N)!}{\left[\left(\frac{N}{4}\right)!\right]^3\ \left(\frac{N}{2}\right)!\ \ \left(\frac{7N}{4}\right)!} \qquad (5\text{-}35)$$

By substituting Equations 5-34 and 5-35 in Equation 5-27 and by using all of the simplifying procedures of the ideal solution derivation, the entropy of mixing a normal with an inverse spinel can be shown to be[13]

$$\Delta S^M = -R\left[\ Y\ \ln\ Y\ +\ (1-Y)\ \ln\ (1-Y)\ +\ (2-Y)\ln\ (2-Y)\right.$$
$$\left.+\ (1-Y)\ \ln\ 4\right]. \qquad (5\text{-}36)$$

The graph of Equation 5-36, (Fig. 19) exhibits a maximum at Y = 0.45 and is skewed toward the $ZnFe_2O_4$ side. The general configuration of the graph resembles those of the experimental results, implying that the structure of the real system approaches this model more closely than that of the ideally random solution. This would suggest that the normal and the inverse structures substantially maintain their identity in the solid solution, even at the very high temperatures of this investigation.

---

[13] See Appendix C for the complete derivation.

CHAPTER VI

THERMODYNAMIC EVALUATION OF THE Zn-Fe-S-O SYSTEM

Thus far, the investigation has been concerned with the thermodynamic properties of the spinel solid solution region of the $ZnO-Fe_2O_3-Fe_3O_4$ system and with the effect of temperature and oxygen pressure on these properties. The experimental results of Chapter IV and the data in Figures 5, 6, and 7 showed that high temperatures and low oxygen pressures promote the dissociation of $ZnFe_2O_4$ and that the composition of the resultant spinel solid-solution is a function of temperatures and oxygen pressure. However, the question of why zinc metallurgists have found an increase in ferrite formation with increased roasting temperatures has not been answered.

In an attempt to answer this question, the thermodynamic properties of the Zn-Fe-S-O system were calculated from data of this investigation together with data from other investigators. Because of the complexity of the problem, the thermodynamic properties of the ternary system of Zn-S-O and Fe-S-O were calculated first; then the thermodynamic properties of the ternary systems were combined to give the Zn-Fe-S-O system. The calculations were further simplified by assuming the following conditions:

1. The free energy of reaction equations are linear functions of temperature.
2. Reactions regarding basic sulfates were not considered.
3. All solid phases are pure and are completely immiscible in one another, with the exception of ZnO, Fe_2O_3 and Fe_3O_4.

4. Only two types of reactions were considered: those involving oxygen or oxygen plus SO_2, and those involving solid-solid ion exchanges.

By applying the foregoing conditions, compound stability diagrams were constructed for each ternary system from the thermodynamic properties of the system. These diagrams depict regions of compound stability, separated by boundary lines that represent the equations of equilibrium for the compounds.

In order to show the effects of temperature and oxygen pressure on compound stability during roasting, the coordinates of the diagrams are plotted as logarithm of oxygen pressure versus the reciprocal of absolute temperature, at a constant SO_2 pressure. The effects of SO_2 pressure were shown by constructing the diagrams at two different SO_2 pressures. In constructing the diagrams of the Zn-Fe-S-O systems, the SO_2 pressures of $1X10^{-1}$ and $1X10^{-5}$ atmospheres were selected. The first of these was selected because roasters frequently operate in this range whereas the second was selected to illustrate the effect very low SO_2 pressures have on the system. Only the 0.1 atmosphere systems of Zn-S-O and Fe-S-O are illustrated in this report; however, both pressure levels are shown for the Zn-Fe-S-O system.

Zn-S-O System. Because of the interest in roasting ZnS, considerable data have been tabulated on the thermodynamic properties of the Zn-S-O system.[1] Within the system, the following compounds are

---

[1] L. Wohler, W. Phuddemann, and P. Wohler. Ber. deut Chem. Ges., Vol. 41 (1908), p. 703.
G. Hoschek. Monatsh Chem., Vol. 93, No. 4 (1962), p. 826.
H. Floud and N. Boye. Z. Elektrochem. Vol. 66, No. 2 (1962), p. 184.
T. R. Ingraham and H. H. Kellogg. Trans. Met. Soc. AIME, Vol. 227 (1963), p. 1419.

known to exist: ZnS, ZnO, $ZnSO_4$, $ZnSO_4$, $ZnO.2ZnSO_4$, SO_2 and SO_3. However, because of the conditions found in a roaster and because of the simplifications noted previously, only the compounds of ZnS, and ZnO, $ZnSO_4$, and SO_2 were considered in this study. Table XII gives equations for the free energy of formation of these compounds, as presented in the literature. These equations were used to calculate the free energy of reaction equations 1, 2, 3, and 4, which are also shown in Table XII. The reaction equations were then used to establish the boundary lines between regions of stability. An example of this procedure follows:

When reaction No. 1 is considered[2], the low temperature free energy equation is given as

$$\Delta F = -156,800 + 125.28T \quad .$$

However, the free energy equation can also be written as

$$\Delta F = 12.303\ RT \log_{10} K_{eq}, \qquad (6\text{-}1)$$

where K_{eq} is defined as the equilibrium constant. Since the condensed phases are considered pure and immiscible according to condition 3, the equilibrium constant can be expressed as

$$K_{eq} = (P_{O_2})^{-1} \ (P_{SO_2})^{-2} \quad ,$$

where P_{O_2} and P_{SO_2} are the pressure of oxygen and the pressure of SO_2,

---

[2] T. R. Ingraham and H. H. Kellogg, Ibid., p. 1425. Ingraham and Kellogg showed that this reaction does not exist and that the basic sulfate $ZnO.2ZnSO_4$ is an intermediate phase between ZnO and $ZnSO_4$. However, the SO_2 and oxygen pressure range, over which the basic sulfate is stable, is small in comparison with the stability range of ZnO and $ZnSO_4$; therefore, the basic sulfate was neglected in this investigation.

TABLE XII

FREE ENERGY DATA FOR THE Zn-S-O SYSTEM

Reaction	Temperature Range °K	ΔF° cal/mole	Reference
$Zn_{\substack{\text{solid}\\\text{liquid}\\\text{gas}}} + \frac{1}{2}S_{2(gas)} + 2O_{2(gas)} \rightarrow ZnSO_{4(sol)}$	298-1180 1180-	249,500 + 105.5T 277,000 + 128.8T	a*
$Zn_{\substack{\text{solid}\\\text{liquid}\\\text{gas}}} + \frac{1}{2}S_{2(gas)} \rightarrow ZnS_{(solid)}$	298-693 693-180 1180-1500	-60,565 + 22.70T -61,740 + 24.27T -89,165 + 47.50T	b
$Zn_{\substack{\text{solid}\\\text{liquid}\\\text{gas}}} + \frac{1}{2}O_{2(gas)} \rightarrow ZnO_{(solid)}$	298-693 693-1180 1180-1500	-83,100 + 23.57T -84,480 + 25.55T -110,140 + 47.35T	c
$\frac{1}{2}S_{2(gas)} + O_{2(gas)} \rightarrow SO_{2(gas)}$	298-	-86,620 + 17.31T	c
$SO_2 + \frac{1}{2}O_2 \rightarrow SO_3$	298-	-22,600 + 21.36T	d
(1) $2ZnO + 2SO_2 + O_2 \rightarrow 2ZnSO_4$	693-1180 1180-1500	-156,800 + 125.28T -160,400 + 128.28T	
(2) $ZnS + \frac{3}{2}O_2 \rightarrow ZnO + SO_2$	693-1180	-109,360 + 18.59T -107,595 + 17.16T	

* See references at the end of table.

TABLE XII
(continued)

Reaction	Temperature Range °K	ΔF^{o} cal/mole	Reference
(3) $ZnS + 2O_2 \longrightarrow ZnSO_4$	298-693 693-1180	-188,935 + 82.2T -187,760 + 81.2T	
(4) $3ZnSO_4 + ZnS \longrightarrow 4ZnO + 4SO_2$	693-1180	+125,700 - 169.4T	

[a]C. H. Mathewson, Zinc, The Science and Technology of Metal, Its Alloys and Compounds. Amer. Chem. Soc. Monograph Ser. No. 142, Reinhold Pub. Corp.

[b]F. D. Richardson and J.H.E. Jeffes, J. Iron Steel Inst., Vol. 170, p. 165 (1952).

[c]J. P. Coughlin, U.S. Bureau of Mines, Bull. 542 (1954).

[d]The remaining reactions were derived by addition or subtraction of the proper free energy of formation equations given above.

respectively. By substituting this expression into Equation 6.1, setting the equation equal to the tabulated free energy equation, and simplifying, an expression of $\log_{10} P_{O_2}$ can be obtained in terms of temperature and $\log_{10} P_{SO_2}$,

$$\log_{10} P_{SO_2} = (-34{,}280/T) + 27.38 - 2\log_{10} P_{SO_2}.$$

This equation is then used to establish the boundary line between ZnO and $ZnSO_4$ at a constant SO_2 pressure, as shown in Figure 20. From Equation 1 and the application of Le Chatelier's principle, it can be seen that sustained oxygen pressure greater than the equilibrium values would force the system completely to the $ZnSO_4$ side of the equation. Therefore, $ZnSO_4$ is the stable compound above the number 1 boundary line. Application of similar procedures to Equations 2 and 3 results in a completed diagram (Figure 20) with three regions of stability. The solutions to equations 1, 2, 3, and 4, together with the material needed to construct Figure 20, are shown in Table XIII. Equation 4 represents the point of intersection of all three boundaries and gives the invarient point in Figure 20, because the SO_2 pressure is held constant.

Fe-S-O System. There has been less interest in roasting FeS; therefore, fewer thermodynamic properties have been tabulated for the Fe-S-O system. Although the compounds of FeS_2, FeS, FeO, Fe_3O_4, Fe_2O_3, $FeSO_4$, $Fe_2(SO_4)_3$, SO_2, and SO_3 are known to exist, there are probably a number of basic sulfates and other complex compounds that also exist within the system. Of the known compounds, experimentally determined free energy data exist for FeS_2, FeS, FeO, Fe_3O_4, and Fe_2O_3.

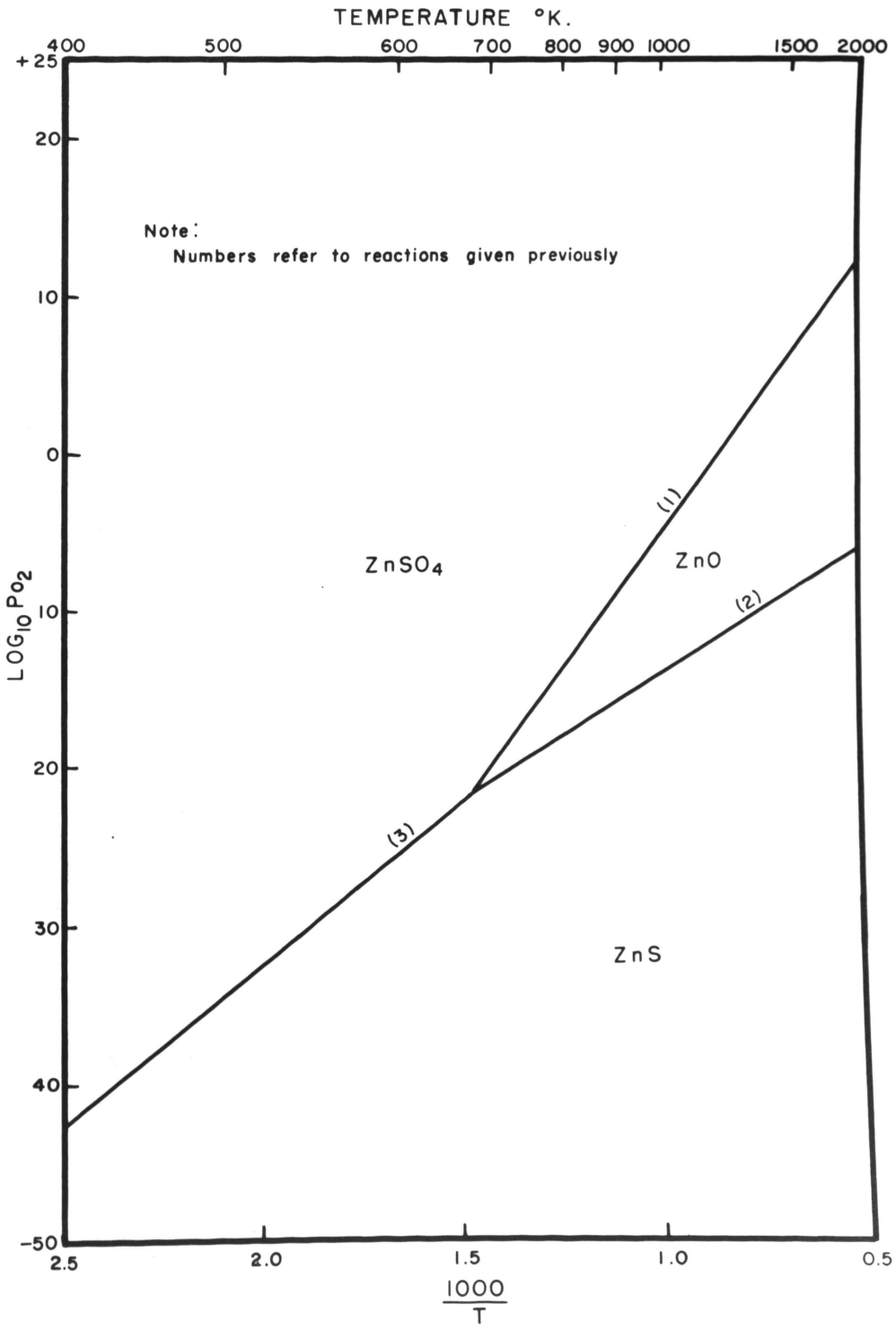

FIGURE 20. - Zn-S-O Compound Stability Diagram at a Constant SO_2 Pressure of 0.1 Atmospheres.

TABLE XIII

TEMPERATURE AND OXYGEN PRESSURE DATA FOR THE Zn-S-O COMPOUND STABILITY DIAGRAM

Reaction	Temperature °K	ΔF^{o}	P_{SO_2} Atmospheres	$\log_{10} P_{O_2}$
(1) $ZnO + SO_2 + \frac{1}{2} O_2 \rightleftharpoons ZnSO_4$	1200	3,100	0.1	+0.9
			$1X10^{-5}$	+7.5
	700	-34,600	0.1	-19.6
			$1X10^{-5}$	-11.5
(2) $ZnS + \frac{3}{2} O_2 \rightleftharpoons ZnO + SO_2$	1200	-87,100	0.1	-11.2
			$1X10^{-5}$	-14.1
	700	-96,300	0.1	-20.7
			$1X10^{-5}$	-23.3
(3) $ZnS + 2 O_2 \rightleftharpoons ZnSO_4$	600	-139,635	0.1	25.0
			$1X10^{-5}$	25.0
	400	-156,085	0.1	42.8
			$1X10^{-5}$	42.8
(4) $3ZnSO_4 + ZnS \rightleftharpoons 4ZnO + 4SO_2$	670	12,200	0.1	-21.8
	482	12,200	$1X10^{-5}$	-34.2

In addition, Moore and Kelly[3] have published ΔH°_{298} and ΔS°_{298} values for $FeSO_4$ which permit the estimation of the free energy of formation at any temperature. This estimate employs the assumption that the change in heat capacity (ΔC_p) for the reaction equals zero at all temperatures and that

$$\Delta F_T = \Delta H^{\circ}_{298} - T\Delta S^{\circ}_{298}$$

Although this assumption is not necessarily true, the equation does give a good first approximation for the free energy of reaction at any temperature.[4]

The foregoing free energy data were not sufficient to construct a compound stability diagram, however, and a free energy of formation equation for $Fe_2(SO_4)$ had to be developed. The equation was developed from published[5] decomposition pressures of the sulfate. In general, the decomposition pressure measured is the sum of the partial pressures of SO_3, SO_2 and O_2, because the decomposition occurs in two steps. The first of these is the decomposition of the sulfate,

$$Fe_2(SO_4)_3 \rightleftharpoons Fe_2O_3 + 3SO_3 \qquad (6\text{-}2)$$

the second is the decomposition of the sulfur trioxide

$$2SO_3 \rightleftharpoons 2SO_2 + O_2$$

By considering the thermodynamic properties[6] and stoichiometry of the second reaction, the partial pressures of SO_3, SO_2, and O_2 can be

---

[3] G. E. Moore, K. K. Kelley. J. Amer. Chem. Soc., Vol. 64 (1942), p. 2949.

[4] O. Kubaschewski and E. Evans. Metallurgical Thermochemistry. New York, Pergamon Press (1958).

[5] N. A. Warner and T. R. Ingraham. Can. J. Chem., Vol. 38 (1960), p. 2196.

[6] K. K. Kelley. U. S. Bureau of Mines Bull. 406 (1937), p. 14.

calculated. Employing this procedure, Warner and Ingraham[7] derived the equation

$$\log_{10} \left(P_{SO_3}\right)^3 = 28.34 - (29{,}600/T) \qquad (6\text{-}3)$$

where P_{SO_3} is expressed in atmospheres, and the temperature (T) is between 630° and 724° C.

Applying the relationship

$$\Delta F = -2.303\ RT \log_{10} \left(P_{SO_3}\right)^3$$

to Equation 6-3, a linear free energy equation

$$\Delta F = 135{,}400 - 129.7T \qquad (6\text{-}4)$$

was derived for the reaction given in 6-2.

By combining this equation with the free energy of formation equations of SO_3 and Fe_2O_3[8], it was possible to calculate the free energy equation of $Fe_2(SO_4)_3$ from its elements according to the reaction

$$2Fe_{(\alpha)} + \tfrac{3}{2}S_2\ (gas) + 6O_2 = Fe_2(SO_4)_3\ (solid) \qquad (6\text{-}5)$$

The value of this free energy equation is

$$\Delta F = -656{,}620 + 305.1T\ . \qquad (6\text{-}6)$$

In order to determine if Equation 6-6 was a fair estimate of the free energy and to determine if it was valid over a wide range of temperature, an alternate method was used to calculate a free energy

---

[7]N. A. Wagner and T. R. Ingraham. Can. J. Chem., Vol. 38 (1960), p. 2196.

[8]J. P. Coughlin, U. S. Bureau of Mines Bull. 542 (1954).

equation. This method employs the approximation, mentioned earlier, of

$$\Delta F_T = \Delta H^\circ_{298} - T\Delta S^\circ_{298} \qquad (6\text{-}7)$$

where ΔH°_{298} and ΔS°_{298} now represent the standard heat of formation and entropy change, respectively, of $Fe_2(SO_4)_3$, according to the reaction given in Equation 6-5.

Utilizing the heats of the reactions

$$Fe_{\alpha} + 3S_{(rh)} + 6O_{2(gas)} = Fe_2(SO_4)_{3(solid)}$$

$$\Delta H^\circ_{298} = 640{,}000 \text{ cal}^*$$

and

$$\tfrac{3}{2}S_{2(gas)} = 3S_{(rh)}$$

$$\Delta H^\circ_{298} = -46{,}500^{**}$$

it was possible to calculate the heat of formation for $Fe_2(SO_4)_3$

$$\Delta H^\circ_{298} = -686{,}500 \text{ cal} \qquad (6\text{-}8)$$

as it is shown in the reaction of 6-2.

Calculation of the entropy change (ΔS°_{298}) for Equation 6-7 was not as easy, however, because standard entropy values for all of the constituents were not available. It was necessary to estimate the entropy value of $Fe_2(SO_4)_3$ with a method devised by Latimer.[9] In this method the compound is considered to be the sum of an equivalent number of cations and anions for example:

$$Fe_2(SO_4)_3 = 2Fe^{+3} + 3(SO_4)^{-2}.$$

---

* J. A. Hedvall and Heuberger. Z. Anorg. Ch., Vol. 128 (1923), p. 5.
** K. K. Kelley. Op. Cit., p. 6.

[9] W. M. Latimer. J. Amer. Chem. Soc., Vol. 73 (1951), p. 1480.

The standard entropy of this compound is likewise the sum of an equivalent number of cationic and anionic entropies which have been empirically determined from the size, the charge, and the mass of the ions.

Employing the ionic entropies given in Table XIV, the standard entropy of $Fe_2(SO_4)_3$ was estimated as

$$S_{298} = 2(10.4) + 3\ (13.7) = 61.9 \text{ cal/degree.} \qquad (6\text{-}9)$$

The value was combined with the standard entropies of the elements given in Table XIV to calculate the entropy change of the reaction given in 6-2:

$$\Delta S^{o}_{298} = -326.9 \text{ cal/degree} \qquad (6\text{-}10)$$

TABLE XIV

STANDARD ENTROPY VALUES OF THE CONSTITUENTS OF $Fe_2(SO_4)_3$

Constituent	Entropy value at 298°K cal/degree	Reference
$Fe\ \alpha$	6.49	a
$S_{2(gas)}$	54.50	a
$O_{2(gas)}$	49.01	a
Fe^{+3}	10.4	b
$(SO_4)^{-2}$	13.7	b

[a]K. K. Kelley, E. G. Kin. U. S. Bureau of Mines Bull. 592 (1961).
[b]W. M. Latimer. J. Amer. Chem. Soc., Vol. 73 (1951), p. 1480.

Substituting Equations 6-8 and 6-10 into 6-7 gives the estimated free energy equation

$$\Delta F_T = -686{,}500 + 326.9T \qquad (6\text{-}11)$$

Free energy values from this equation are in good agreement with the values from Equation 6-6, varying from 4 to 7 percent within the temperature range from 298° to 1500°K. This would indicate the Equation 6-6 is probably a good estimate of the free energy of formation equation of $Fe_2(SO_4)_3$.

Equation 6-6 together with the free energy of formation equations for FeS, FeO, Fe_3O_4, Fe_2O_3, $FeSO_4$, SO_2, and SO_3 are listed in Table XV. The values of FeS_2 are not shown because it decomposes quite readily into FeS and S. Also given in the table are the free energy of reaction equations needed to calculate the boundary lines in Figure 21. The solutions to the reaction equations, in terms of $\log_{10}P_{O_2}$ and temperature, are given in Table XVI and are shown graphically in Figure 21. It can be seen from the figure that only reactions a, b, c, d, and e are stable within the temperature and atmospheric conditions of the figure (temperature, between 400° and 2000°K, $\log_{10} P_{O_2}$, between -50 and +25; and SO_2 pressure, equal to 0.1 atmospheres). The expressions of $\log_{10}P_{O_2}$ in terms of temperature were obtained by the same procedures used in the Zn-S-O system. The Fe-S-O system shows two invarient points, which are given by Equations m and n.

Zn-Fe-S-O System. The compound stability diagrams of the Zn-Fe-S-O system were constructed by superimposing the Zn-S-O system onto the Fe-S-O system. The reactions of the individual systems were assumed to be independent of each other, and the boundaries were assumed not altered by the superposition. By combining the two ternary systems, the Zn-Fe-S-O diagram was divided into areas where a zinc compound was stable with an iron compound. Reactions between

TABLE XV

FREE ENERGY DATA FOR THE Fe-S-O SYSTEM

Reaction	Temperature Range °K	ΔF° cal/mole	Reference
$Fe_{\alpha}^{\gamma} + \frac{1}{2} S_{2(gas)} \longrightarrow FeS_{(solid)}$	412-1300	-36,020 + 12.65T	* α
$0.947Fe_{(\alpha,\gamma)} + \frac{1}{2} O_{2(gas)} \longrightarrow Fe_{0.947}O$ (solid)	298-1650	-63,200 + 15.47T	β
$3Fe_{\alpha}^{\gamma} + 2O_{2(gas)} \longrightarrow Fe_3O_4$(magnetite)	298-900 900-1803	-265,660 + 76.81T -261,200 + 71.36T	β
$2Fe_{\alpha}^{\gamma} + \frac{3}{2} O_{2(gas)} \longrightarrow Fe_2O_3$(hematite)	298-950 950-1800	-195,450 + 61.38T -192,680 + 58.21T	γ
$2Fe_{(solid)} + \frac{1}{2} S_{2(gas)} + 2O_{2(gas)} \longrightarrow FeSO_4$ (solid)	298-	-221,300 + 106.22T	ε
$2Fe_{(solid)} + \frac{3}{2}S_{2(gas)} + 6O_{2(gas)} \longrightarrow Fe_2(SO_4)_3$ (solid)	298-1500	-656,620 + 305.1T	ζ
$\frac{1}{2} S_{2(gas)} + O_{2(gas)} \longrightarrow SO_{2(gas)}$	298-2000	-86,520 + 17.48T	β
$\frac{1}{2} S_{2(gas)} + \frac{3}{2} O_{2(gas)} \longrightarrow SO_{3(gas)}$	298-1500	-109,550 + 39.09	β
(a) $Fe_2O_3 + \frac{3}{2} O_2 + 3SO_2 \rightleftharpoons Fe_2(SO_4)_3$	298-950 950-1500	-201,610 + 188.3T -204,380 + 194.4T	
(b) $4Fe_3O_4 + O_2 \rightleftharpoons 6Fe_2O_3$	298-900 900-1803	-110,060 + 61.04T -111,280 + 63.82T	

* See references at the end of table.

TABLE XV
(continued)

Reaction	Temperature Range °K	ΔF^{o} cal/mole	Reference
(c) $3FeS + 5O_2 \rightleftharpoons Fe_3O_4 + 3SO_2$	412-900 900-1300	-417,160 + 91.30T -412,700 + 85.85T	
(d) $2FeS + \frac{7}{2} O_2 \rightleftharpoons Fe_2O_3 + 2SO_2$	412-950 950-1300	-397,730 + 80.60T -394,880 + 77.40T	
(e) $2FeS + 5O_2 \rightleftharpoons Fe_2(SO_4)_3$	412-1300	-498,060 + 262.3T	
(f) $2FeSO_4 + SO_2 + O_2 \rightleftharpoons Fe_2(SO_4)_3$	298-	-137,500 + 75.2T	
(g) $Fe_2O_3 + \frac{1}{2} O_2 + 2SO_2 \rightleftharpoons 2FeSO_4$	298-950 950-1800	-74,110 + 116.1T -76,960 + 119.3T	
(h) $Fe_3O_4 + 3SO_2 + O_2 \rightleftharpoons 3FeSO_4$	298-900 900-1803	-138,680 + 189.41T -143,140 + 194.86T	
(i) $FeS + 2O_2 \rightleftharpoons FeSO_4$	412-1300	-185,420 + 93.52T	
(j) $FeS + \frac{3}{2} O_2 \rightleftharpoons FeO + SO_2$	298-1300	-113,700 + 20.3T	[illegible]
(k) $3FeO + \frac{1}{2} O_2 \rightleftharpoons Fe_3O_4$	298-900 900-1650	-76,060 + 30.4T -71,600 + 24.9T	[illegible]
(m) $10Fe_2O_3 + 27SO_2 \rightleftharpoons 7Fe_2(SO_4)_3 + 6FeS$	412-950	-521,920 + 1125.8T	
(n) $7Fe_3O_4 + SO_2 \rightleftharpoons 10Fe_2O_3 + FeS$	412-900	-44,380 + 71.3T	

TABLE XV
(continued)

[α] F. D. Richardson and J.H.E. Jeffes. J. Iron Steel Inst., Vol. 170, p. 165 (1952).

Average of two equations: $Fe + \frac{1}{2} S_{2(gas)} \quad FeS$, 412-1179°K, 35,910 + 12.56T

$Fe + \frac{1}{2} S_{2(gas)} \quad FeS$, 1179-1300°K, 36,070 + 12.74T

[β] J. P. Coughlin, U. S. Bureau of Mines Bull. 542 (1954).

[γ] Ibid.

Average of two equations: $2Fe + \frac{3}{2}O_2 \quad Fe_2O_3$ (,) 950-1179°K, 192,800 + 58.30T

$2Fe + \frac{3}{2}O_2 \quad Fe_2O_3$ ( ) 1179-1800°K, 192,550 + 58.12T

[ε] G. E. Moore and K. K. Kelley. J. Amer. Chem. Soc., Vol. 64, pp. 2949-2951 (1942)

Assuming $F_T = H_{298} - T\ S_{298}$

[ζ] Derived from equation in the text and the above free energies of formation.

[η] For simplicity, $Fe_{0.947}O$ was assumed to be stoichometric FeO.

TABLE XVI

TEMPERATURE AND OXYGEN PRESSURE DATA FOR THE Fe-S-O COMPOUND STABILITY DIAGRAMS

Reaction	Temperature °K	ΔF^{o} Cal	SO_2 Pressure Atmosphere	$\log_{10} P_{O_2}$
(a) $Fe_2O_3 + \frac{3}{2} O_2 + 3SO_2 \rightleftharpoons Fe_2(SO_4)_3$	400	-126,290	0.1	-44.01
			$1X10^{-5}$	-36.01
	750	-60,385	0.1	-9.73
			$1X10^{-5}$	-1.73
	1000	-13,310	0.1	+0.06
			$1X10^{-5}$	+8.06
	1500	-80,840	0.1	+9.85
			$1X10^{-5}$	+17.85
(b) $4Fe_3O_4 + O_2 \rightleftharpoons 6Fe_3O_4$	400	-85,640		-46.8
	750	-64,280		-18.7
	1000	-47,460		-10.3
	1500	-15,550		-2.2

TABLE XVI
(continued)

Reaction	Temperature °K	ΔF^{o} Cal	SO_2 Pressure Atmosphere	$\log_{10} P_{O_2}$
(c) $3FeS + 5O_2 \rightleftharpoons Fe_3O_4 + 3SO_2$	400	-380,640	0.1	-46.8
			$1X10^{-5}$	-42.2
	750	-348,685	0.1	-18.7
			$1X10^{-5}$	-20.9
	1000	-326,850	0.1	-10.3
			$1X10^{-5}$	-14.8
	1500	-283,925	0.1	-2.2
			$1X10^{-5}$	-8.8
(d) $2FeS + \frac{7}{2} O_2 \rightleftharpoons Fe_2O_3 + 2SO_2$	400	-286,034	0.1	-42.4
			$1X10^{-5}$	-44.7
	750	-243,170	0.1	-20.8
			$1X10^{-5}$	-23.1
	1000	-225,810	0.1	-14.6
			$1X10^{-5}$	-16.9
	1500	-191,875	0.1	-8.5
			$1X10^{-5}$	-10.8

TABLE XVI
(continued)

Reaction	Temperature °K	F° Cal	SO_2 Pressure Atmosphere	$\log_{10} P_{O_2}$
(e) $2FeS + 5O_2 + SO_2 \rightleftharpoons Fe_2(SO_4)_3$	400	-393,140	0.1	-42.6
			$1X10^{-5}$	-41.8
	1500	-104,710	0.1	-2.8
			$1X10^{-5}$	-2.5
(f) $2FeSO_4 + SO_2 + O_2 \rightleftharpoons Fe_2(SO_4)_3$	400	-97,418	0.1	-52.2
			$1X10^{-5}$	-48.2
	1500	-14,730	0.1	-1.1
			$1X10^{-5}$	+2.8
(g) $Fe_2O_3 + \frac{1}{2}O_2 + 2SO_2 \rightleftharpoons 2FeSO_4$	400	-27,670	0.1	-26.2
			$1X10^{-5}$	-10.2
	750	+12,965	0.1	+11.5
			$1X10^{-5}$	+27.5
(h) $Fe_3O_4 + 3SO_2 + O_2 \rightleftharpoons 3FeSO_4$	400	-62,916	0.1	-31.3
			$1X10^{-5}$	-19.3
	750	+3,377	0.1	+3.9
			$1X10^{-5}$	+15.9

TABLE XVI
(continued)

Reaction	Temperature °K	ΔF^{o} Cal	SO_2 Pressure Atmosphere	$\log_{10} P_{O_2}$
(i) $FeS + 2O_2 \rightleftharpoons FeSO_4$	400	-147,872		-40.4
	1500	-45,000		-3.2
(j) $FeS + \frac{3}{2} O_2 \rightleftharpoons FeO + SO_2$	400	-32,500	0.1 $1X10^{-5}$	-12.5 -15.1
	1000	-83,250	0.1 $1X10^{-5}$	-8.7 -11.4
(k) $3FeO + \frac{1}{2} O_2 \rightleftharpoons Fe_3O_4$	400	-63,900		-69.8
	750	-53,260		-31.0
	1000	-46,650		-20.4
	1500	-34,175		-9.9
(m) $10Fe_2O_3 + 27SO_2 \rightleftharpoons 7Fe_2(SO_4)_3 + 6FeS$	420	-49,170	0.1	-39.8
(n) $7Fe_3O_4 + SO_2 \rightleftharpoons 10Fe_2O_3 + FeS$	584	-2,640	0.1	-27.7
	471	-10,800	$1X10^{5}$	-37.4

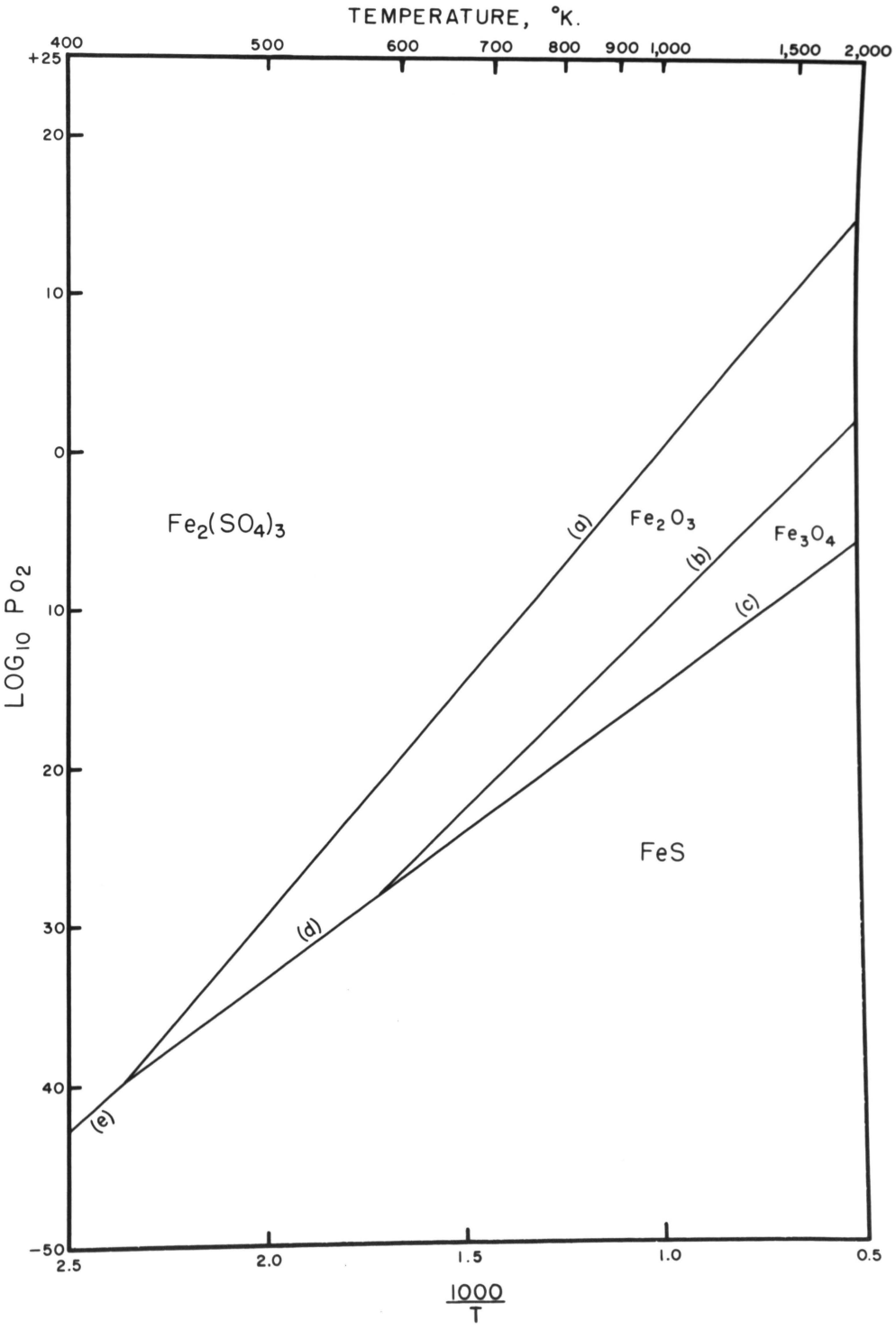

FIGURE 21. - Fe-S-O Compound Stability Diagram at a Constant SO_2 Pressure of 0.1 Atmospheres.

the compounds were considered and, with the exception of ZnO plus Fe_2O_3 or Fe_3O_4, were found to be thermodynamically unstable. The reactions between ZnO and Fe_2O_3 or Fe_3O_4 were assumed to produce $ZnFe_2O_4$ and the free energy of this reaction was assumed to be small in comparison with reaction between ZnO and $ZnSO_4$ (reaction 1). Thus, when the ternary systems were superimposed, line 1 was not altered. Under actual conditions, however, line 1 is probably displaced slightly to the left of its position in Figures 22 and 23.

If attention is now confined to the ordinary conditions of roasting ($\log_{10}P_{O_2}$ between minus 1 and minus 2). Figure 22 shows three regions of stability: $ZnSO_4$ plus $Fe_2(SO_4)_3$, $ZnSO_4$ plus Fe_2O_3, and $ZnFe_2O_4$. These same three regions have been observed by Umethu and Suzuki[10] in their investigation of recovery of zinc from $ZnFe_2O_4$. What is more significant, however, is that they reported the boundary temperatures (reactions a and 1 on the figure) to be approximately 630°C and 750°C, which are in fair agreement with those shown in the figure at approximately 670°C (943°K) and 800°C (1070°K). They have also noted that these boundary temperatures tend to decrease as the SO_2 pressure is decreased, substantially what is found when Figure 22 is compared with Figure 23.

All of these experimental findings indicate that Figures 22 and 23 give a good qualitative representation of the Zn-Fe-S-O system under roasting conditions. They also indicate that the conditions assumed in

---

[10] Y. Umethu and S. Suzuki. J. Mining Inst. Japan, Vol. 68 (1952), p. 529.

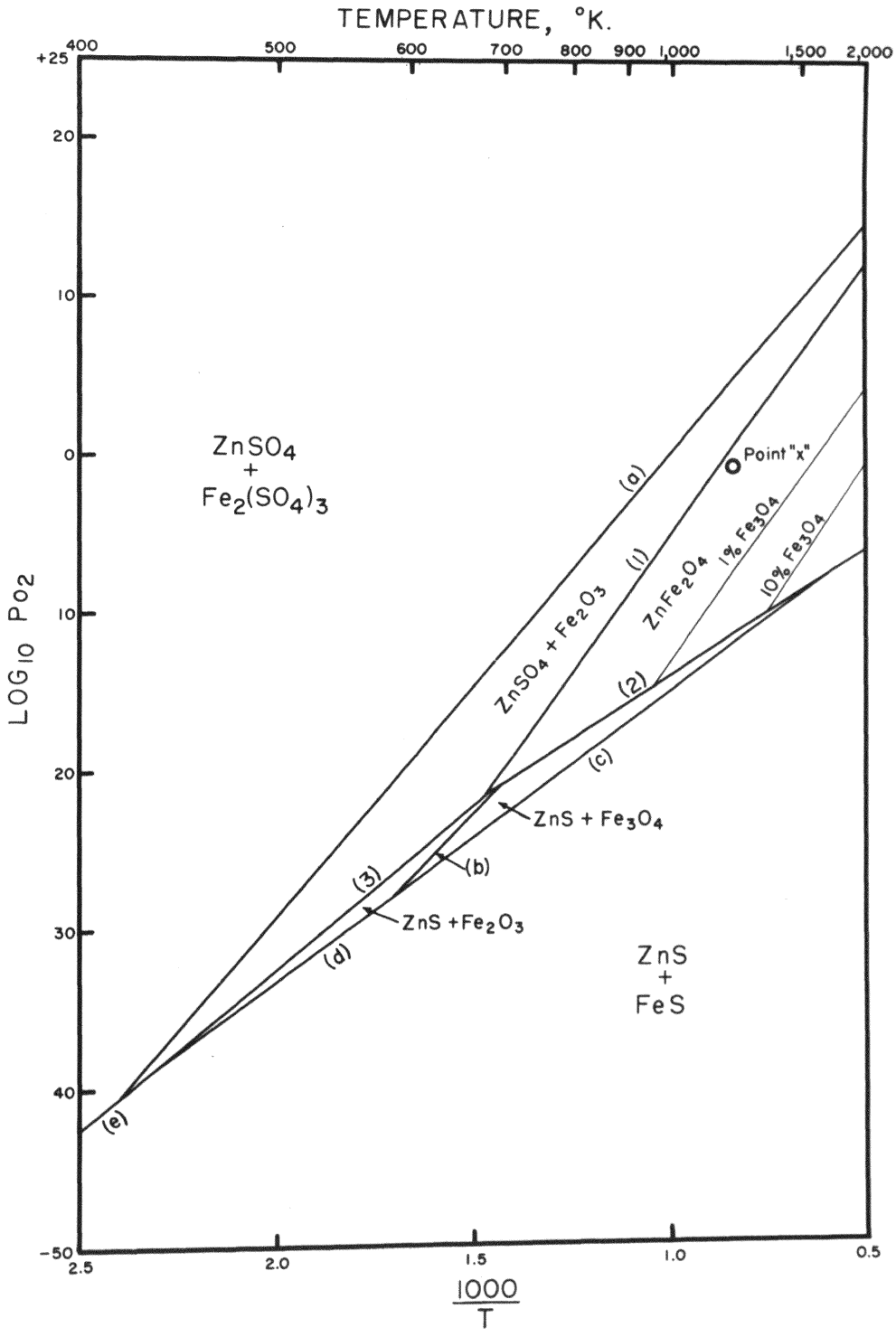

FIGURE 22. - Zn-Fe-S-O Compound Stability Diagram at a Constant SO_2 Pressure of 0.1 Atmospheres.

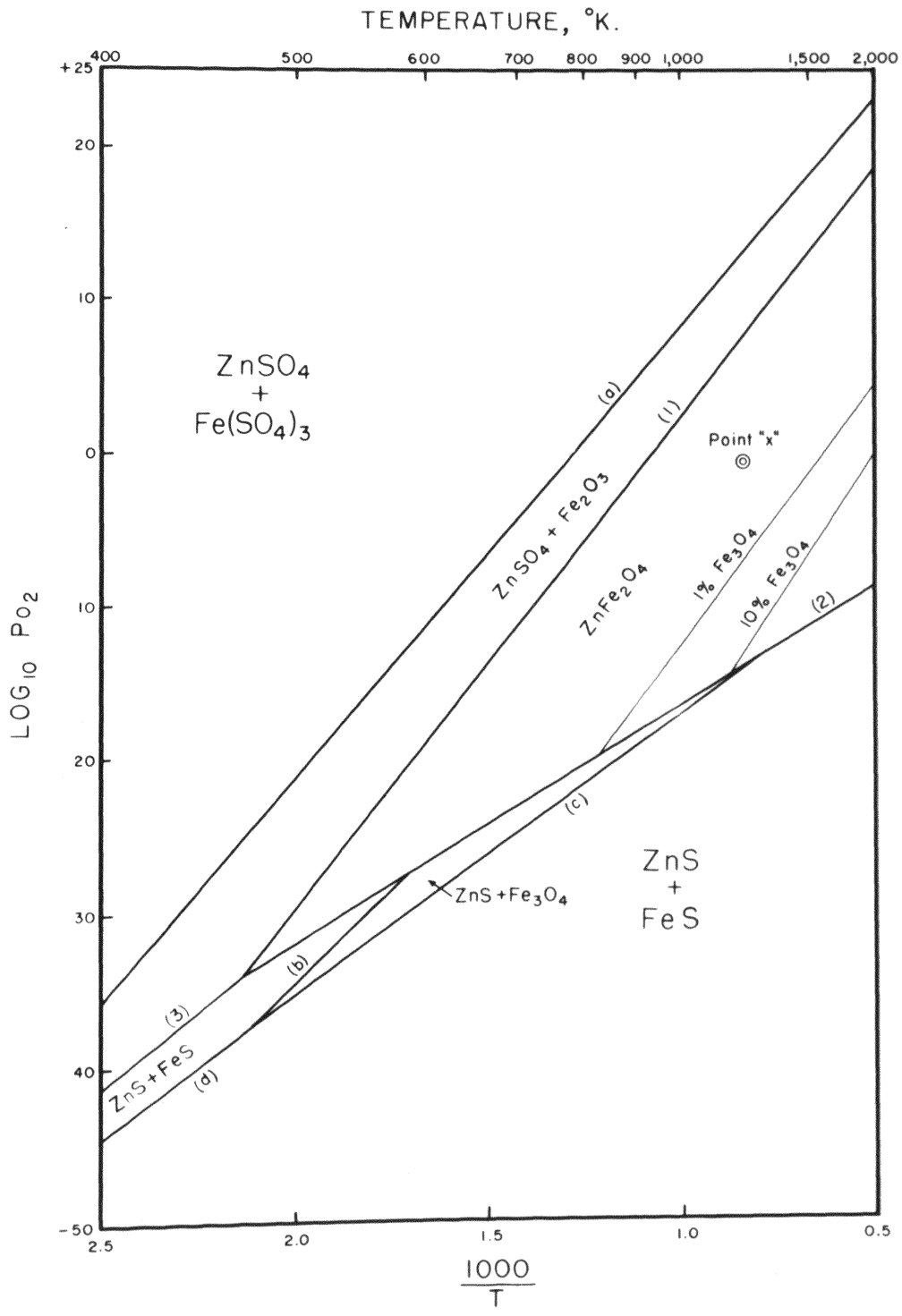

FIGURE 23. - Zn-Fe-S-O Compound Stability Diagram at a Constant SO_2 Pressure of $1X10^{-5}$ Atmospheres.

the beginning of the chapter did not introduce much error in the construction of the figures.

Figures 22 and 23 can now offer a simple explanation as to why zinc metallurgists have found $ZnFe_2O_4$ to be more prevalent at higher roasting temperatures. Apparently, the higher roasting temperatures are the only temperatures at which ZnO and Fe_2O_3 can coexist with the oxygen and SO_2 in the atmosphere; therefore, it is the only condition at which they can combine to form $ZnFe_2O_4$.

To show how the Zn-Fe-S-O system is affected by high temperature roasting, the experimental results of this investigation were incorporated into the $ZnFe_2O_4$ regions of Figures 22 and 23. As was shown in the experimental results, the composition of the ferrite solid solution is a function of temperature and oxygen pressure; likewise, the composition of the $ZnFe_2O_4$ region, shown in the figures, varies with the temperature and oxygen pressure. In order to graphically represent the composition within this region and to show how it varies, the system was assumed to contain excess ZnO. This required the regional composition to exhibit the same temperature and oxygen dependence as the boundary between the solid solution and solid solution plus ZnO regions shown in Figures 5, 6, and 7. The Fe_3O_4 content of the boundary was used to denote the composition. The variation of Fe_3O_4 with temperature and oxygen pressure was determined by plotting the mole percent of Fe_3O_4 on the boundary versus $\log_{10} P_{O_2}$, as shown in Figure 24. Straight lines were drawn through the Fe_3O_4 composition of the boundary. Greater significance was placed on the higher Fe_3O_4 contents because the logarithmic plot of composition tends

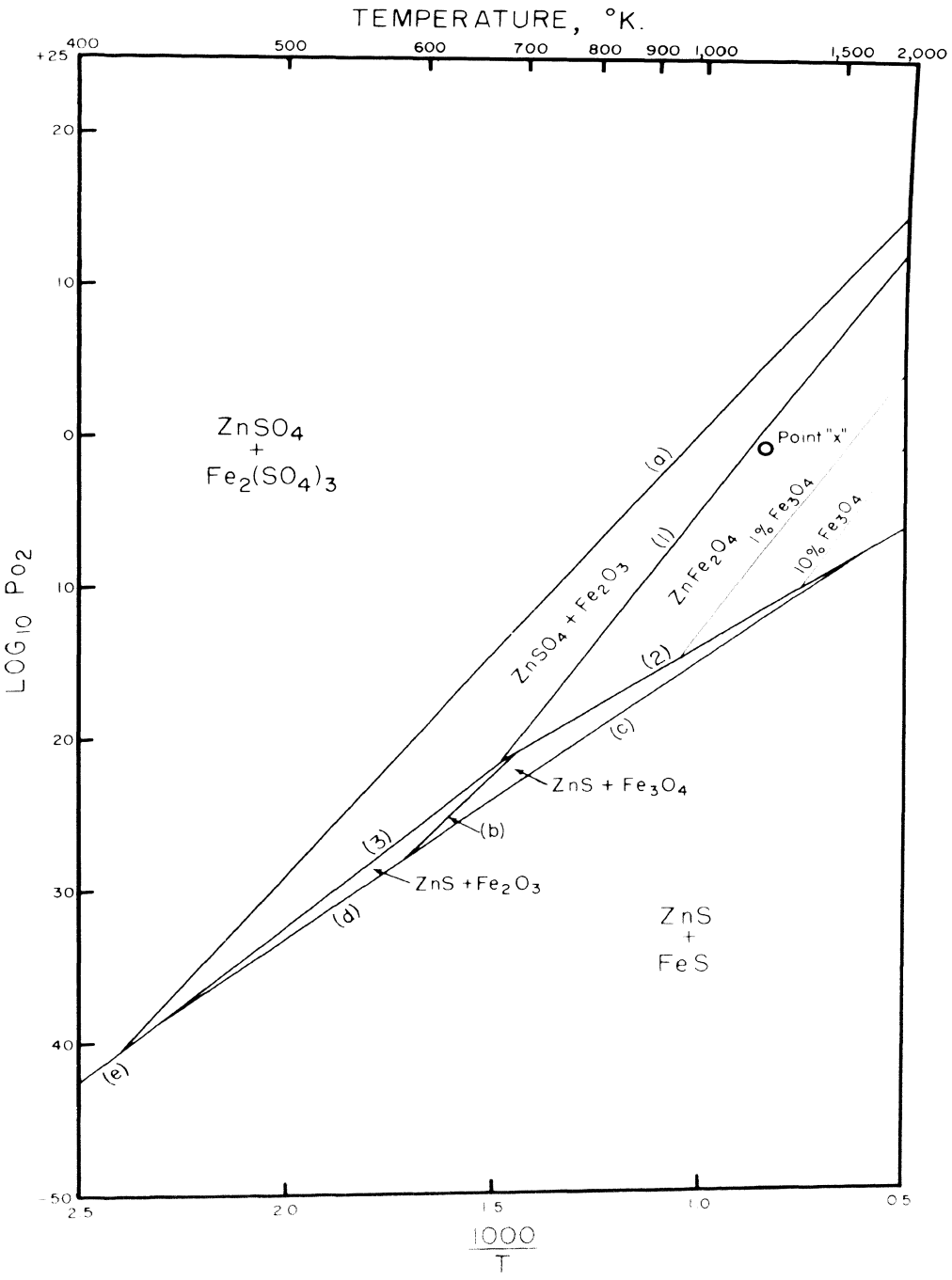

FIGURE 22. - Zn-Fe-S-O Compound Stability Diagram at a Constant SO_2 Pressure of 0.1 Atmospheres.

to magnify errors in analysis at low Fe_3O_4 content. The temperatures and the logarithm of oxygen pressures for a series of constant compositions were then taken from this figure and plotted in Figures 22 and 23, where they appear as straight lines approximately parallel to Reaction 1.

Analysis of Roasting. If the roasting process is now considered in the light of Figures 22 and 23, a number of interesting observations can be made regarding the effect of temperature, oxygen and SO_2 pressure on zinc recovery. This is easily accomplished by considering a sample system such as Point X on Figures 22 and 23.

Effect of Temperature. If only the temperature is varied, the zinc recovery can be increased in two ways: (1) Increasing the temperature would move Point X closer to the 1 percent Fe_3O_4 line, thereby decomposing some of the $ZnFe_2O_4$ and releasing free ZnO. However, considerable amounts of ZnO will still be retained in the ferrite solid solution, as can be seen in the $ZnO-Fe_2O_3-Fe_3O_4$ isothermal sections of Figures 5, 6, and 7; (2) Decreasing the temperature would move Point X into the $ZnSO_4$ plus Fe_2O_3 region where the zinc is no longer retained in the ferrite solid solution. On the other hand, as temperature is decreased the kinetics of the roasting process are decreased, and the probability of retaining unoxidized ZnS is increased.

Effect of Oxygen Pressure. Because of the practical difficulties of increasing the oxygen pressure above one atmosphere, only reductions in oxygen pressure can be effective in increasing zinc recovery. Decreasing the oxygen pressure would move Point X toward

the 1 percent Fe_3O_4 line, however, not as effectively as an equivalent temperature increase. In this instance, a temperature increase of 120°C will move the point the same amount as a 100 fold decrease in oxygen pressure.

Effect of SO_2 Pressure. As can be noted in the comparison of Figures 22 and 23, changing the SO_2 pressure is only effective in moving the boundary with respect to Point X and not in moving the point toward the 1 percent Fe_3O_4 line. This would mean very little zinc recovery would be possible by decreasing the SO_2 pressure. On the other hand, the SO_2 pressure could not be increased enough economically to force boundary 1 to the right of Point X. Therefore varied SO_2 pressure, by itself, probably would not affect zinc recovery in the $ZnFe_2O_4$ region.

As was pointed out, temperature is probably the most effective variable for increasing zinc recovery. However, oxygen and SO_2 pressure can be effectively used in combination with temperature to increase zinc recovery.

CHAPTER VII

SUMMARY AND CONCLUSIONS

This investigation has been primarily concerned with the thermodynamic properties of the ZnO-Fe_2O_3-Fe_3O_4 system and their relationship to: (1) the effect of temperature and oxygen pressure on the decomposition of $ZnFe_2O_4$, (2) the normal and inverse spinel structure, (3) the conversion of zinc to $ZnFe_2O_4$ to ZnO during roasting.

The thermodynamic properties of the system were determined from a series of isobaric oxygen lines in isothermal sections of the ZnO-Fe_2O_3-Fe_3O_4 system. The isothermal sections were derived from the chemical composition of ZnO-Fe_2O_3 mixtures that were equilibrated with a series of oxygen-argon gas mixtures at 1100°, 1300°, and 1400° C. These sections revealed a number of interesting properties of the system:

1. There are three regions of stability within the oxygen pressure range of the experiment: (a) a large spinel solid solution region; (b) a ZnO plus solid solution region; (c) a Fe_2O_3 plus solid solution region.
2. The boundary line between the spinel solid solution region and the ZnO plus solid solution region follows a direction of constant mole percent ZnO (a line between 50 percent ZnO-50 percent Fe_2O_3 and 50 percent ZnO-50 percent Fe_3O_4). The direction of this line does not appear to be affected by temperature or oxygen pressure, only the distance the line extends into the ternary system is affected.

3. The boundary line between the spinel solid solution region and the Fe_2O_3 plus solid solution region follows an approximate straight line between $ZnFe_2O_4$ and the composition of the magnetite in equilibrium with Fe_2O_3, as determined by Darken and Gurry.[1] This boundary is greatly affected by temperature and, as the temperature is reduced, approaches a straight line between $ZnFe_2O_4$ and Fe_3O_4.

4. The constant pressure of oxygen lines, in the isothermal sections, tend to cluster in the region of 66 percent $ZnFe_2O_4$-34 percent Fe_3O_4, indicating the possibility of compound formation within that region. Lattice parameter measurements of the $ZnFe_2O_4$-Fe_3O_4 pseudo-binary system did not bear out this indication, however, but showed the lattice parameter of the system to follow Vegard's law.

In addition to the isothermal sections, the chemical compositions of the equilibrated ZnO-Fe_2O_3 mixtures showed that free ZnO promotes the decomposition of $ZnFe_2O_4$, especially at high temperatures. This was probably brought about by a solubility of ferrous ion in the ZnO lattice. This solubility was indicated by an expansion of the hexagonal lattice in the c-direction.

Lattice parameter and X-ray studies of the spinel solid solution region showed that excess ZnO (defined as ZnO greater than the amount needed to form the pseudo-binary system $ZnFe_2O_4$) tends to expand the

---

[1] L. S. Darken and R. W. Gurry. J. Amer. Chem. Soc., Vol. 68 (1959), p. 798.

spinel lattice, whereas excess Fe_2O_3, by similar definition, tends to contract the lattice. This behavior suggests that the zinc ions continue to occupy the smaller tetrahedral voids and, as the number of filled voids is increased, the lattice parameter increases. Likewise, the ferric ions continue to enter the larger octahedral voids and, because of the higher electrostatic-attractive force, contract the lattice. However, X-ray analysis of much greater precision is needed to test this hypothesis. On the other hand, the X-ray studies do show that the lattice parameter, by itself, could not be used to calculate the composition of the spinel solid solution, as was done in another thermodynamic investigation of this system.[2]

The activities of ZnO, Fe_2O_3, and Fe_3O_4 derived from the constant oxygen pressure lines, showed that the spinel solid solution region is far from ideal with regard to the activities of the components. This was made more apparent in the activity curves of the $ZnFe_2O_4$-Fe_3O_4 pseudo-binary system where both $ZnFe_2O_4$ and Fe_3O_4 show large positive deviations from Raoult's law, especially at high Fe_3O_4 contents. This positive deviation suggested the possibility of repulsive forces between the two components of the system, and it had the following significant effects upon the partial molar quantities which were calculated from the activities:

1. The molar free energy curves were skewed toward the $ZnFe_2O_4$ side (Figure 17) and show a minimum in the region

---

[2]G. P. Popov, M. L. Simonova, T. A. Vgolnikova, and G. I. Chufavov. Dokl. Akad. Nauk. SSSR, Vol. 148, No. 2 (1963).

of 35 percent Fe_3O_4 (the same general region in which the clustering of constant-oxygen-pressure lines was noted). If the system behaved more ideally, the minimum would be closer to the 50 percent Fe_3O_4 region.

2. The molar enthalpy of mixing curve was also skewed toward the $ZnFe_2O_4$ side (Figure 18) but showed a maximum at 45 percent Fe_3O_4. The enthalpy of mixing for an ideal system, on the other hand, is zero throughout the system.

3. The entropy of mixing, however, did exhibit some ideal behavior when compared with a theoretically calculated entropy of mixing for a normal and an inverse spinel, where the cations must occupy the same type of void (tetrahedral or octahedral) which they would occupy in the pure component ($ZnFe_2O_4$ or Fe_3O_4). The oxygen ions, on the other hand, were assumed to be fixed in a rigid lattice. Figure 19 has shown that the experimental entropy of mixing curves bears a close resemblance to the configuration of this calculated curve, and both sets of curves show a maximum at 45 percent Fe_3O_4. This similarity might suggest that the cations of the components (zinc, ferrous and ferric ions) are the major contributing factor to the thermodynamic properties of the system. This might also offer an explanation as to why the lattice

---

[3] J. Smit, H.P.J. Wijn. Ferrites. Physical Properties of Ferri-Magnetic Oxides in Relation to Their Technical Application. N.Y., John Wiley and Sons (1959).

the activities of the components show positive deviations from ideality; that is, show repulsive forces toward each other. Because of the ratio of voids to cations occupying voids (8 tetrahedral voids per tetrahedral cation and 2 octahedral voids per octahedral cation), these repulsive forces would have little effect upon the anion lattice, but would distribute the cations so as to minimize the forces they exert on each other.

In order to determine why the zinc industry found $ZnFe_2O_4$ more prevalent at higher roasting temperatures and to determine the effect that properties of the ZnO-Fe_2O_3-Fe_3O_4 system have on the recovery of zinc from $ZnFe_2O_4$, it was found necessary to construct phase stability diagrams for the Zn-S-O and Fe-S-O systems.

The regions of stability were determined from free energy of reaction equations between the sulfates, sulfides, and oxides of each system.

To construct the Fe-S-O system, however, it was found necessary to estimate a free energy of formation equation for $Fe_2(SO_4)_3$ from decomposition pressures of the sulfate that were published in the literature. The value of this equation, in calories, was found to be

$$\Delta F^{o} = -656{,}620 + 305.1T$$

To determine whether this equation was a fair estimate of the free energy of formation, an alternate method was used to estimate the parameter (twice the unit cell dimension of a face-centered cubic arrangement of oxygen ions)^3 behaves ideally, whereas,

free energy of formation equation. This equation gave free energy values that differed by less than 7 percent of the values given by the foregoing equation. The phase stability diagrams of the Zn-S-O and Fe-S-O ternary systems consisted of a plot of logarithm of oxygen pressure versus reciprocal of temperature; these diagrams showed regions of stability for the sulfates, sulfides, and oxides at a constant SO_2 pressure. These regions of stability are separated by lines representing the equilibrium equations between the sulfates, sulfides, and oxides and are the phases which should be stable at a particular temperature, oxygen pressure, and SO_2 pressure.

The two ternary systems were superimposed to form the Zn-Fe-S-O system, and the superposition divided the systems into regions where a zinc compound was stable with an iron compound. Interactions between these compounds were considered and, with the exception of ZnO plus Fe_2O_3 or Fe_3O_4, were found to be thermodynamically unstable.

When the system was considered in the area of roasting conditions, three regions were found to be stable: (1) the $ZnSO_4$ plus $Fe_2(SO_4)_3$ region, (2) the $ZnSO_4$ plus Fe_2O_3 region, (3) the $ZnFe_2O_4$ region. It was also noted that, as the SO_2 pressure was decreased, the boundary lines between the regions shift toward lower temperatures. All of these findings agree with the experimental results of other investigators[4], indicating that the diagrams give a good qualitative representation of the Zn-Fe-S-O system, at least within the region of roasting conditions.

---

[4] Y. Umethu and S. Suzuki, loc. cit.

The diagrams also show that the higher roasting temperatures are the only conditions under which ZnO and Fe_2O_3 can coexist with the oxygen and SO_2 in the roaster atmosphere; therefore these are the only conditions under which ZnO and Fe_2O_3 can combine to form $ZnFe_2O_4$.

In addition, the results of this investigation were applied to the $ZnFe_2O_4$ region to show the effect of temperature and oxygen pressure on the composition of this region. These results showed that temperature is the most effective variable for increasing zinc recovery, and that the oxygen and SO_2 pressures can be effectively used in combination with temperatures to increase zinc recovery.

BIBLIOGRAPHY

American Zinc Institute. "Zinc--The Science and Technology of the Metal, Its Alloys and Compounds", Am. Chem. Soc. Monograph No. 142, Reinhold Publ. Corp., New York, N.Y. (1959), pp. 1-7.

Claisse, F. Norelco Reporter, Vol. 4, No. 1, p. 3 (1957).

Coughlin, J. P. U. S. Bureau of Mines Bull. 542 (1954).

Darken, L. S. J. Am. Chem. Soc., Vol. 72, 2909 (1950).

_____, and R. W. Gurry. J. Amer. Chem. Soc., Vol. 67, (1945) p. 1398.

_____, and R. W. Gurry. J. Amer. Chem. Soc., Vol. 68, (1959) p. 798.

Floud, H. and N. Boye, Z. Elektrochem, Vol. 66, No. 2 (1962), p. 184.

Gokcen, N. A. J. Phys. Chem. Vol. 64, 401 (1960).

Greig, Posnjak, Merwin, and Sosman. Amer. J. Sci. Vol. 30, (1935) p. 293.

Hedvall, J. A. and Heuberger. Z. Anorg. Ch. Vol. 128 (1923), p. 5.

Hommel. Metallurgie, Vol. 9 (1912), p. 281.

Hopkins, D. W. J. Electrochem. Soc. Vol. 96, p. 195 (1949).

_____, and A. G. Adlington. Inst. of Mining and Metallurgy Trans. Vol. 60 (1950-51), pp. 117-128.

Hoschek, G. Monatsh Chem., Vol. 93, No. 4 (1962), p. 826.

Ingraham, T. R. and H. H. Kellogg. Trans. Met. Soc. AIME, Vol. 227 (1963), p. 1419.

Kubaschewski, O. and E.L.L. Evans. Metallurgical Thermochemistry, New York, Pergammon Press (1958).

Kushima, I. and T. Amanuma. Mem. Fac. Imp. Kyoto Univ. Vol. 16 (1954), p. 191.

Latimer, W. M. J. Amer. Chem. Soc., Vol. 73, (1951), p. 1480.

McKay, H.A.C. Nature Vol. 169, 464 (1952).

Minerals Yearbook. (1961) Vol. I, Metals and Minerals U. S. Dept. of the Interior, Bureau of Mines.

Miyata, N. J. Phys. Soc. Vol. 16, p. 1291 (1961).

Moore, G. E. and K. K. Kelley. J. Amer. Chem. Soc. Vol. 64 (1942), p. 2949.

Pippin, J. E. and C. L. Hogan. The Preparation of Polycrystalline Ferrites for Microwave Applications. ASTIA Document No. AD117295.

Popov, G. P., M. I. Simonova, T. A. Vgolnikova, and G. I. Chufavor. Dokl. Akad. Nauk SSSR, Vol. 148, No. 2 (1963).

Prost and Van DePutte. Rev. Univ. Des. Mines June 1, 1926.

Ralston, O. C. "Electrolytic Deposition and Hydrometallurgy of Zinc", McGraw-Hill Book Co., New York, N.Y. (1921), p. 5.

Roggero, C. E. Trans. Met. Soc. AIME, Vol. 227, p. 105 (1963).

Schuhmann, R. Jr. Acta Met. Vol. 3, 219 (1955).

Tafel and Grosse. Metall u. Erz. Vol. 26 (1929), p. 354.

Takei, T. and Y. Kato. Trans Electrochem Soc. Vol. 57 (1930), pp. 297-312.

Toropov, N. A. and A. I. Borisenko. Doklady Akad. Nauk SSSR, Vol. 82 (1952), p. 607.

Umethu, Y. and S. Suzuki. J. Mining Inst. Japan Vol. 68 (1952) p. 529.

Wohler, L., W. Phuddemann and P. Wohler. Ber. Deut. Chem. Ges., Vol. 41 (1908), p. 703.

Yamaguchi, T. and T. Takei. Sci. Papers Inst. Phy. Chem. Research Tokyo, Vol. 53, p. 207 (1959).

- APPENDIXES -

APPENDIX -A-

CALCULATION OF Fe_2O_3 ACTIVITIES, USING ZINC OXIDE, IRON, AND OXYGEN AS COMPONENTS

Schuhmann[1] has presented an alternate method for the derivation of ternary molar quantities which is, sometimes, easier to follow but somewhat less rigorous. This method will be used here.

For zinc oxide, iron, and oxygen, the Gibbs-Duhem equation can be written

$$n_O \, d\ln \alpha_O + n_{Fe} d\ln \alpha_{Fe} + n_{ZnO} d\ln \alpha_{ZnO} = 0 \qquad \text{(A-1)}$$

Multiplying this equation by $2/n_{Fe}$, and then adding and subtracting $3\ln \alpha_O$ gives:

$$\left(2 \frac{n_O}{n_{Fe}} - 3\right) d\ln \alpha_O + 2 \frac{n_{ZnO}}{n_{Fe}} \, d\ln \alpha_{ZnO} + 2 d\ln \alpha_{Fe} + 3 \, d\ln \alpha_O = 0 \qquad \text{(A-2)}$$

But

$$2 \, d\ln \alpha_{Fe} + 3 \, d\ln \alpha_O = d \, \ln (\alpha_{Fe})^2 (\alpha_O)^3 = d\ln \alpha_{Fe_2O_3}$$

Therefore, Equation A-2 reduces to

$$\left(2 \frac{n_O}{n_{Fe}} - 3\right) d\ln \alpha_O + 2 \frac{n_{ZnO}}{n_{Fe}} \, d\ln \alpha_{ZnO} + d\ln \alpha_{Fe_2O_3} = 0 \qquad \text{(A-3)}$$

By considering a path of constant α_O and n_{ZnO} and then dividing by dn_{Fe}, Equation A-3 reduces to

$$\frac{d\ln \alpha_{Fe_2O_3}}{dn_{Fe}} + 2 \frac{n_{ZnO}}{n_{Fe}} \frac{d\ln \alpha_{ZnO}}{dn_{Fe}} = 0 \qquad \text{(A-4)}$$

Differentiating this with respect to $\ln \alpha_O$ at constant n_{Fe} and n_{ZnO} yields

---

[1] R. Schuhmann, Jr. Acta Met., Vol. 3, 219 (1955).

$$\frac{d^2 \ln \alpha_{Fe_2O_3}}{d\ln\alpha_O \, dn_{Fe}} + 2\frac{n_{ZnO}}{n_{Fe}} \frac{d^2 \ln \alpha_{ZnO}}{d \ln \alpha_O \, dn_{Fe}} = 0 . \qquad \text{(A-5)}$$

If Equation A-3 is now multiplied through by $n_{Fe}/d\ln_O$ and if a path of constant n_{Fe} and n_{ZnO} is considered, the equation reduces to

$$(2n_O - 3n_{Fe}) + (n_{Fe}) \frac{d\ln\alpha_{Fe_2O_3}}{d\ln\alpha_O} + (2n_{ZnO}) \frac{d\ln\alpha_{ZnO}}{d\ln\alpha_O} = 0 \qquad \text{(A-6)}$$

Differentiating this with respect to n_{Fe} a constant $_O$ and n_{ZnO} gives

$$2\frac{dn_O}{dn_{Fe}} - 3 + \frac{d\ln\alpha_{Fe_2O_3}}{d\ln\alpha_O} + (n_{Fe}) \frac{d^2\ln\alpha_{Fe_2O_3}}{dn_{Fe} d\ln\alpha_O} + (2n_{ZnO}) \frac{d^2 \ln \alpha_{ZnO}}{dn_{Fe} d\ln\alpha_O} = 0 \qquad \text{(A-7)}$$

Dividing Equation A-7 by n_{Fe} and substituting in Equation A-5 gives

$$\frac{d\ln\alpha_{Fe_2O_3}}{d\ln\alpha_O} = 3 - \frac{dn_O}{dn_{Fe}} \qquad \text{(A-8)}$$

However,

$$\frac{dn_O}{dn_{Fe}} = \frac{n_O}{n_{Fe}} = \frac{3N_{Fe_2O_3} + 4N_{Fe_3O_4}}{2N_{Fe_2O_3} + 3N_{Fe_3O_4}} \qquad \text{(A-9)}$$

therefore,

$$3 - \frac{dn_O}{dn_{Fe}} = \frac{N_{Fe_3O_4}}{2N_{Fe_2O_3} + 3N_{Fe_3O_4}} = \frac{1}{3+2\dfrac{N_{Fe_2O_3}}{N_{Fe_3O_4}}} \qquad \text{(A-10)}$$

Substituting Equation A-10 into A-8 and integrating according to the restrictions of the derivation yields

$$\ln {}_{Fe_2O_3} = \ln {}_{Fe_2O_3 I} + \int_I^{II} \left(\frac{1}{3+2\dfrac{N_{Fe_2O_3}}{N_{Fe_3O_4}}} \right)_{\ln\alpha_O, N_{ZnO}} d\ln\alpha_O \qquad \text{(A-11)}$$

$$\frac{N_{Fe_2O_3}}{N_{ZnO}}$$

which is equivalent to Equation 5-12 of the text.

APPENDIX -B-

CALCULATIONS OF THE Fe_3O_4 ACTIVITIES FROM THOSE OF Fe_2O_3 AND OXYGEN

In order to derive the relationship between the activities of Fe_3O_4 and the activities of oxygen and Fe_2O_3, two equilibrium reactions must be considered, together with their equilibrium constants.

The first of these reactions consists of the sum of two reactions

$$Fe_3O_4 \rightleftharpoons 3Fe_{Mag} + 2O_2$$

$$K_1 = \frac{\left[\alpha_{Fe_{Mag}}\right]^3 \left[P_{O_2}\right]^2}{\left[\alpha_{Fe_3O_4}\right]} \qquad (B\text{-}1)$$

and $$3Fe_{Hem} + \frac{9}{4} O_2 \rightleftharpoons \frac{3}{2} Fe_2O_3$$

$$K_2 = \frac{\left[\alpha_{Fe_2O_3}\right]^{\frac{3}{2}}}{\left[\alpha_{Fe_{Hem}}\right]^3 \left[P_{O_2}\right]^{\frac{9}{4}}} \qquad (B\text{-}2)$$

which equals

$$Fe_3O_4 + \frac{1}{4} O_2 \rightleftharpoons \frac{3}{2} Fe_2O_3$$

$$K_3 = \left[K_1\right]\left[K_2\right] = \frac{\left[\alpha_{Fe_2O_3}\right]^{\frac{3}{2}}}{\left[\alpha_{Fe_3O_4}\right]\left[P_{O_2}\right]^{\frac{1}{4}}} \qquad (B\text{-}3)$$

The second reaction consists of the decomposition of 3/2 of a mole of Fe_2O_3 into a mole of Fe_3O_4. The decomposition in this case,

however, is done in a spinel solid solution. This decomposition is represented by the reaction

$$(ZnO)_X \cdot (Fe_2O_3)_Y \cdot (Fe_3O_4)_Z + \frac{3}{2}(Fe_2O_3)_* \rightleftharpoons (ZnO)_X \cdot (Fe_2O_3)_Y \cdot (Fe_3O_4)_{Z+1} + \frac{1}{4}O_2$$

$$K_4 = \frac{\left[P_{O_2}\right]^{\frac{1}{4}}}{\left[\alpha_{Fe_2O_3}\right]^{\frac{3}{2}}} \qquad (B\text{-}4)$$

In this equation the values of X, Y, and Z are very much greater than 3/2; therefore the composition of the spinel solid solution as well as the activities of the individual components are practically unchanged. In addition, the activity of $(Fe_2O_3)_*$ is equal to the activity of the $(Fe_2O_3)_Y$. Adding Equations B-3 and B-4 gives

$$(ZnO)_X(Fe_2O_3)_Y \cdot (Fe_3O_4)_Z + Fe_3O_4 \rightleftharpoons (ZnO)_X \cdot (Fe_3O_4)_Y \cdot (Fe_3O_4)_{Z+1} \qquad (B\text{-}5)$$

which is the reaction defining the partial molar free energy of mixing Fe_3O_4 in the spinel solid solution.

The partial molar free energy of mixing Fe_3O_4 is defined as

$$\Delta F_{Fe_3O_4} = RT \ln \alpha_{Fe_3O_4}$$

which is also the free energy change for this reaction

$$\Delta F = -RT \ln K_5$$

where

$$K_5 = \left[K_3\right]\left[K_4\right] = K_3 \frac{\left[P_{O_2}\right]^{\frac{1}{4}}}{\left[\alpha_{Fe_2O_3}\right]^{\frac{3}{2}}} \qquad (B\text{-}6)$$

This equation is equivalent to what is found in Equation B-3, therefore the activity of Fe_3O_4 in the spinel solid solution is defined as

$$\alpha_{Fe_3O_4} = \frac{\left[\alpha_{Fe_2O_3}\right]^{\frac{3}{2}}}{\left[K_3\right]\left[P_{O_2}\right]^{\frac{1}{4}}}$$

APPENDIX C

COMPLETION OF THE DERIVATION FOR THE ENTROPY OF MIXING A NORMAL WITH AN INVERSE SPINEL

The entropy of position of a substance (S_p) is defined as

$$S_p = K \ln W_p \tag{C-1}$$

where K is Boltzmann's constant and W_p is the total number of ways of arranging the positions within the structure of the substance. Employing this definition and the W_p of equation 5-33,

$$W_p = \frac{(2N)!\ (N)!}{(\frac{N}{4}-X)!(\frac{N}{2}-X)!\ [(X)!]^2\ (\frac{7N}{4})!(\frac{N}{2})!}$$

the entropy of position for mixing an inverse with a normal spinel is

$$S_p = K\left[\ln 2N\ !+\ln N!-\ln(\tfrac{N}{4}-X)!-\ln(\tfrac{N}{2}-X)!-2\ln X!-\ln\tfrac{7N}{4}!-\ln\tfrac{N}{2}!\right] \tag{C-2}$$

Applying Stirling's approximation to this equation gives

$$S_p = K\left[2N\ln 2N+\ln N-(\tfrac{N}{4}-X)\ln(\tfrac{N}{4}-X)-(\tfrac{N}{2}-X)\ln(\tfrac{N}{2}-X)-2X\ln X-\tfrac{7N}{4}\ln\tfrac{7N}{4}\right.$$

$$\left.-\tfrac{N}{2}\ln\tfrac{N}{2}-2N-N+(\tfrac{N}{4}-X)+(\tfrac{N}{2}-X)+2X+\tfrac{7N}{4}+\tfrac{N}{2}\right] \tag{C-3}$$

Combining terms and letting $N=4N_o$, where N_o is Avagadro's number, Equation C-3 reduces to

$$S_p=KN_o\left[8\ln 8N_o+4\ln 4N_o-(1-Y)\ln(1-Y)N_o-(2-Y)\ln(2-Y)N_o-2Y\ln YN_o-7\ln 7N_o-2\ln 2N_o\right] \tag{C-4}$$

where $Y=XN_o$ which is equal to the mole fraction of Fe_3O_4.

Separating the logarithms of the products into the sum of the logarithms for example

$$8\ln 8N_o = 8\ln 8 + 8\ln N_o,$$

and combining terms, gives the equation

$$S_p = R\left[\ln\left(\frac{8^8\,4^4}{7^7\,2^2}\right) - (1-Y)\ln(1-Y) - (2-Y)\ln(2-Y) - 2Y\ln Y\right] , \qquad (C\text{-}5)$$

where R, the gas constant, equals KN_o.

Combining this equation with the position entropies of Fe_3O_4 and $ZnFe_2O_4$, as shown in Equation 5-27 of the text, gives the entropy of mixing

$$\Delta S^m = -R\left[Y\ln Y + (1-Y)\ln(1-Y) + (2-Y)\ln(2-Y) + (1-Y)\ln\frac{8^8 4^3}{7^7} - (1-Y)\ln\frac{8^8 2^4}{7^7}\right] ,$$

which is further simplified to

$$\Delta S^m = -R\left[Y\ln Y + (1-Y) + (1-Y)\ln(1-Y) + (2-Y) + (1-Y)\ln 4\right] , \qquad (C\text{-}6)$$

the same equation as is shown in Equation 5-36 of the text.

VITA

The author was born on December 9, 1933, in Elizabeth, New Jersey. He received his primary education in Denville, New Jersey, and his secondary education in Dover, New Jersey. Upon graduation from high school, he served a two-year apprenticeship as a tool and die maker.

From June 1953 to June 1957 he served in the United States Navy as a Machinery Repairman. In September 1957, he enrolled in the University of Missouri School of Mines and Metallurgy and received his Bachelor of Science degree and Master of Science Degree in June 1961 and August 1962, respectively.

He has been enrolled in the Graduate School of the University of Missouri since September, 1962, and has worked on the research presented here under the auspices of a Bureau of Mines cooperative Fellowship.